

Particle-hole instability in the AdS_4 holography

E. Gubankova *

Institute for Theoretical Physics, J. W. Goethe-University, D-60438 Frankfurt am Main, Germany

E-mail: gubankova@th.physik.uni-frankfurt.de

ABSTRACT: We show that particle-hole pairing is realized in the background of a charged black hole in magnetic field. The pairing instability occurs for sufficiently large fermion charges, which correspond to the Fermi liquid regime. The critical temperature for Fermi liquids is proportional to the magnetic field and vanishes as we approach the non-Fermi liquid state. The pairing order parameter leads to a relative shift of the Fermi surfaces corresponding to the bulk fermions with spin up and down. The value of the shift in Fermi momentum k_F and the critical temperature T_c are proportional to the effective density of states at the Fermi surface. Our one-loop calculations provide a dual description of the magnetic catalysis for the lowest Landau level in graphene. This analyses may be relevant for the antiferromagnetic behavior in the cuprate superconductors and for the chiral spirals in the chiral magnetic effect.

We also discuss thermodynamic and transport properties of a system at the boundary at zero magnetic field. The scaling behavior of the specific heat is $c \sim T$ for Fermi liquid and $c \sim T^{2\nu}$ for non-Fermi liquid, while the behavior of the DC conductivity is the same $\sigma \sim T^{-2\nu}$ in both cases. While it can be difficult to extract transport and hydrodynamic from the lattice, the AdS/CFT approach provides a robust frame for nonperturbative calculation of these properties.

KEYWORDS: AdS/CFT correspondence, strongly correlated electrons, transport.

*Also at ITEP, Moscow, Russia

Contents

1. Introduction	1
2. Dyonic black hole and infrared CFT	3
3. Variational calculations of the pairing gap	6
3.1 Effective action for interacting fermions in a magnetic field	6
3.2 Variational calculations of magnetic catalysis in a charged black hole geometry AdS_4	8
4. Pairing instability in the Ginsburg-Landau formalism	12
4.1 Microscopic calculations of magnetic catalysis. Ginsburg-Landau in a holographic approach	12
4.2 Solving for the zero modes and finding the critical temperature	17
5. Equation of state and transport properties of the boundary field theory at zero magnetic field	28
5.1 Equation of state and specific heat	29
5.2 DC conductivity	33
6. Discussion	35
A. Dirac equation in the AdS_4	37
A.1 Dirac equation with magnetic field in a charged black hole geometry AdS_4	37
A.2 Dirac equation. Conformal dimension in the low frequency limit	41
B. Dirac equation in the AdS_2	44
B.1 Dirac equation and conformal dimension	44
B.2 Two-point functions for charged fermions in AdS_2	46
C. One-loop calculations in a $(2 + 1)$ dimensional field theory	48
D. Critical temperature from the AdS_4 variational calculations	51

1. Introduction

Particle-hole pairing appears in different contexts in condensed matter physics. We consider here magnetic catalysis, i.e., generation of the T-odd mass parameter in the presence of a magnetic field. It is a well established phenomenon in $(2 + 1)$ -dimensions and it is believed to explain the anomalous quantum Hall effect in graphene, i.e., the appearance

of the additional plateaus in the Hall conductivity σ_{xy} for the lowest Landau level [1] (see [2] for the magnetic catalysis in $(3 + 1)$ -dimensions). Electron-hole pairing is responsible for the spin density order parameter and the antiferromagnetic nature of the cuprate superconductors at half filling. Spin-density wave in the form of spin-orbit ordering can trigger the superconducting pairing, while both superconducting electron-electron and spin density wave electron-hole orders are essential to describe physics of Mott insulating and pseudogap phases. Recently, there was an interest to the particle-hole pairing in the form of chiral spirals in the context of the chiral magnetic effect and the quarkyonic matter [3].

These phenomena involve strongly coupled physics. We therefore use the *AdS/CFT* correspondence which is a powerful tool in understanding strongly coupled quantum field theories. It is formulated as a duality between classical gravitational theory in the anti-de Sitter (*AdS*) space and a strongly coupled conformal field theory (*CFT*) in the limit of large N and large 't Hooft coupling λ defined on the boundary of the *AdS* space. Recently the *AdS/CFT* correspondence was applied to different phenomena which arise in the context of condensed matter systems [4, 5, 6, 7, 8, 9]. Many of the above studies were initiated by the original papers on a holographic superconductor [10, 11], the non-Fermi liquid behavior [12], and quantum phase transitions [13]. In particular, there have been significant developments in understanding the superconducting instability near a charged black hole. It was shown that charged black holes are unstable to forming hair, which means that a (free) charged (or neutral) scalar field develops a vacuum expectation value and breaks spontaneously the corresponding symmetry when put in the charged black hole background with asymptotic *AdS* geometry [10, 11]. This was linked to the Breitenlohner-Freedman instability that provides a gravitational mechanism for superconductivity: if the charge of the boson is sufficiently large compared to its mass it will condense. This mechanism does not give microscopic details behind the superconductivity like the BCS pairing does. It provides the evidence for the bosonic condensate and suggests a holographic mechanism for the superconductivity. Using the Cooper pair picture the critical temperature has been calculated in Ref.[14].

In describing the particle-hole pairing we follow the same route as used to address superconductivity [15]. Both graphene and the cuprate superconductors are systems at finite charge density in $(2 + 1)$ -dimensions. Therefore the gravity dual description is given by a charged black hole in $(3 + 1)$ -dimensional anti-de Sitter space-time *AdS*₄. Strong coupling and large N limit of the boundary theory translates into a gravity theory at small curvature and low energy, which reduces to a universal sector of classical Einstein gravity plus matter fields. The global $U(1)$ symmetry of the conformal field theory (CFT) with current J_μ is mapped to a $U(1)$ local gauge symmetry with a gauge field A_M in the *AdS*₄. In the *AdS*₄, A_M is an actual (not background) $U(1)$ field, which is dynamic.

In this paper we add a four-Fermi contact interaction between the charged fermions. We choose the channel favoring the magnetic catalysis and look for the particle-hole instability that shows up when the one-loop effective action has negative modes. There is important difference between showing the instability for the bosonic field $\langle \Phi \rangle \neq 0$ and for fermions $\langle \bar{\psi}\psi \rangle \neq 0$. Calculation for bosons is classical in the black hole background, whereas for fermions it involves one loop computation. We use variational approach where

we utilize the formula for the one loop fermion determinant expressed through a sum over quasinormal modes of the black hole [16, 17]. As discussed in [16, 17], the quasinormal modes are given by the poles of the retarded fermion Green function. The structure of the poles for the retarded Green function has been obtained in [18] for various relative relations between the charge and the mass of the fermion. We also do a one-loop calculation in the bulk to obtain a non-local in the radial direction Ginsburg-Landau action. The latter calculation involves bulk fermion propagators and a radial profile for the pairing order parameter. The idea of calculation follows the Ginsburg-Landau approach.

In this paper we consider application of particle-hole pairing to the magnetic catalysis. Magnetic catalysis has been shown in $(2 + 1)$ [1] and $(3 + 1)$ [2] dimensional relativistic models. The general result is that a constant magnetic field leads to the generation of a fermion dynamical mass even at the weakest attractive interaction between fermions. The essence of the effect is that in the magnetic field the dimension of the system effectively reduces $d \rightarrow d - 2$, i.e., to $(0 + 1)$ and $(1 + 1)$ dimensional systems, that favors the dynamics of the particle-hole pairing (therefore the name of magnetic catalysis) [1]. We can choose different forms of the four-Fermi interaction, that will generate a mass term for the fermions with needed symmetry properties. For simplicity, we choose a contact interaction $G_{int}(\bar{\psi}i\Gamma^2\Gamma^5\psi)^2$ with the strength G_{int} written through the mass scale of the interaction $G_{int} = 1/M_{int}^2$. We show that this interaction triggers the generation of the mass term $\Delta\bar{\psi}i\Gamma^2\Gamma^5\psi$ which is odd both under time-reversal and parity transformations (see the representation of Γ matrices). Contrary to the Dirac mass term $m\bar{\psi}\psi$, the generation of the T -odd mass $\Delta\bar{\psi}i\Gamma^2\Gamma^5\psi$ does not break any symmetry, e.g. $U(1)_L \times U(1)_R$ in the NJL model or spin (flavor) symmetry $SU(2)$ ($U(2)_+ \times U(2)_-$) in the case of graphene [1]. Because no symmetry is spontaneously broken by the T -odd mass, no gap opens in the spectrum. In this sense, the condensate $\Delta\bar{\psi}i\Gamma^2\Gamma^5\psi$ is similar to the spin density wave $\langle \psi^\dagger \vec{\sigma} \psi \rangle$, where the former couples to the mass and the latter one to the chemical potential.

The paper is organized in the following way. In section 2 we introduce the black hole geometry and consider the near horizon limit which is dual to the IR CFT. In section 3 we perform the variational calculation for the particle-hole pairing order parameter. In section 4 we perform Ginsburg-Landau calculations in the AdS_4 bulk geometry, and calculate the critical temperature. In section 5 we consider thermodynamic and transport properties of a system on the boundary at zero magnetic field. Appendices contain solution of the Dirac equation in magnetic field and calculation of the Landau levels in the AdS_4 holography (Appendix A.1), calculation of the conformal dimension in the IR CFT₃ (Appendix A.2), solution of the Dirac equation in the AdS_2 and obtaining the IR CFT₁ conformal dimension (Appendix B.1), derivation of the AdS_2 Green function (Appendix B.2), one-loop calculation in $(2 + 1)$ -dimensional field theory (Appendix C), calculation of the critical temperature in the AdS_4 (Appendix D).

2. Dyonic black hole and infrared CFT

We consider 3-dimensional conformal field theory (CFT) with global $U(1)$ symmetry that has a gravity dual. At finite charge density and in the presence of magnetic field, the

system can be described by a dyonic black hole in 4-dimensional anti-de Sitter space-time, AdS_4 , with the current J_μ in the CFT mapped to a $U(1)$ gauge field A_M in AdS .

The action for a vector field A_M coupled to AdS_4 gravity can be written as

$$S = \frac{1}{2\kappa^2} \int d^4x \sqrt{-g} \left(\mathcal{R} + \frac{6}{R^2} - \frac{R^2}{g_F^2} F_{MN} F^{MN} \right), \quad (2.1)$$

where g_F^2 is an effective dimensionless gauge coupling and R is the curvature radius of AdS_4 . The equations of motion following from eq.(2.1) are solved by the geometry of the dyonic black hole, i.e., with both electric and magnetic charges,

$$ds^2 = g_{MN} dx^M dx^N = \frac{r^2}{R^2} (-f dt^2 + d\vec{x}^2) + \frac{R^2}{r^2} \frac{dr^2}{f}, \quad (2.2)$$

where the redshift factor, f , and the vector field A_M reflect the fact that the system is at finite charge density and in the magnetic field,

$$f = 1 + \frac{Q^2 + H^2}{r^4} - \frac{M}{r^3},$$

$$A_t = \mu \left(1 - \frac{r_0}{r} \right), \quad A_x = -\mathcal{H}y, \quad (2.3)$$

where we chose the Landau gauge; the chemical potential μ and the magnetic field \mathcal{H} are given by

$$\mu = \frac{g_F Q}{R^2 r_0}, \quad \mathcal{H} = \frac{g_F H}{R^4}. \quad (2.4)$$

Here r_0 is the horizon radius determined by the largest positive root of the redshift factor, $f(r_0) = 0$,

$$M = r_0^3 + \frac{Q^2 + H^2}{r_0} \quad (2.5)$$

and the CFT is defined at the boundary $r \rightarrow \infty$. The geometry eqs.(2.2),(2.3) describes the boundary theory at a finite density, i.e., a system in the medium at chemical potential μ , with the charge, energy, and entropy densities given, respectively, by

$$\rho = 2 \frac{Q}{\kappa^2 R^2 g_F}, \quad \epsilon = \frac{M}{\kappa^2 R^4}, \quad s = \frac{2\pi}{\kappa^2} \frac{r_0^2}{R^2}. \quad (2.6)$$

The temperature of the system is identified with the Hawking temperature of the black hole, $T_H \sim |f'(r_0)|/4\pi$,

$$T = \frac{3r_0}{4\pi R^2} \left(1 - \frac{Q^2 + H^2}{3r_0^4} \right). \quad (2.7)$$

Since Q and H have dimensions of $[L]^2$, it is convenient to parametrize them as

$$Q^2 = 3r_*^4, \quad Q^2 + H^2 = 3r_{**}^4. \quad (2.8)$$

In terms of r_0 , r_* and r_{**} the expressions are

$$f = 1 + \frac{3r_{**}^4}{r^4} - \frac{r_0^3 + 3r_{**}^4/r_0}{r^3},$$

$$A_t = \mu \left(1 - \frac{r_0}{r} \right), \quad A_x = -\mathcal{H}, \quad (2.9)$$

with

$$\mu = \sqrt{3}g_F \frac{r_*^2}{R^2 r_0}, \quad \mathcal{H} = \sqrt{3}g_F \frac{\sqrt{r_{**}^4 - r_*^4}}{R^4}. \quad (2.10)$$

The expressions for the charge, energy and entropy densities, and for the temperature are simplified as

$$\begin{aligned} \rho &= \frac{2\sqrt{3}}{\kappa^2 g_F} \frac{r_*^2}{R^2}, \quad \epsilon = \frac{1}{\kappa^2} \frac{r_0^3 + 3r_{**}^4/r_0}{R^4}, \quad s = \frac{2\pi}{\kappa^2} \frac{r_0^2}{R^2}, \\ T &= \frac{3}{4\pi} \frac{r_0}{R^2} \left(1 - \frac{r_{**}^4}{r_0^4}\right). \end{aligned} \quad (2.11)$$

In the first part of the paper we consider the zero temperature limit, i.e., extremal black hole,

$$T = 0 \quad \rightarrow \quad r_0 = r_{**}, \quad (2.12)$$

which in original variables is $Q^2 + H^2 = 3r_0^4$. In the zero temperature limit, eq.(2.12), the redshift factor f , eq.(2.9), develops a double zero at the horizon

$$f = 6 \frac{(r - r_{**})^2}{r_{**}^2} + \dots. \quad (2.13)$$

As a result, near the horizon the AdS_4 metric reduces to $AdS_2 \times R^2$ with the curvature radius of AdS_2 given by

$$R_2 = \frac{1}{\sqrt{6}} R. \quad (2.14)$$

This is a very important property of the metric, which simplifies calculations. This metric reduction can be seen explicitly by considering the scaling limit

$$\begin{aligned} r - r_{**} &= \lambda \frac{R_2^2}{\zeta}, \quad t = \frac{\tau}{\lambda}, \\ \lambda &\rightarrow 0 \text{ with } \zeta, \tau \text{ finite,} \end{aligned} \quad (2.15)$$

then the metric eq.(2.2) describes a black hole in $AdS_2 \times R^2$

$$ds^2 = \frac{R_2^2}{\zeta^2} (-d\tau^2 + d\zeta^2) + \frac{r_{**}^2}{R^2} d\vec{x}^2, \quad (2.16)$$

with

$$A_\tau = \frac{g_F}{\sqrt{12}} \frac{r_*^2}{r_{**}^2} \frac{1}{\zeta}, \quad A_x = -\mathcal{H}y. \quad (2.17)$$

Physically, the scaling limit eq.(2.15) with finite τ corresponds to the long time limit of the original time coordinate t , which translates to the low frequency limit of the boundary theory

$$\frac{\omega}{\mu} \rightarrow 0, \quad (2.18)$$

where ω is the frequency conjugate to t . (One can think of λ as being a frequency ω). Near the AdS_4 horizon, we expect that gravity of the AdS_2 region of an extremal dyonic black hole is described by a CFT_1 dual. We refer to [18] for an account of the AdS_2/CFT_1

duality. In what follows we use the horizon of AdS_2 region at $\zeta \rightarrow \infty$ (coefficient in front of $d\tau$ vanishes at the horizon) and the infrared CFT ($IR CFT$) defined at the AdS_2 boundary, $\zeta = 0$. The scaling picture eqs.(2.15),(2.16) suggests that in the low frequency limit, the 2-dimensional boundary theory is described by this $IR CFT$ (which is a CFT_1). The Green function for operator \mathcal{O} in the boundary theory is obtained as a small frequency expansion and by a matching procedure of different regions along radial direction, and is expressed through the Green function of the $IR CFT$ [18].

3. Variational calculations of the pairing gap

In this section we perform variational calculations of the particle-hole pairing gap in the bulk. The logic of calculations is the same as in a field theory, except for arising radial dependence of bulk quantities, e.g. for the gap parameter $\Delta(r)$ as opposed to the BCS with a constant gap. The radial profile is important to keep, since it insures convergence of radial integrals and for different bulk behavior characterizes different systems on the boundary. Our variational calculations in the bulk are possible due to the one-loop formula for an effective action obtained in [16, 17] and expressions for the poles of the fermion Green function obtained in [18].

3.1 Effective action for interacting fermions in a magnetic field

We consider a spinor field ψ in the AdS_4 of charge q and mass m , which is dual to an operator \mathcal{O} in the boundary CFT_3 of charge q and dimension

$$\Delta_\psi = \frac{3}{2} + mR, \quad (3.1)$$

with $mR \geq \frac{1}{2}$ and corresponding to the “stable” CFT . In the black hole geometry, eq.(2.2), the quadratic action for ψ is written as

$$S_0 = i \int d^4x \sqrt{-g} (\bar{\psi} \Gamma^M \mathcal{D}_M \psi - m \bar{\psi} \psi), \quad (3.2)$$

where $\bar{\psi} = \psi^\dagger \Gamma^t$, and

$$\mathcal{D}_M = \partial_M + \frac{1}{4} \omega_{abM} \Gamma^{ab} - iq A_M, \quad (3.3)$$

with ω_{abM} the spin connection, and $\Gamma^{ab} = \frac{1}{2}[\Gamma^a, \Gamma^b]$; here M and a, b denote the bulk space-time and tangent space indices respectively, and μ, ν denote indices along the boundary directions, i.e. $M = (r, \mu)$.

As discussed in the introduction, we can add to S_0 the contact interacting part

$$S_{int} = - \int d^4x \sqrt{-g} G_{int} (\bar{\psi} i \hat{\Gamma}^2 \hat{\Gamma}^5 \psi) (\bar{\psi} i \hat{\Gamma}^2 \hat{\Gamma}^5 \psi), \quad (3.4)$$

where $G_{int} = 1/M_{int}^2$, M_{int} is a mass scale of the interaction. The representation for Γ matrices is given by eq.(A.15), and hat indices on Γ matrices always refer to tangent space indices. In this representation of Γ matrices,

$$i \hat{\Gamma}^2 \hat{\Gamma}^5 = \begin{pmatrix} 1 & 0 \\ 0 & -1 \end{pmatrix}. \quad (3.5)$$

We also have $i\Gamma^2\Gamma^5 = -\Gamma^{\hat{r}}\Gamma^{\hat{t}}\Gamma^{\hat{1}}$. The form of interaction eq.(3.4) is motivated by the form of the projectors eq.(A.37) which decouple ψ into two components.

We add the magnetic Zeeman splitting of the spin degeneracy

$$S_B = \int d^4x \sqrt{-g} q \mathcal{H} \bar{\psi} \Gamma^{\hat{t}} \sigma^3 \psi, \quad (3.6)$$

where σ^3 acts on spin indices. The resulting action is the following sum $S = S_0 + S_{int} + S_B$.

We solve the four-Fermi interaction, S_{int} , in the mean-field approximation by performing standard Hubbard-Stratonovich transformation. We introduce a composite order parameter

$$\Delta = 2G_{int} \langle \bar{\psi} i \Gamma^{\hat{t}} \Gamma^{\hat{5}} \psi \rangle \quad (3.7)$$

and decouple the interaction into a quadratic form

$$S_{int} = \int d^4x \sqrt{-g} \left(\frac{\Delta^2}{4G_{int}} - (\Delta \bar{\psi} i \Gamma^{\hat{t}} \Gamma^{\hat{5}} \psi + h.c.) \right). \quad (3.8)$$

The order parameter Δ is T-odd, i.e. $T(\Gamma^{\hat{0}} i \Gamma^{\hat{t}} \Gamma^{\hat{5}}) T^\dagger = -(\Gamma^{\hat{0}} i \Gamma^{\hat{t}} \Gamma^{\hat{5}})$, with

$$T = C \Gamma^{\hat{5}} = i \begin{pmatrix} 0 & -1 \\ 1 & 0 \end{pmatrix}, \quad C = \begin{pmatrix} -\sigma^2 & 0 \\ 0 & -\sigma^2 \end{pmatrix} \quad (3.9)$$

and charge conjugation is fixed by $C \Gamma^{\hat{t}} = \Gamma^{\hat{r}}$. The exact form of the four-Fermi interaction is not important. With any interaction $G_{int}(\bar{\psi} \Gamma \psi)(\bar{\psi} \Gamma \psi)$ respecting the symmetries, where Γ stands for a collective combination of Gamma matrices, the gap given by eq.(D.4) can be generated. Its effective action is given by $S_{eff} = -i \text{Tr} (\ln G^{-1} + \frac{1}{2}(G_0^{-1} G - 1))$ which satisfies the stationarity condition (or gap equation) $\delta S_{eff} / \delta G = 0$ [1].

To get an effective action for Δ , we integrate out the fermion fields with the result

$$S_{eff} = \int d^4x \sqrt{-g} \left(\frac{|\Delta|^2}{4G_{int}} - \frac{1}{2} \text{Tr} \ln G^{-1} \right), \quad (3.10)$$

where the full fermion propagator $G(x, x') = \langle \psi(x) \bar{\psi}(x') \rangle$ and its inverse is given by

$$G^{-1}(x, x') = \Gamma^M \mathcal{D}_M - m - \Delta i \Gamma^{\hat{t}} \Gamma^{\hat{5}} \pm q \mathcal{H} \Gamma^{\hat{t}}. \quad (3.11)$$

In the one-loop effective action eq.(3.13), the trace and the logarithm are taken in the functional sense. The coordinate $x = \{r, t, \vec{x}\}$ includes the radial r and $(2+1)$ boundary directions $\{t, \vec{x}\}$ in AdS_4 . If we assume translational invariance along boundary directions, then the Fourier transform is given by

$$G(x, x') = T \sum_n \int \frac{d^2k}{(2\pi)^2} G(i\omega_n, k, r, r') e^{-i\omega_n(t-t') + i\vec{k}(\vec{x}-\vec{x}')}, \quad (3.12)$$

where fermionic Matsubara frequency is $\omega_n = (2n+1)\pi T$. We furthermore assume that the condensate is a function of only the radial coordinate in the AdS_4 , $\Delta(r, \omega, k) = \Delta(r)$. The effective action is given by

$$S_{eff} = \frac{V_2}{T} \int dr \sqrt{-g} \left(\frac{|\Delta(r)|^2}{4G_{int}} - \frac{T}{2} \sum_n \int \frac{d^2k}{(2\pi)^2} dr' \text{Tr} \ln G^{-1}(i\omega_n, k, r, r') \right). \quad (3.13)$$

In general, it is a difficult task to calculate one loop effective action in the bulk. Here we will use the method suggested in [16, 17] to calculate the free energy (determinants) in a black hole background as a sum over the quasinormal modes of the black hole. We will also use the recent analytical results [18] for the fermion quasinormal modes.

3.2 Variational calculations of magnetic catalysis in a charged black hole geometry AdS_4

To calculate one-loop fermion action eq.(3.13) we need to know eigenvalues of the Dirac equation eq.(A.42), which can be written symbolically for each mode as [16, 17]

$$M(z, l)\Phi = \lambda(z, l)\Phi \quad (3.14)$$

with $z = i\omega_n$. The zero modes $\lambda(z_*(l), l) = 0$ define as solutions the quasinormal frequencies $z_*(l)$. As was shown in [16, 17], the quasinormal frequencies z_* of a wave equation in a black hole space-time are actually poles in the corresponding retarded Green function in the black hole background, where

$$M(i\omega_n, l)G(i\omega_n, l, r, r') = r^4\delta(r, r'). \quad (3.15)$$

Indeed representing the Green function as a sum over eigenfunctions we have

$$\text{Tr} \frac{1}{M(i\omega_n, l)} = \int_0^{r^+} dr G(i\omega_n, l, r, r), \quad (3.16)$$

which is the usual representation of G . This equation is shown to be true for general complex $z = i\omega_n$ and G satisfies the ingoing boundary condition at $\omega \neq 0$ and regularity at $\omega = 0$ at the horizon [16, 17]. Therefore, as was shown in [16, 17], the fermion determinant given by a sum over the quasinormal frequencies of the black hole, i.e. when $M(z, l)$ has a zero eigenvalue, is equivalent to the sum over the poles of the analytically continued to complex frequencies fermion Green function with ingoing boundary conditions at the horizon. This method is also used in color superconductivity [19].

Analytic results have been obtained for the Green function in the AdS_4 [18]. (Numerically it has been obtained in [20].) A general form for the retarded Green function is given by [18, 21, 22]

$$G_R(\omega, k) = \frac{B_+ + B_- G^{IR}(\omega)}{A_+ + A_- G^{IR}(\omega, k)}, \quad (3.17)$$

where the ratio of numerator to denominator comes from expansion of the solution of Dirac equation at the boundary $r \rightarrow \infty$, therefore the ratio B/A is the AdS_4 retarded Green function, G_R . The coefficients A_\pm, B_\pm are expansions (rows) in small frequency ω . The low-frequency limit is equivalent to the expansion near the horizon at small ω , where metric reduces to $AdS_4 \rightarrow AdS_2 \times R^2$. Therefore A_+ (B_+) and A_- (B_-) components arise from expansion (and matching procedure) near the AdS_2 boundary, that relates ratio A_+/A_- (B_+/B_-) via the IR Green function G^{IR} obtained in the $AdS_2 \times R^2$ calculation. Non-analytical frequency behavior of G is controlled by the IR CFT, G^{IR} , while coefficients A_\pm and B_\pm carry the UV information. In section 4, we find the coefficients A_\pm, B_\pm to the leading order in frequency, that requires solution of the Dirac equation in the AdS_4 .

It was found in [20] and [18], that the fermion Green function develops a sharp pick indicating the existence of the Fermi surface and quasiparticle poles. Expansion of the Green function near the Fermi surface is given by [18]

$$\begin{aligned} G_R(\omega, k) &= \frac{(-h_1 v_F)}{\omega - v_F k_\perp + \Sigma(\omega, k_F)}, \\ \Sigma(\omega, k_F) &= h v_F G^{IR}(\omega, k_F) = h v_F c(k_F) \omega^{2\nu_{k_F}}, \end{aligned} \quad (3.18)$$

where we keep notations for constants introduced in [18]. Here $k_\perp = k - k_F$, h_1, h, v_F are governed by the UV physics, and were obtained numerically in [18] and here in section 4. Eq.(4.17) gives the rough structure for the boundary Green function. Further, in section 4, we use a more detailed description for G_R . As $T \rightarrow 0$, $\Sigma(\omega, k_F) \rightarrow \omega^{2\nu_{k_F}}$, therefore at zero temperature there is no dependence on Δ coming from G^{IR} . We are interested in the poles of G_R at zero temperature. In this section UV constants will not be important. There are three characteristic regimes depending on the ν_{k_F} , the low energy ($\omega \ll \mu$) scaling dimension of the dual fermionic operator. The poles of the Green function are located in the lower half complex plane at

$$\omega_c(k) = \omega_*(k) - i\Gamma(k). \quad (3.19)$$

For the three regimes we have the following [18], [22]

- For (quasi-) Fermi liquid, $\nu_{k_F} > \frac{1}{2}$,

$$\omega_*(k) = v_F(k - k_F) + \dots, \quad \frac{\Gamma(k)}{\omega_*(k)} \sim (k - k_F)^{2\nu_{k_F} - 1} \rightarrow 0, \quad (3.20)$$

and the residue of the pole is $Z = h_1 v_F$. The pole represents a stable quasiparticle as one approaches the Fermi surface, with linear dispersion relation and v_F being the Fermi velocity, vanishing decay width and a non-vanishing spectral weight Z at the Fermi surface.

- For non-Fermi liquid, $\nu_{k_F} < \frac{1}{2}$,

$$\omega_*(k) = (k - k_F)^{\frac{1}{2\nu_{k_F}}}, \quad \frac{\Gamma(k)}{\omega_*(k)} = \text{const}, \quad (3.21)$$

and the residue of the pole is $Z \sim (k - k_F)^{\frac{1-2\nu_{k_F}}{2\nu_{k_F}}} \rightarrow 0$. The pole represents an unstable quasiparticle as one approaches the Fermi surface, with exponent in dispersion relation greater than one, the imaginary part is comparable to the real part of the pole, and a vanishing spectral weight Z at the Fermi surface. Non-Fermi liquid is example of a Fermi surface without sharp quasiparticle picks.

- For marginal Fermi liquid, $\nu_{k_F} = \frac{1}{2}$,

$$\Sigma(\omega) \approx \tilde{c}_1 \omega \log \omega + i d_1 \omega, \quad \frac{d_1}{\tilde{c}_1} = -\frac{\pi}{1 + e^{-\frac{2\pi q}{\sqrt{12}}}}, \quad (3.22)$$

where $\tilde{c}_1 < 0$ and d_1 are real constants. The single-particle scattering rate is linear in ω , while it is still suppressed compared to the real part as the Fermi surface is approached, but

the suppression is only logarithmic. The quasiparticle residue also vanishes logarithmically at the Fermi surface. We use this summary on quasiparticle poles below.

Following [16, 17], we represent the fermion determinant in an effective action eq.(3.13) as a sum over poles of the retarded Green function in the black hole background. We obtain an analog to eq.(C.9) of one-loop action

$$S_{eff} = \frac{V_2}{T} \left(\int dr \sqrt{-g} \frac{|\Delta(r)|^2}{4G_{int}} + \frac{T|q\mathcal{H}|}{2\pi} \sum_{z_*[\Delta(r)]} \ln \left(\frac{1}{2\pi} \left| \Gamma \left(\frac{iz_*[\Delta(r)]}{2\pi T} + \frac{1}{2} \right) \right|^2 \right) \right), \quad (3.23)$$

where $z_*[\Delta(r)]$ is a functional of the order parameter $\Delta(r)$, V_2 is the boundary spatial volume. In order to make a connection with the field theory eq.(C.9), the following equations has been used for the complex frequency z_*

$$\left| \Gamma \left(\frac{1}{2} + iz \right) \right|^2 = \frac{\pi}{\cosh(\pi z)}. \quad (3.24)$$

It was shown in [17], that it holds for a complex z by matching poles and zeros of the two meromorphic functions. Here $|\Gamma(\frac{1}{2} + iz)|^2 = \Gamma(\frac{1}{2} + iz)\Gamma(\frac{1}{2} - iz)$. We will consider the zero temperature limit, therefore as explained in [16], the sum in eq.(3.23) is saturated by one pole eq.(3.19),

$$z_*[\Delta(r)] = \omega_*[\Delta(r)] - i\Gamma[\Delta(r)], \quad (3.25)$$

where the real and imaginary parts of the dispersion are functionals of the order parameter $\Delta(r)$. As was shown in [17], equation (3.23) for the fermion determinant captures only the singular contributions incorporated by the closest to $\omega = 0$ pole eq.(3.19), and smooth analytic terms are not important.

We take the functional derivative,

$$\delta S_{eff} = \frac{V_2}{T} \int dr \sqrt{-g} \left(\frac{2\Delta(r)}{4G_{int}} + \frac{T|q\mathcal{H}|}{2\pi} \frac{\delta}{\delta\Delta(r)} \ln \left(\frac{1}{2\pi} \left| \Gamma \left(\frac{iz_*[\Delta(r)]}{2\pi T} + \frac{1}{2} \right) \right|^2 \right) \right) \delta\Delta(r), \quad (3.26)$$

with $\frac{\delta\Delta(r')}{\delta\Delta(r)} = \delta(r - r')$ and therefore the dimension of the functional derivative $\frac{\delta}{\delta\Delta(r)}$ is $\frac{1}{[r\Delta]}$. For the gap equation, $\frac{\delta S_{eff}}{\delta\Delta(r)} = 0$, we have

$$\Delta(r) = \frac{G_{int}|q\mathcal{H}|}{\pi} \frac{1}{\pi} \left(\frac{\delta\omega_*[\Delta(r)]}{\delta\Delta(r)} \text{Im}\Psi \left(\frac{iz_*[\Delta(r)]}{2\pi T} + \frac{1}{2} \right) - \frac{\delta\Gamma[\Delta(r)]}{\delta\Delta(r)} \text{Re}\Psi \left(\frac{iz_*[\Delta(r)]}{2\pi T} + \frac{1}{2} \right) \right), \quad (3.27)$$

where Ψ is the digamma function, $\Psi(x) = \frac{d \ln \Gamma(x)}{dx}$.

In the zero temperature limit, $T \sim 0$, we have

$$\Delta(r) = \frac{G_{int}|q\mathcal{H}|}{\pi} \frac{1}{\pi} \left(\frac{\delta\omega_*[\Delta(r)]}{\delta\Delta(r)} \left(\frac{\pi}{2} - \arctan \frac{\Gamma[\Delta(r)]}{\omega_*[\Delta(r)]} \right) + \frac{\delta\Gamma[\Delta(r)]}{\delta\Delta(r)} \ln \frac{2\pi T}{\sqrt{\omega_*[\Delta(r)]^2 + \Gamma[\Delta(r)]^2}} \right). \quad (3.28)$$

Generally, it is difficult to find the dependence for the pole $z_*[\Delta(r)]$ [21]. However, here we have simplifications. First, the order parameter enters the Dirac equation essentially

as a mass term on the diagonal, i.e. it does not mix ψ^\dagger and ψ as a superconducting gap does. Therefore in the pole of the Green function eq.(4.17), the frequency is not affected, and there is only a shift in the Fermi momentum k_F . Second, we can consider the order parameter Δ to be small. The procedure of finding the Fermi momentum is reduced to finding the bound state of the Schrodinger equation with zero energy [18] or to finding a solution to the Dirac equation which is normalizable at the boundary [14]. Since the order parameter contributes to the potential term in the Dirac equation, the shift in k_F is given by the first order perturbative correction

$$k_F \rightarrow k_F \pm \delta k_F[\Delta(r)],$$

$$\delta k_F[\Delta(r)] = \frac{bh_1}{v_F R^3} \int dr \sqrt{-g} \psi^0(r)^\dagger \sigma^1 \psi^0(r) \Delta(r), \quad (3.29)$$

where the zero modes ψ^0 are solutions of the (free, without Δ) Dirac equation with $\omega = 0$ and $k = k_F$ introduced in the next section, the signs \pm refer to components F_1/F_2 of the Dirac equation (A.42), b is a dimensionless constant which has to be determined from the equation for the Fermi momentum k_F in the presence of the gap Δ . Note that $\Gamma^{\hat{t}} = \text{diag}(i\sigma^1, i\sigma^1)$. The unperturbed Fermi momentum is $k_F = \sqrt{q^2 \mu^2 - m^2}$ and R is the *AdS* radius. In eqs.(3.20)-(3.22), the following substitution should be made $k \rightarrow \sqrt{2|q\mathcal{H}l}$ (this substitution in the pole was shown to be true in [16] based on scaling arguments, see also Appendix A.1). Introducing magnetic field lowers the Fermi energy. For large magnetic field the lowest Landau level $l = 0$ dominates and higher Landau levels are not important, while for small magnetic field all Landau levels should be included in the sum to correctly reproduce the limit of zero magnetic field. Following [16], we tune magnetic field to the point when $k \sim k_F$, and once the pole crosses the Fermi surface it is counted in the fermion determinant of the effective action.

For the Fermi liquid, $\nu_{k_F} > \frac{1}{2}$,

$$\omega_*[\Delta(r)] = v_F \delta k_F[\Delta(r)], \quad \Gamma[\Delta(r)] \sim (\delta k_F[\Delta(r)])^{2\nu_{k_F}}. \quad (3.30)$$

Near the Fermi surface we have for small $\Delta \sim 0$

$$\frac{\delta \omega_*[\Delta(r)]}{\delta \Delta(r)} \sim \frac{h_1 v_F^3}{R^3} \psi^0(r)^\dagger \sigma^1 \psi^0(r), \quad \frac{\delta \Gamma[\Delta(r)]}{\delta \Delta(r)} \sim \frac{\psi^0(r)^\dagger \sigma^1 \psi^0(r)}{R^4} (\delta k_F[\Delta(r)])^{2\nu_{k_F}-1} \rightarrow 0,$$

$$\frac{\Gamma[\Delta(r)]}{\omega_*[\Delta(r)]} \sim (\delta k_F[\Delta(r)])^{2\nu_{k_F}-1} \rightarrow 0. \quad (3.31)$$

Therefore at $T = 0$, the gap equation gives the following solution

$$\Delta(r) = \frac{G_{int} |q\mathcal{H}| b h_1 v_F^3}{2\pi R^3} \psi^0(r)^\dagger \sigma^1 \psi^0(r), \quad (3.32)$$

where $G_{int} = \frac{1}{M_F^2}$, and b is a dimensionless constant. The difference in factor 2 with the $(2+1)$ -dimensional case eq.(C.12) is due to taking one pole eq.(3.19) instead of two poles in the field theory, which does not affect our conclusions. Eq.(3.32) contains the radial profile of the order parameter, $\psi^0(r)^\dagger \sigma^1 \psi^0(r)$ shown in Fig.(2). The prefactor in eq.(3.32)

contains information about the magnetic catalysis for the lowest Landau level at $T = 0$. At zero temperature, the only solution is a nonzero gap which is proportional to the magnetic field and a radius of the four-Fermi interaction $\Delta \sim \frac{1}{M_F} |q\mathcal{H}|$. For a finite T , from eq.(3.27), there exist also a trivial solution $\Delta = 0$, and a critical temperature T_c separates the phases with zero and nonzero gaps. This is in complete analogy with a $(2 + 1)$ field theory case [1]. We consider the regime around T_c and the corresponding phase transition in the next section.

For the non-Fermi liquid, $\nu_{k_F} < \frac{1}{2}$,

$$\omega_*[\Delta(r)] \sim \Gamma[\Delta(r)] \sim (\delta k_F[\Delta(r)])^{\frac{1}{2\nu_{k_F}}}. \quad (3.33)$$

Near the Fermi surface we have for small $\Delta \sim 0$

$$\frac{\delta\omega_*[\Delta(r)]}{\delta\Delta(r)} \sim \frac{\delta\Gamma[\Delta(r)]}{\delta\Delta(r)} \sim (\delta k_F[\Delta(r)])^{\frac{1}{2\nu_{k_F}} - 1} \rightarrow 0, \quad (3.34)$$

zeros for both term in the gap equation mean that there is no instability. Therefore in this case

$$\Delta(r) = 0, \quad (3.35)$$

i.e. no gap is generated in a magnetic field. Thus, for Fermi liquids, particle-hole pairing $\bar{\psi}\Gamma\psi$, is favorable in the magnetic field, while non-Fermi liquids do not support the pairing. The same conclusion has been reached for the case of the superconducting pairing $\langle \psi\Gamma\psi \rangle$ where Γ contains Γ^5 in [14]. There, it was suggested that taking the long-range four-Fermi interaction may generate the instability for non-Fermi liquids. On a technical ground, the momentum/frequency dependent four-Fermi interaction will change a simple shift in the Fermi momentum eq.(3.29), so that the derivatives of the real and/or imaginary parts of the pole will not vanish.

4. Pairing instability in the Ginsburg-Landau formalism

In this section we consider the pairing particle-hole instability using Ginsburg-Landau approach in the bulk. Our calculation closely follows the leading order (one loop) Ginsburg-Landau procedure, with the only difference of using bulk fermion propagators. The prescription to construct propagators and vertices on the gravity side is given in [14], [22].

4.1 Microscopic calculations of magnetic catalysis. Ginsburg-Landau in a holographic approach

In the mean field approximation, the four-Fermi (contact) interaction $\bar{\psi}(x)\Gamma\psi(x)\bar{\psi}(x)\Gamma\psi(x)$ gives the following bilinear terms

$$\bar{\psi}\Gamma\psi\Delta + \bar{\psi}\bar{\Gamma}\psi\Delta^\dagger, \quad (4.1)$$

where the second term is hermitian conjugate to the first one and $\bar{\Gamma} = \Gamma^{\hat{t}}\Gamma^\dagger\Gamma^{\hat{t}}$, and the order parameter

$$\Delta = G_{int}\langle\bar{\psi}\Gamma\psi\rangle \quad (4.2)$$

is a singlet (number) in spin space. Here $\Gamma = i\Gamma^2\Gamma^5$. The one-loop (Euclidean) action is given to the second order in Δ

$$S^{(2)} = \int d^4x \sqrt{g} \frac{|\Delta|^2}{4G_{int}} - 2 \int d^4x d^4x' \text{tr} \mathcal{G}(x', x) \Gamma \Delta(x) \mathcal{G}(x, x') \bar{\Gamma} \Delta(x')^\dagger, \quad (4.3)$$

where the Euclidean non-interacting Green function in the bulk is $\mathcal{G}(x, x') = -\langle \psi(x) \bar{\psi}(x') \rangle$. Assuming translational invariance along the spacetime $\{\tau, \vec{x}\}$, we perform the Fourier transform

$$\mathcal{G}(x, x') = T \sum_n \int \frac{d^2k}{(2\pi)^2} \mathcal{G}(r, r', i\omega_n, \vec{k}) e^{-i\omega_n(\tau-\tau') + i\vec{k}(\vec{x}-\vec{x}')}, \quad (4.4)$$

where the radial coordinate is r and the boundary directions are $\{\tau, \vec{x}\}$; the fermionic Matsubara frequencies are $\omega_n = \pi T(2n+1)$. We assume that the gap depends only on the radial direction, $\Delta = \Delta(u)$. The one-loop effective action is given by

$$S^{(2)} = \frac{V_2}{T} \int dr \sqrt{g(r)} \left(\frac{|\Delta|^2}{4G_{int}} + \int dr' \sqrt{g(r')} \Delta(r) \Delta(r')^* F(r, r') \right) \\ F(r, r') = -2T \sum_n \int \frac{d^2k}{(2\pi)^2} \text{tr} \mathcal{G}(r', r, i\omega_n, \vec{k}) \Gamma \mathcal{G}(r, r', -i\omega_n, -\vec{k}) \bar{\Gamma}. \quad (4.5)$$

We make analytic continuation of the Euclidean Green function into the lower (upper) half plane in imaginary frequency plane, and use the following expressions relating Euclidean and retarded (advanced) Green functions [14]

$$\mathcal{G}(z) \mathcal{G}(-z) = \mathcal{G}^R(z) \mathcal{G}^A(-z) \\ \mathcal{G}^A(r, r') = -\mathcal{G}^R(r, r')^*, \quad (4.6)$$

where $z = i\omega_n$, in order to rewrite the action in terms of retarded (advanced) Green functions

$$F(r, r') = i \int \frac{d^2k}{(2\pi)^2} \int_{-\infty}^{\infty} \frac{d\Omega}{\pi} \tanh \frac{\Omega}{2T} \text{tr} \mathcal{G}^R(r', r, \Omega, \vec{k})^* \Gamma \mathcal{G}^R(r, r', -\Omega, -\vec{k}) \bar{\Gamma}, \quad (4.7)$$

where we substituted the Matsubara sum by the contour integral, $i\omega_n \rightarrow z$, and Ω is on the real axis of z . In order to calculate this integral, we express the bulk Green function through the boundary one as given in [14]. The bulk Green function is a solution of the free Dirac equation, eq.(A.32),

$$D(\Omega, k) \mathcal{G}^R(r, r', \Omega, k) = \frac{1}{\sqrt{-g}} i \delta(r, r'), \quad (4.8)$$

with the free radial Dirac operator $D(\Omega, k)$, which includes the mass term and the magnetic field but has zero gap, $\Delta = 0$. The bulk Green function is constructed through the modes $\psi(r)$, $\bar{\psi} = e^{-i\Omega t + i\vec{k}x} \psi(r)$, which are solutions of the free Dirac equation eq.(A.32)

$$D(\Omega, k) \psi_{radial}(r) = 0. \quad (4.9)$$

Due to the choice of the Gamma matrices, eq.(A.15), ψ decouples into two-component spinors, $\psi = (\psi_1, \psi_2)^T$, which are eigenfunctions with definite eigenvalue of $\Gamma^{\hat{r}}\Gamma^{\hat{t}}\Gamma^{\hat{1}}$. Therefore the bulk retarded Green function has the block-diagonal form, eq.(A.40), where the components \mathcal{G}_α , $\alpha = 1, 2$, are constructed from the solutions of the Dirac equation as [14]

$$\mathcal{G}_\alpha^R(r, r') = \frac{G_\alpha(\Omega, k)}{R^3} \times \begin{cases} -\psi_\alpha^{bdy}(r)\tilde{\psi}_\alpha^{in}(r') & r > r' \\ -\psi_\alpha^{in}(r)\tilde{\psi}_\alpha^{bdy}(r') & r < r' \end{cases}, \quad (4.10)$$

with $\tilde{\psi}_\alpha = i\psi_\alpha^T\sigma^1$. Note that $\Gamma^{\hat{0}} \equiv \Gamma^{\hat{t}} = \text{diag}(i\sigma^1, i\sigma^1)$ and the dimension of ψ is $[\psi] \sim L^{3/2}$; the minus sign comes from the definition of the bulk Green function $\mathcal{G} = -\langle \psi\bar{\psi} \rangle$. Here the prefactor arises from the Wronskian [14], and includes the retarded Green function of the boundary field theory (later we refer to it as the boundary Green function). Since the Wronskian is a constant related to the conserved charge current, it is simpler to calculate it at the conformal boundary [14] with the result given by eq.(4.10).

There is the following reasoning behind construction of the bulk Green function in eq.(4.10). At the boundary, $r, r' \rightarrow \infty$, the behavior is given by two terms (we omit prefactors)

$$G \sim r^{\Delta_\psi-d} + r^{-\Delta_\psi}, \quad (4.11)$$

and we put to zero the non-normalizable part $\sim r^{\Delta_\psi-d}$, and leave the normalizable part $\sim r^{-\Delta_\psi}$. At the horizon, $r, r' \rightarrow r_0$, there are two terms

$$G \sim e^{-ikr_0} + e^{ikr_0}, \quad (4.12)$$

where we throw away the outgoing solution e^{-ikr_0} , and leave the ingoing one e^{ikr_0} . In this way we obtain the retarded Green function. Note that $e^{\pm ikr_0} \sim (r - r_0)^{\pm i\omega/T}$ with the Lorentzian signature. In the Euclidean space, this means that when the behavior of the Green function is fixed at the horizon, $r, r' \rightarrow r_0$ as $G \sim (r - r_0)^{\pm\omega/T}$, then the retarded Green function has asymptotics $G_R \sim (r - r_0)^{\omega/T}$, with $\omega > 0$ (and corresponds to the ingoing solution), and the advanced Green function has asymptotics $G_A \sim (r - r_0)^{-\omega/T}$, with $\omega < 0$ (and corresponds to the outgoing solution).

The boundary conditions are fixed as follows for the solutions of the Dirac equation. The (free) solution of the Dirac equation has the following behavior near the boundary, $r \rightarrow \infty$, eq.(A.39) with $\Delta = 0$,

$$\psi_\alpha \sim a_\alpha r^{mR} \begin{pmatrix} 0 \\ 1 \end{pmatrix} + b_\alpha r^{-mR} \begin{pmatrix} 1 \\ 0 \end{pmatrix}. \quad (4.13)$$

The two spinors $(1, 0)$ and $(0, 1)$ are eigenstates of $\Gamma^{\hat{r}}$ with opposite eigenvalues, implying that a_α and b_α are canonically conjugate (in a radial Hamiltonian slicing) [23]. Therefore a boundary condition must be imposed on one, with the other allowed to fluctuate. For $mR > \frac{1}{2}$, we choose the fluctuating piece to be the normalizable mode at the boundary (with regular behavior) proportional to $(1, 0)$. This gives us the solution ψ^{bdy} . More generally, the quantization choice for $mR > \frac{1}{2}$ is to impose the boundary condition $a_\alpha = 0$ on the fluctuating mode. Another quantization choice for $mR > \frac{1}{2}$ is discussed in [23, 18]. For the

solution ψ^{in} we impose ingoing boundary conditions at the horizon, $r = r_0$. Thus, there are two normalizable solutions with the following behavior at the conformal boundary $r \rightarrow \infty$

$$\begin{aligned}\psi_\alpha^{bdy} &= r^{-mR} \begin{pmatrix} 1 \\ 0 \end{pmatrix} \\ \psi_\alpha^{in} &= \frac{1}{G_\alpha} r^{mR} \begin{pmatrix} 0 \\ 1 \end{pmatrix} + r^{-mR} \begin{pmatrix} 1 \\ 0 \end{pmatrix},\end{aligned}\quad (4.14)$$

where the boundary Green function G_α was introduced in ψ_α^{in} following its definition being proportional to b_α/a_α in the ingoing solution. Using representation eq.(4.10), we can show that $\mathcal{G}^R(r, r', \Omega, \vec{k})^* = -\mathcal{G}^A(r, r', \Omega, \vec{k})$, since $\psi^{bdy*} = \psi^{bdy}$ and $\psi^{in*} = \psi^{out}$. Also $\mathcal{G}^A(r, r', \Omega, \vec{k}) = \Gamma^{\hat{t}} \mathcal{G}^R(r', r, \Omega, \vec{k})^\dagger \Gamma^{\hat{t}}$, since $i\sigma^1 \mathcal{G}_\alpha^R(r', r, \Omega, \vec{k})^\dagger i\sigma^1 = -\mathcal{G}_\alpha^R(r, r', \Omega, \vec{k})^*$. Therefore we can rewrite the kernel eq.(4.7) in equivalent form

$$F(r, r') = -i \int \frac{d^2k}{(2\pi)^2} \int_{-\infty}^{\infty} \frac{d\Omega}{\pi} \tanh \frac{\Omega}{2T} \text{tr} \Gamma^{\hat{t}} \mathcal{G}^R(r, r', \Omega, \vec{k})^\dagger \Gamma^{\hat{t}} \Gamma \mathcal{G}^R(r, r', -\Omega, -\vec{k}) \bar{\Gamma}. \quad (4.15)$$

Using the relation eq.(4.10), we obtain

$$\begin{aligned}F(r, r') &= \frac{i}{R^6} \int \frac{d^2k}{(2\pi)^2} \int_{-\infty}^{\infty} \frac{d\Omega}{\pi} \tanh \frac{\Omega}{2T} G_1(\Omega, \vec{k})^* G_1(-\Omega, -\vec{k}) \times \\ &\quad \begin{cases} \psi_2^{in}(r', \Omega, \vec{k})^\dagger \sigma^1 \psi_2^{in}(r', -\Omega, -\vec{k}) \psi_1^{bdy}(r, \Omega, \vec{k})^\dagger \sigma^1 \psi_1^{bdy}(r, -\Omega, -\vec{k}), & r > r' \\ \psi_2^{bdy}(r', \Omega, \vec{k})^\dagger \sigma^1 \psi_2^{bdy}(r', -\Omega, -\vec{k}) \psi_1^{in}(r, \Omega, \vec{k})^\dagger \sigma^1 \psi_1^{in}(r, -\Omega, -\vec{k}), & r < r' \end{cases} \\ &\quad + (1 \leftrightarrow 2),\end{aligned}\quad (4.16)$$

where we used $\psi_\alpha^{in}(-\Omega) = \psi_\alpha^{out}$ and $\psi_\alpha^{in}(\Omega)^* = \psi_\alpha^{out}(\Omega)$ which follows from the definition of in(out)going solution, the solution ψ^{bdy} is real, and $\psi_1(-\vec{k}) = \psi_2(\vec{k})$ which follows from the symmetry of the Dirac equation [20]; we omitted other arguments by ψ 's.

All quantities in eq.(4.16) can be obtained numerical. However, at low temperatures $T \ll \mu$, calculations can be done analytically, due to the fact that the main contribution comes from the pole in a retarded Green function describing the Fermi surface, i.e., the closest to the origin pole $\omega_* \sim 0$ as $k \sim k_F$. The same argument that physics occurs close to the Fermi surface in the bulk was used in [16] describing phenomena in magnetic field and for the BCS theory in a holographic approach by [14]. This repeats the reasoning of the field theory, as in the BCS theory. Close to the Fermi surface and at low temperatures, i.e. at $T \ll \Omega \ll \mu$, the boundary Green function, $G \equiv G_1$, to the leading order is given by [18]

$$G(\Omega, k) = \frac{(-h_1 v_F)}{\Omega - v_F k_\perp - h_2 v_F e^{i\theta - i\pi\nu} \Omega^{2\nu}}, \quad (4.17)$$

where $k_\perp = k - k_F$ is the perpendicular distance of the momentum from the Fermi surface, h_1 and v_f are real constants and are calculated below, h_2 is positive and the phase θ is such that poles of the Green function are in the lower half complex frequency plane, ν is the zero temperature conformal dimension at the Fermi momentum, $\nu \equiv \nu_{k_F}$, given by eq.(A.46) with $\Delta = 0$.

We perform the momentum and frequency integrals in eq.(4.16). We make the same assumption as in [16] and as in our variational calculations. We consider only contributions near the Fermi momentum $k \sim k_F$ (see discussion after eq.(3.29)). Therefore, in the leading order, there is no momentum dependence in the boundary Green functions, and the momentum integral d^2k is trivially performed, which gives in the magnetic field a factor $|q\mathcal{H}|$. In the frequency integral, for $T \ll \Omega$, we substitute $\tanh \frac{\Omega}{2T} \rightarrow 1$, and we have

$$F(r, r') = \frac{1}{R^6} \text{Re} \int_0^\infty \frac{d\Omega}{\pi^2} \frac{h_1}{-\Omega/v_F + h_2 e^{-i\theta + i\pi\nu\Omega/2\nu}} \frac{h_1}{\Omega/v_F + h_2 e^{i\theta + i\pi\nu\Omega/2\nu}} \times \begin{cases} \psi_2^{in}(r', \Omega)^\dagger \sigma^1 \psi_2^{in}(r', -\Omega) \psi_1^{bdy}(r, \Omega)^\dagger \sigma^1 \psi_1^{bdy}(r, -\Omega) & r > r' \\ \psi_2^{bdy}(r', \Omega)^\dagger \sigma^1 \psi_2^{bdy}(r', -\Omega) \psi_1^{in}(r, \Omega)^\dagger \sigma^1 \psi_1^{in}(r, -\Omega) & r < r' \end{cases}, \quad (4.18)$$

where the wave functions are evaluated at the Fermi momentum. In the frequency integral, depending on the critical exponent ν either the first or the second term in each denominator dominates. To make this comparison, note that h_2 has a dimension, i.e. $h_2 \sim \mu^{1-2\nu}$. At small frequencies $\Omega \ll \mu$, for $\nu > \frac{1}{2}$ the first term $\sim \Omega$ dominates, while for $\nu < \frac{1}{2}$ the second term $\sim \mu \left(\frac{\Omega}{\mu}\right)^{2\nu}$ dominates, as also shown in [18]. As discussed in [14], the range $T \ll \Omega \ll \mu$ implies that the fermion wavefunctions should be evaluated at $\Omega = 0$ and $k = k_F$ in the extremal $T = 0$ black hole background. This means, they are exactly zero modes at the Fermi surface, $\psi^{bdy} = \psi^{in} = \psi^0$, which will be calculated below.

For $\nu > \frac{1}{2}$, the leading behavior of eq.(4.18) at small temperatures $T \ll \mu$ is

$$F(r, r') = -\frac{|q\mathcal{H}|h_1^2 v_F^3}{2\pi^2 R^6} \frac{1}{T} \psi^0(r)^\dagger \sigma^1 \psi^0(r) \psi^0(r')^\dagger \sigma^1 \psi^0(r'), \quad (4.19)$$

where ψ^0 is the $T = 0$ fermion zero mode at the fermi surface.

For $\nu < \frac{1}{2}$, the leading behavior of eq.(4.18) at small temperatures $T \ll \mu$ is

$$F(r, r') = -\frac{|q\mathcal{H}|h_1^2 v_F}{2\pi^2 h_2^2 R^6} \cos(2\pi\nu) \frac{\mu^{1-4\nu} - T^{1-4\nu}}{1 - 4\nu} \psi^0(r)^\dagger \sigma^1 \psi^0(r) \psi^0(r')^\dagger \sigma^1 \psi^0(r'), \quad (4.20)$$

that for $\nu < \frac{1}{4}$ becomes to the leading order in expansion T/μ temperature independent

$$F(r, r') = -\frac{|q\mathcal{H}|h_1^2 v_F}{2\pi^2 h_2^2 R^6} \cos(2\pi\nu) \frac{\mu^{1-4\nu}}{1 - 4\nu} \psi^0(r)^\dagger \sigma^1 \psi^0(r) \psi^0(r')^\dagger \sigma^1 \psi^0(r'), \quad (4.21)$$

and for $\frac{1}{4} < \nu < \frac{1}{2}$ has a wrong sign for the kernel F to give a nontrivial solution of the gap equation. This means that there is no instability in particle-antiparticle pairing for $\nu < \frac{1}{2}$. We observed this already before in variational calculations, where non-Fermi liquids did not support $\psi\bar{\psi}$ -pairing while the Fermi liquids did, see eqs.(3.32) and (3.35).

For the Fermi liquids, we obtain the equation for the critical temperature from the effective action eq.(4.5)

$$\frac{\Delta(r)}{2G_{int}} + \int dr' \sqrt{-g(r')} \Delta(r') F(r', r) = 0, \quad (4.22)$$

which is an analog of the gap equation but with free propagators (Green functions). As in [14], we use the factorisation of $F(r, r')$ to write an ansatz for the gap function

$$\Delta^0(r) \sim \psi^0(r)^\dagger \sigma^1 \psi^0(r). \quad (4.23)$$

Using this ansatz back in the equation, we get the following critical temperature for $\nu > \frac{1}{2}$

$$T_c = \frac{G_{int} |q\mathcal{H}| h_1^2 v_F^3}{\pi^2 R^6} \int dr \sqrt{-g(r)} (\psi^0(r)^\dagger \sigma^1 \psi^0(r))^2. \quad (4.24)$$

The radial form of the gap function eq.(4.23) was obtained by variational calculations in eq.(3.32). Eq.(3.32) can be considered as a one loop mass gap equation (self-energy correction) with a four-Fermi vertex G_{int} and the bulk fermion propagator $\mathcal{G}^R(r, r')$ given by eq.(4.10) and modified as in eq.(3.29) to include the gap. The mass gap equation reads $\Delta(r) \sim G_{int} \int \frac{d^2 k}{(2\pi)^2} \int d\omega \mathcal{G}(\omega, \vec{k}, r, r)$, where integration gives $\sim |q\mathcal{H}| h_1 v_F$ and the resulting gap as in eq.(3.32). Substituting eq.(3.32) in eq.(3.29) for δk_F , we have

$$\begin{aligned} T_c &\sim v_F \delta k_F \sim \frac{G_{int} v_F^3}{R^3} N_{eff}, \\ N_{eff} &\sim \frac{|q\mathcal{H}| h_1^2}{R^3} \int dr \sqrt{-g(r)} (\psi^0(r)^\dagger \sigma^1 \psi^0(r))^2, \end{aligned} \quad (4.25)$$

where N_{eff} is the effective density of states at the Fermi surface.

In the next section we calculate the constants h_1 and v_F for the different fermion charges q , and find the zero mode wave function $\psi^0(r)$. We follow procedure outlined in [14]. We then find the critical temperature T_c as a function of the charge q and the magnetic field.

4.2 Solving for the zero modes and finding the critical temperature

In this section we follow the procedure of [14]. We solve the Dirac equation for the zero mode in black hole background, that amounts to finding a solution at zero frequencies $\omega = 0$ (we use here $\omega \equiv \Omega$) in the $T = 0$ background. We will also set mass $m = 0$. As was shown in [14], analytic solution can be found in this case. The Dirac equation in the magnetic field

$$\mathcal{D}_M \psi = 0, \quad (4.26)$$

where $\mathcal{D}_M = \partial_M + \frac{1}{4} \omega_{abM} \Gamma^{ab} - iqA_M$ is defined in Appendix A.1. The Dirac equation can be written explicitly including the spin connection as

$$\begin{aligned} &\left(-\frac{\sqrt{g_{ii}}}{\sqrt{g_{rr}}} \sigma^1 \partial_r + \sqrt{g_{ii}} i \sigma^2 m - \frac{\sqrt{g_{ii}}}{\sqrt{-g_{tt}}} \sigma^3 (\omega + qA_t) + \frac{\sqrt{g_{ii}}}{\sqrt{-g_{tt}}} \sigma^1 \frac{1}{2} \omega_{\hat{r}\hat{t}} \right. \\ &\quad \left. - \sigma^1 \frac{1}{2} \omega_{\hat{x}\hat{r}\hat{x}} - \sigma^1 \frac{1}{2} \omega_{\hat{y}\hat{r}\hat{y}} - \lambda \right) \otimes 1 \begin{pmatrix} \psi_1 \\ \psi_2 \end{pmatrix} = 0, \end{aligned} \quad (4.27)$$

where $\lambda \rightarrow \sqrt{2|q\mathcal{H}|l}$ is the eigenvalue for the Landau levels which takes into account $\{x, y\}$ -plane physics in the magnetic field (Appendix A), and $\psi = (\psi_1, \psi_2)^T$, and the Γ matrices

are given by eq.(A.15). In the basis eq.(A.15) the two components decouple, therefore below we solve for the first component. Substituting the spin connection we have

$$\left(-\frac{r^2\sqrt{f}}{R^2}\sigma^1\partial_r + \frac{r}{R}i\sigma^2m - \frac{1}{\sqrt{f}}\sigma^3(\omega + qA_t) - \sigma^1\frac{r\sqrt{f}}{2R^2}\left(3 + \frac{rf'}{2f}\right) - \lambda\right)F = 0, \quad (4.28)$$

with $F = (y_1, y_2)$. As in the AdS_2 , it is convenient to change the basis eq.(B.14)

$$\begin{pmatrix} \tilde{y}_1 \\ \tilde{y}_2 \end{pmatrix} = \begin{pmatrix} 1 & -i \\ -i & 1 \end{pmatrix} \begin{pmatrix} y_1 \\ y_2 \end{pmatrix}, \quad (4.29)$$

that simplifies the second order differential equation for one component. The Dirac equation is given

$$\left(-\frac{r^2\sqrt{f}}{R^2}\sigma^1\partial_r + \frac{r}{R}i\sigma^3m + \frac{1}{\sqrt{f}}\sigma^2(\omega + qA_t) - \sigma^1\frac{r\sqrt{f}}{2R^2}\left(3 + \frac{rf'}{2f}\right) - \lambda\right)\tilde{F} = 0, \quad (4.30)$$

with $\tilde{F} = (\tilde{y}_1, \tilde{y}_2)^T$.

We introduce dimensionless variables with the goal to scale away the AdS_4 radius R and the horizon radius r_0

$$\begin{aligned} r &\rightarrow r_0r, \quad m \rightarrow \frac{m}{R}, \quad r_* \rightarrow r_0r_*, \quad r_{**} \rightarrow r_0r_{**} \\ M &\rightarrow r_0^3M, \quad Q \rightarrow r_0^2Q, \quad H \rightarrow r_0^2H \end{aligned} \quad (4.31)$$

and

$$\begin{aligned} (t, \vec{x}) &\rightarrow \frac{R^2}{r_0}(t, \vec{x}), \quad A_M \rightarrow \frac{r_0}{R^2}A_M, \quad \omega \rightarrow \frac{r_0}{R^2}\omega, \\ \lambda &\rightarrow \frac{r_0}{R^2}\lambda, \quad T \rightarrow \frac{r_0}{R^2}T, \\ ds^2 &\rightarrow R^2ds^2. \end{aligned} \quad (4.32)$$

In the new variables we have

$$\begin{aligned} T &= \frac{3}{4\pi}(1 - r_{**}^4), \quad f = 1 + \frac{3r_{**}^4}{r^4} - \frac{1 + 3r_{**}^4}{r^3}, \\ A_t &= \mu\left(1 - \frac{1}{r}\right), \quad \mu = \sqrt{3}g_F r_*^2, \end{aligned} \quad (4.33)$$

and the metric is given by

$$ds^2 = r^2(-f dt^2 + d\vec{x}^2) + \frac{1}{r^2} \frac{dr^2}{f}, \quad (4.34)$$

with the horizon at $r = 1$, and the conformal boundary at $r \rightarrow \infty$; the red shift factor is

$$f = 1 + \frac{3r_{**}^4}{r^4} - \frac{1 + 3r_{**}^4}{r^3}. \quad (4.35)$$

The Dirac equation is given by

$$\left(-r^2\sqrt{f}\sigma^1\partial_r + ri\sigma^3m + \frac{1}{\sqrt{f}}\sigma^2(\omega + qA_t) - \sigma^1\frac{r\sqrt{f}}{2}\left(3 + \frac{rf'}{2f}\right) - \lambda\right)\tilde{F} = 0. \quad (4.36)$$

We set $m = 0$. Then we get the following second order equations for each component

$$\left(r^4 f \partial_r^2 + (5r^3 f + r^4 f') \partial_r + \frac{15}{4} r^2 f + 2r^3 f' + \frac{r^4 f''}{4} + \frac{1}{f} \left((\omega + qA_t) \pm \frac{ir^2 f'}{4} \right)^2 \mp r^2 i q A_t' - \lambda^2 \right) \tilde{y}_{1;2} = 0, \quad (4.37)$$

with $A_t = \mu(1 - \frac{1}{r})$, and the upper/lower sign is for \tilde{y}_1/\tilde{y}_2 . At $T = 0$, from eq.(4.33) we have $r_{**} = 1$, and the red shift factor develops the double zero near the horizon,

$$f = \frac{(r-1)^2(r^2 + 2r + 3)}{r^4}. \quad (4.38)$$

Due to this fact, the metric near horizon reduces to $AdS_2 \times R^2$, and calculations in AdS_4 are possible to do analytically at small frequencies [18],[14]. We will utilize that below.

We introduce a new radial variable z ,

$$r = \frac{1}{1-z}, \quad (4.39)$$

then the second order differential equation is given by

$$\left(f \partial_z^2 + \left(\frac{3f}{1-z} + f' \right) \partial_z + \frac{15f}{4(1-z)^2} + \frac{3f'}{2(1-z)} + \frac{f''}{4} + \frac{1}{f} \left((\omega + qA_t) \pm \frac{if'}{4} \right)^2 \mp i q A_t' - \lambda^2 \right) \tilde{y}_{1;2} = 0, \quad (4.40)$$

with

$$f = 3z^2(z - z_0)(z - \bar{z}_0), \quad z_0 = \frac{1}{3}(4 + i\sqrt{2}), \\ A_t = \mu z, \quad \mu = \sqrt{3} g_F r_*^2, \quad (4.41)$$

and horizon is at $z = 0$, the conformal boundary is at $z = 1$. Due to the double zero of the red shift factor near the horizon, the second order differential equation eq.(4.40) can be solved analytically at $\omega = 0$ [14].

We put for completeness the second order equations for the components when spin connection has been eliminated using transformation eq.(A.8)

$$\psi = (r^3 \sqrt{f})^{-1/2} \Phi, \quad (4.42)$$

where equations for ψ contain the spin connection, and for Φ do not. The second order equations in dimensionless variables without spin connection read

$$\left(r^4 f \partial_r^2 + (2r^3 f + \frac{r^4 f'}{2}) \partial_r + \frac{r^4 f'^2}{16f} + \frac{1}{f} (\omega + qA_t \pm \frac{ir^2 f'}{4})^2 \mp r^2 i q A_t' - \lambda^2 \right) \tilde{y}_{1;2} = 0, \quad (4.43)$$

and we use the same notations for the components for $\Phi = (\tilde{y}_1, \tilde{y}_2)^T$ as for ψ ; again the upper/lower sign is for \tilde{y}_1/\tilde{y}_2 . Using the radial coordinate z , these equations are written as

$$\left(f \partial_z^2 + \frac{f'}{2} \partial_z + \frac{f'^2}{16f} + \frac{1}{f} (\omega + qA_t \pm \frac{if'}{4})^2 \mp i q A_t' - \lambda^2 \right) \tilde{y}_{1;2} = 0. \quad (4.44)$$

These equations look simpler than the corresponding equations with spin connection. However, they are not readily recognized by MAPLE program, and we will not use them. Writing the transformation which removes the spin connection explicitly as

$$\psi = \left(\frac{z}{(1-z)^3} \sqrt{3(z-z_0)(z-\bar{z}_0)} \right)^{-1/2}. \quad (4.45)$$

gives an idea about the prefactor that we should expect to get in the solution. As mentioned, these equations are not recognized by MAPLE. We therefore proceed with eq.(4.40) which contains spin connection.

Near the horizon, $z = 0$, we have $f = 6z^2$ and

$$6z^2 \tilde{y}'' + 12z \tilde{y}' + \left(\frac{3}{2} + \frac{(q\mu)^2}{6} - \lambda^2 \right) \tilde{y} = 0 \quad (4.46)$$

and the same for \tilde{z} , giving the behavior near horizon

$$\tilde{y}_1 \sim \tilde{y}_2 \sim z^{-\frac{1}{2} \pm \nu}, \quad \nu = \frac{1}{6} \sqrt{6\lambda^2 - (q\mu)^2}, \quad (4.47)$$

with $\mu = \sqrt{3}g_F r_*^2$. We will be interested in this scaling exponent given at the Fermi momentum,

$$\nu \rightarrow \nu_{k_F} = \frac{1}{6} \sqrt{6k_F^2 - 3q^2 g_F^2 r_*^4}, \quad (4.48)$$

which is the conformal dimension found in eq.(A.45). Note that $r_{**} = 1$ at $T = 0$.

Putting $\omega = 0$ eqs.(4.40,4.41) and using MAPLE, we find the analytic solution for the zero mode [14] (see also [24]). The first solution with regular behavior $z^{-\frac{1}{2} + \nu}$ at the horizon, $z \sim 0$, is given by

$$\begin{aligned} \tilde{y}_{1;2}^0 &= N_{1;2} (z-1)^{\frac{3}{2}} z^{-\frac{1}{2} + \nu_\lambda} (z-\bar{z}_0)^{-\frac{1}{2} - \nu_\lambda} \left(\frac{z-z_0}{z-\bar{z}_0} \right)^{\frac{1}{4}(-1 \mp \sqrt{2}q\mu/z_0)}, \\ &\times {}_2F_1 \left(\frac{1}{2} + \nu_\lambda \mp \frac{\sqrt{2}}{3} q\mu, \nu_\lambda \pm i \frac{q\mu}{6}, 1 + 2\nu_\lambda, \frac{2i\sqrt{2}z}{3z_0(z-\bar{z}_0)} \right), \end{aligned} \quad (4.49)$$

where ${}_2F_1$ is the hypergeometric function, N_1, N_2 are normalizations defined later, and upper/lower sign is for \tilde{y}_1/\tilde{y}_2 ; the role of momentum is played by $\lambda \rightarrow \sqrt{2|q\mathcal{H}l|}$. The second solution, with behavior $z^{-\frac{1}{2} - \nu}$ at the horizon, is obtained by replacing $\nu_\lambda \rightarrow -\nu_\lambda$ in eq.(4.49)

$$\tilde{\eta}_{1;2}^0 = \tilde{N}_{1;2} \left(\frac{\tilde{y}_{1;2}^0}{N_{1;2}} \text{ with } \nu_\lambda \rightarrow -\nu_\lambda \right), \quad (4.50)$$

and it will be required to have a regular behavior at $z \sim 0$ for small frequencies. Since normalization factors are constants, we find their relative weight by substituting solutions back into first order differential equations eq.(4.40,4.41) at $z \sim 0$,

$$\frac{N_1}{N_2} = -\frac{6i\nu_\lambda + q\mu}{\sqrt{6}\lambda} \left(\frac{z_0}{\bar{z}_0} \right)^{q\mu/\sqrt{2}z_0}, \quad \frac{\tilde{N}_1}{\tilde{N}_2} = \frac{6i\nu_\lambda - q\mu}{\sqrt{6}\lambda} \left(\frac{z_0}{\bar{z}_0} \right)^{q\mu/\sqrt{2}z_0}. \quad (4.51)$$

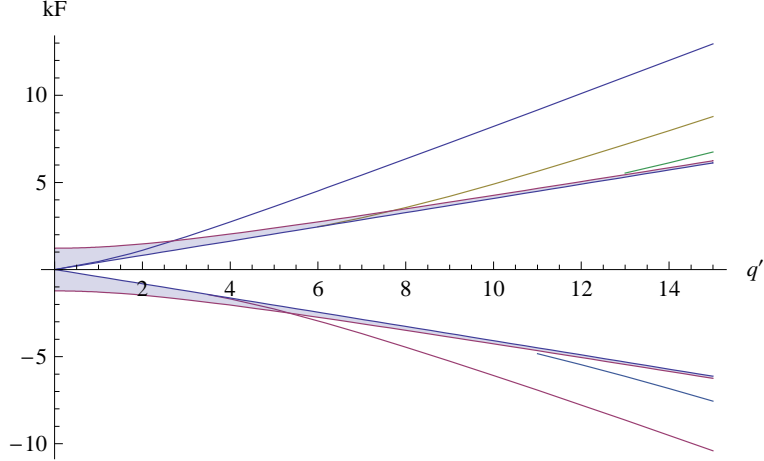


Figure 1: Fermi momentum k_F vs. charge of the fermion field $q' = \sqrt{3}q$. We choose $r_* = 1$, $g_F = 1$, therefore $\mu = \sqrt{3}$. The inner (closer to x-axis) line of the filled/shaded area is $\nu_{k_F} = 0$ and the outer line is $\nu_{k_F} = \frac{1}{2}$, so that the shaded region corresponds to $0 < \nu_{k_F} < \frac{1}{2}$. At a given q there are multiple Fermi surfaces. From left to right are the first, second etc. Fermi surfaces. They disappear at $\nu_{k_F} = 0$. Positive and negative k_F correspond to Fermi surfaces in G_1 and G_2 Green functions respectively. At $q = 1$, which on the plot is $q'\sqrt{3}$ $k_F \approx 0.92$ in agreement with [20]. The first Fermi surface hits the border-line between a Fermi and non-Fermi liquids $\nu = \frac{1}{2}$ at $q' = 2.71$.

The same relations are obtained when calculations are done for any z . The zero mode equals to $\psi^0 = \frac{1}{2}(\tilde{y}_1 + i\tilde{y}_2, \tilde{y}_2 + i\tilde{y}_1)$ with $\tilde{y}_{1;2} = \tilde{y}_{1;2}^0 + \tilde{\eta}_{1;2}^0$.

To obtain the Fermi momentum, we can follow [18] and search for a normalizable solution of the Dirac equation with the certain boundary conditions, which is equivalent of looking for a bound state in a zero-energy Schrodinger equation. We use an alternative way suggested in [14], that also uses that the solution should be regular at the horizon and obey certain falloff conditions near the boundary of AdS_4 . To construct ψ^{bdy} , we required the boundary condition $a = 0$ on the fluctuating mode, i.e. at the conformal boundary $z \rightarrow 1$

$$\psi^0 = \frac{1}{2} \begin{pmatrix} \tilde{y}_1 + i\tilde{y}_2 \\ \tilde{y}_2 + i\tilde{y}_1 \end{pmatrix} \sim (1-z)^{3/2} \begin{pmatrix} 1 \\ 0 \end{pmatrix} + \dots \quad (4.52)$$

Therefore the equation for the Fermi momentum k_F is

$$\lim_{z \rightarrow 1} (z-1)^{-3/2} (\tilde{y}_2 + i\tilde{y}_1) = 0. \quad (4.53)$$

Using the zero mode solution eq.(4.49) in the eq.(4.53), we have

$$\frac{{}_2F_1(1 + \nu_{k_F} + \frac{iq\mu}{6}, \frac{1}{2} + \nu_{k_F} - \frac{\sqrt{2}q\mu}{3}, 1 + 2\nu_{k_F}, \frac{2}{3}(1 - i\sqrt{2}))}{{}_2F_1(\nu_{k_F} + \frac{iq\mu}{6}, \frac{1}{2} + \nu_{k_F} - \frac{\sqrt{2}q\mu}{3}, 1 + 2\nu_{k_F}, \frac{2}{3}(1 - i\sqrt{2}))} = \frac{6\nu_{k_F} - iq\mu}{k_F(-2i + \sqrt{2})}, \quad (4.54)$$

with $\nu_{k_F} = \frac{1}{6}\sqrt{6k_F^2 - (q\mu)^2}$. We solve the equation for the Fermi surface numerically, using MATHEMATICA to evaluate the hypergeometric functions. The solutions of eq.(4.54) are

depicted in Fig.(1). There are multiple Fermi surfaces for a given q . Following [14], the largest $|k_F|$ is called the first Fermi surface, the next $|k_F|$ the second Fermi surface, and so on. For all further plots, we choose $r_* = 1$ and $g_F = 1$; therefore $\mu = \sqrt{3}$. We recover a result of the numerical solution of the Dirac equation [20]: for $q = 1$ which is $\mu q = \sqrt{3}$ we have $k_F = 0.9185$. In Fig.(1), positive and negative k_F correspond to the Fermi surfaces in the Green functions G_1 and G_2 . The relation between two components when $m = 0$ is $G_2(\omega, k) = -\frac{1}{G_1(\omega, k)}$ [20], therefore Fig.(1) is not symmetric with respect to $k_F = 0$ axis.

We substitute the Fermi momentum into the zero mode solution eq.(4.49) and get the radial profile for the pairing gap function Δ^0 given by eq.(4.23). We plot $\Delta^0(z)$ for different charges, Fig.(2). The curves are normalized to have the same maxima. Charges are increased from left to right. For large charge, when $\nu > \frac{1}{2}$, the zero modes are supported away from the horizon, while at smaller charge, when $\nu \rightarrow \frac{1}{2}$, the zero mode functions are supported near the horizon. The same tendency was first observed for the Cooper pairing [14, 21]. This means that for non-Fermi liquids, at $\nu < \frac{1}{2}$, the physics of the Fermi surface is captured by the near horizon $\text{AdS}_2 \times \mathbb{R}^2$ region.

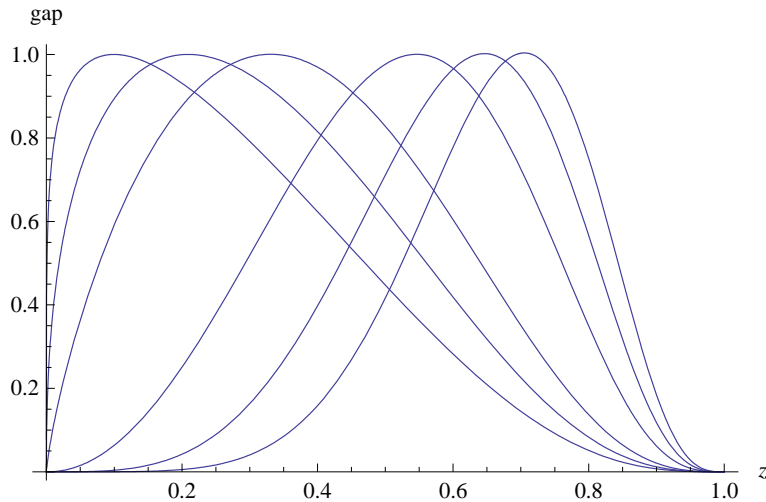


Figure 2: Wavefunction of a pairing mode $\Delta^0 = \psi^{0\dagger} \sigma^1 \psi^0$ as a function of the radial coordinate z , with the horizon at $z = 0$ and the boundary at $z = 1$, for different values of the charge $q' = \sqrt{3}q$ for the first Fermi surface. We set $r_* = 1$, $g_F = 1$. From left to right the values of the charge are $q' = \{3, 3.4, 4, 6, 8, 10\}$. The curves are normalized to have their maxima all the same. At small charge, non-Fermi liquid, the wave function is supported near the horizon. At large charge, Fermi liquid, the wave function is supported away from the horizon.

We express the boundary Green function through the zero mode solutions. To do that we should obtain the solution at small but nonzero frequency and expand the Green function to the leading order in ω . We follow the matching procedure of [14] between the solution in the “near” (to horizon) region (“inner” in terminology of [18]), $z \ll 1$, and in the “far” (from horizon) region (“outer” in terminology of [18]), $z \gg \omega$. Matching the two solutions gives a solution on the full spacetime as long as the near and far regions overlap, $\omega \ll 1$.

Near the horizon, $z \ll 1$ $f(z) = 6z^2$, and the second order wave equation, eq.(4.40), becomes

$$\left(z^2 \partial_z^2 + 2z \partial_z + \frac{1}{36} \left((q\mu + \frac{\omega}{z})^2 \pm 6i \frac{\omega}{z} + 9 - 6\lambda^2 \right) \right) \tilde{y}_{1;2} = 0. \quad (4.55)$$

Using MATHEMATICA, we obtain the following solutions

$$\tilde{y}_{1;2}^{near} = C_{1;2} z^{-\frac{1}{2} - \nu_\lambda} e^{-\frac{i\omega}{6z}} {}_1F_1 \left(\frac{1}{2} \mp \frac{1}{2} + \nu_\lambda + \frac{iq\mu}{6}, 1 + 2\nu_\lambda, \frac{i\omega}{3z} \right) + D_{1;2} (\nu_\lambda \rightarrow -\nu_\lambda), \quad (4.56)$$

with upper/lower sign is for \tilde{y}_1/\tilde{y}_2 . Requiring that the solution is ingoing at the horizon $z \sim 0$, $\sim e^{+i\omega/6z}$, fixes the ratio

$$\frac{C_1}{D_1} \sim \frac{C_2}{D_2} \sim \frac{\Gamma(-2\nu_\lambda)\Gamma(1 + \nu_\lambda - \frac{iq\mu}{6})}{\Gamma(2\nu_\lambda)\Gamma(1 - \nu_\lambda - \frac{iq\mu}{6})} (-i\omega)^{2\nu_\lambda}. \quad (4.57)$$

The near horizon solution is in the matching region $z \gg \omega$,

$$\tilde{y}_{1;2}^{near} = A_{1;2} z^{-\frac{1}{2} - \nu_\lambda} + B_{1;2} z^{-\frac{1}{2} + \nu_\lambda}, \quad (4.58)$$

that corresponds to the AdS_2 boundary, given in eq.(B.24). From eqs.(4.58,4.57) we have

$$G^{IR} \sim \frac{B_1}{A_1} \sim \frac{B_2}{A_2} \sim \frac{\Gamma(-2\nu_\lambda)\Gamma(1 + \nu_\lambda - \frac{iq\mu}{6})}{\Gamma(2\nu_\lambda)\Gamma(1 - \nu_\lambda - \frac{iq\mu}{6})} (-i\omega)^{2\nu_\lambda}, \quad (4.59)$$

since by definition the ratio B_1/A_1 gives the retarded Green function in the IR CFT living on the boundary of AdS_2 . We calculated it in the Appendix C, eq.(B.30).

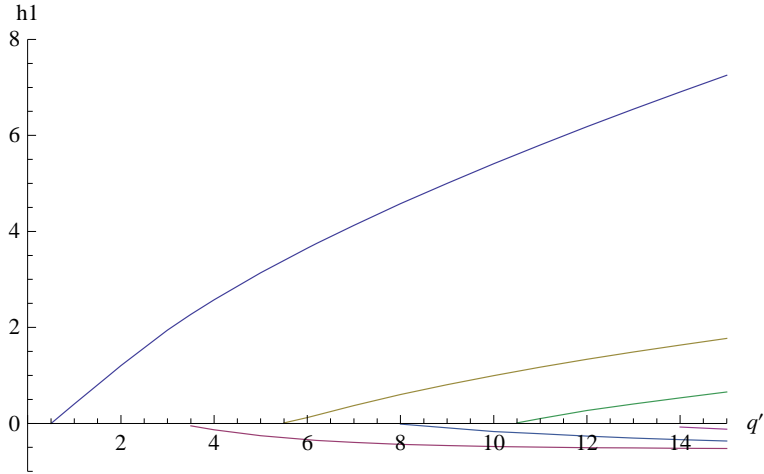


Figure 3: Constant h_1 , reflecting the UV physics of the AdS_4 bulk, vs. charge $q' = \sqrt{3}q$. It vanishes at $\nu_{k_F} = 0$. The multiple lines are for various Fermi surfaces, in ascending order with the first fermi surface on the left. Note, h_1 has the same sign as k_F . As above, positive and negative k_F correspond to Fermi surfaces in the Green functions G_1 and G_2 respectively.

In the asymptotic far region $z \gg \omega$, the second order wave equation is solved perturbatively in ω ,

$$\tilde{y}_{1;2}^{far} = \tilde{y}_{1;2}^{(0)} + \omega \tilde{y}_{1;2}^{(1)}, \quad (4.60)$$

where $\tilde{y}_{1;2}^{(0)}$ includes the zero modes found in before, $\tilde{y}_{1;2}^{(0)} = \tilde{y}_{1;2}^0 + \tilde{\eta}_{1;2}^0$. Expanding $\tilde{y}^{(0)}$ in the matching region, $z \ll 1$,

$$\begin{aligned}\tilde{y}_{1;2}^{far} &= \tilde{N}_{1,2} S_{1;2}(\nu) z^{-\frac{1}{2}-\nu} + N_{1;2} S_{1;2}(-\nu) z^{-\frac{1}{2}+\nu} + O(\omega) \\ S_{1;2}(\nu) &= (-1)^{3/2} (-\bar{z}_0)^{-\frac{1}{2}+\nu\lambda} \left(\frac{z_0}{\bar{z}_0} \right)^{-\frac{1}{4} \mp \frac{\sqrt{2}q\mu}{4z_0}}.\end{aligned}\quad (4.61)$$

Comparing the near solution eq.(4.58) and the far solution eq.(4.61) in the matching region $\omega \ll z \ll 1$, we get

$$\frac{\tilde{N}_1}{N_1} = (-\bar{z}_0)^{-2\nu\lambda} \tilde{G}^{IR}, \quad (4.62)$$

that determines the relative contribution of \tilde{y}^0 and $e\tilde{t}a^0$. We also have relations for N_2 and \tilde{N}_2 given in terms of N_1 and \tilde{N}_1 , eq.(4.51). Comparing eq.(4.59) and eq.(4.62), ω and z scale with the same power in the solution \tilde{y} around the horizon. From eq.(4.62) follows that

$$\tilde{\eta}_{1;2}^0 \sim G^{IR} \sim G^{IR} \sim \omega^{2\nu\lambda}. \quad (4.63)$$

The first order correction $\tilde{y}_{1;2}^{(1)}$ satisfies an inhomogeneous second order wave equation with $\tilde{y}_{1;2}^{(0)}$ as the source. To calculate the retarded boundary Green function, we need only the leading asymptotic behavior near the boundary $z \rightarrow 1$. The asymptotic behavior can be found by integrating the Dirac equation (4.40) as in Appendix C of [18] with the result [14]

$$\tilde{y}_2^{(1)} + i\tilde{y}_1^{(1)} = 2i(1-z)^3 \frac{\int_0^1 dz \sqrt{g/g_{tt}} (|\tilde{y}_1^0|^2 + |\tilde{y}_2^0|^2)}{\tilde{y}_1^{0*} - i\tilde{y}_2^{0*}}. \quad (4.64)$$

Note, that from eq.(4.64) and eq.(4.63), only $\tilde{\eta}$ depends on the frequency, while all other wavefunctions are independent of ω .

The Green function of the dual field theory defined on the boundary of AdS₄, as introduced in eq.(4.14), is

$$G = \lim_{z \rightarrow 1} \frac{\tilde{y}_1 + i\tilde{y}_2}{\tilde{y}_2 + i\tilde{y}_1}. \quad (4.65)$$

Expanding in small frequency ω ,

$$G = \lim_{z \rightarrow 1} \frac{\tilde{y}_1^0 + i\tilde{y}_2^0 + \tilde{\eta}_1^0 + i\tilde{\eta}_2^0}{\tilde{y}_2^0 + i\tilde{y}_1^0 + \tilde{\eta}_2^0 + i\tilde{\eta}_1^0 + \omega(\tilde{y}_2^{(1)} + i\tilde{y}_1^{(1)}) + O(\omega^2)}, \quad (4.66)$$

where the zero mode wavefunctions $\tilde{y}_{1;2}^0$, $\tilde{\eta}_{1;2}^0$ are defined in eq.(B.24) with normalization given in eq.(4.51,4.62) and asymptotic behavior of the last term in denominator given in eq.(4.64). Near the Fermi surface, $k_\perp = k - k_F$, and at $T = 0$ the Green function is written [18]

$$G = \frac{(-h_1 v_F)}{\omega - v_F k_\perp - h_2 v_F e^{i\theta - i\pi\nu} \omega^{2\nu k_F}}, \quad (4.67)$$

which was used in our calculations for T_c , eq.(4.17). Note that all quantities here In the above formula, the last term in the denominator comes from $\tilde{\eta}_{1;2}^0$ and includes $G^{IR} \sim \omega^{2\nu k_F}$,

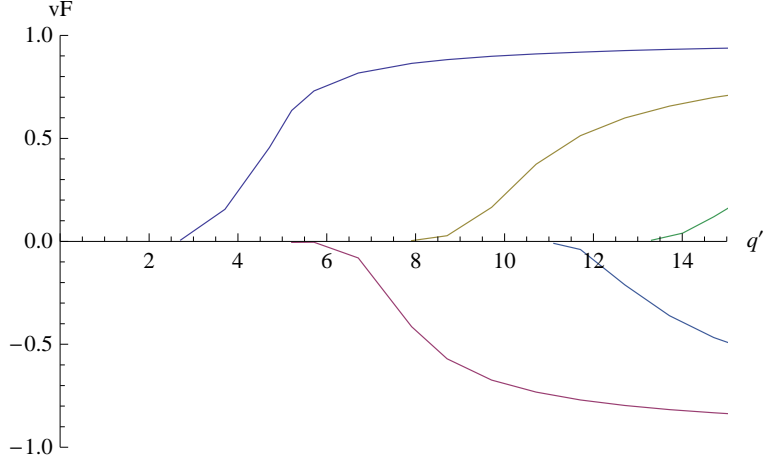


Figure 4: Constant v_F , reflecting the UV physics of the AdS_4 bulk, vs. charge $q' = \sqrt{3}q$. It vanishes at $\nu_{k_F} = \frac{1}{2}$. For the first Fermi surface it happens ($\nu_{k_F} = \frac{1}{2}$) at $q' = 2.71$. The multiple lines are for various Fermi surfaces, in ascending order with the first fermi surface on the left. Note, v_F has the same sign as k_F . As above, positive and negative k_F correspond to Fermi surfaces in the Green functions G_1 and G_2 , respectively.

i.e. it is determined by the $IR AdS_2$ physics near the horizon. Other terms are determined by the UV physics of the AdS_4 bulk. The constants h_1 and v_F are

$$h_1 = \lim_{z \rightarrow 1} \frac{\tilde{y}_1^0 + i\tilde{y}_2^0}{\partial_k(\tilde{y}_2^0 + i\tilde{y}_1^0)}, \quad (4.68)$$

$$v_F = \frac{1}{h_1} \left(\int_0^1 dz \sqrt{g/g_{tt}} \psi^{0\dagger} \psi^0 \right)^{-1} \lim_{z \rightarrow 1} \frac{|\tilde{y}_1^0 + i\tilde{y}_2^0|^2}{(1-z)^3}, \quad (4.69)$$

where all wavefunctions are evaluated at $k = k_F$; the zero mode has components $\psi^0 = (\tilde{y}_1^0 + i\tilde{y}_2^0, \tilde{y}_2^0 + i\tilde{y}_1^0)$; and the wavefunctions $\tilde{y}_{1,2}^0$ are given by analytic expressions, eq.(4.49). The constants h_2, θ can be also obtained from this expression. The constants h_1 and v_F are dimensionless in eqs.(4.68),(4.69), i.e. the scaling is (from dimensional to dimensionless) $h_1 \rightarrow \frac{1}{r_0} h_1, v_F \rightarrow \frac{R^3}{r_0^3} v_F$. Both constants are real. They are plotted as function of $q\mu$ in Figs.(3),(4). The Fermi velocity vanishes at the horizontal line $v_F = 0$ when $\nu_{k_F} = \frac{1}{2}$. The wavefunction renormalization h_1 vanishes when $\nu_{k_F} = 0$. The multiple lines in each plot are for various Fermi surfaces, starting with the first FS at the most left. Positive and negative v_F, h_1 correspond to the Fermi surfaces in the Green functions G_1 and G_2 respectively. Both v_F and h_1 have the same sign as k_F . The Fermi velocity decreases at small charges and tends to the speed of light at large charges. Geometrically this means, that as the charge is lowered the zero mode wavefunction is supported near the black hole horizon, Fig.(2), where the gravitational redshift reduces the local speed of light as compared to the boundary value. This was observed also in [14, 18].

The dimensionless critical temperature is given by

$$T_c = \frac{G_{int} |q\mathcal{H}| h_1^2 v_F^3}{\pi^2} \int dz \sqrt{-g} (\psi^0(z)^\dagger \sigma^1 \psi^0(z))^2, \quad (4.70)$$

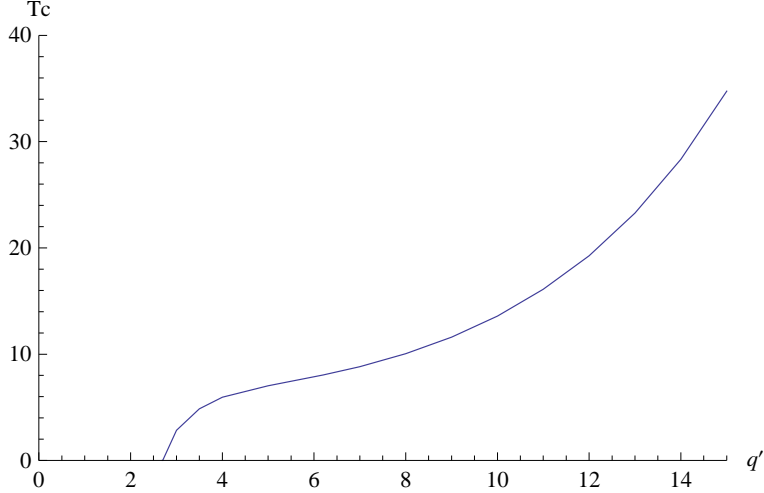


Figure 5: Critical temperature T_c vs. the charge $q' = \sqrt{3}q$ for the first Fermi surface. Only parametric dependence is shown, and the $1/\pi^2$ factor is not included. We set $r_* = 1$, $g_F = 1$. Note that T_c vanishes around $q' = 2.71$ which corresponds to $\nu_{k_F} = \frac{1}{2}$ for the first Fermi surface. This plot illustrates that pairing is supported only for $\nu_{k_F} > \frac{1}{2}$ which is the region of Fermi liquids.

with transformation to the dimensionless variables given by

$$r \rightarrow r_0 r, \quad G_{int} \rightarrow \left(\frac{r_0^2}{R^3}\right)^{-2} G_{int}, \quad \mathcal{H} \rightarrow \frac{r_0^2}{R^4} \mathcal{H}, \quad h_1 \rightarrow \frac{r_0}{R^2} h_1, \quad \psi^0 \rightarrow R^{3/2} \psi^0. \quad (4.71)$$

Using the analytic expression for the zero mode eq.(4.49), and the results for h_1, v_F, k_F calculated for a given charge q , we plot T_c as function of charge for the first Fermi surface, Fig.(5). The next Fermi surfaces give smaller contributions and are not depicted on the plot. The critical temperature vanishes exactly for $\nu = \frac{1}{2}$, which is for the first Fermi surface is at $q\mu = \sqrt{3}q = 2.71$ and with $k_F = 1.65$. Therefore there is no pairing for $\nu \leq \frac{1}{2}$. This happens due to the fact that to the leading order the density of states eq.(4.25) vanishes for the non-Fermi liquids. This conclusion agrees with our variational calculations, where pairing occurs only for the Fermi liquids, while non-Fermi liquids do not support pairing. Note, that in principle fermions from different Fermi surfaces can participate in pairing.

Now we analyze behavior of the boundary field theory with magnetic field. The conformal dimension of the fermionic operator \mathcal{O} in the *IR CFT* eq.(A.46) is

$$\nu_{k_F} = \sqrt{\frac{1}{6} \left(\frac{k_F^2}{r_{**}^2} + \Delta^2 \right) - \frac{q^2 g_F^2}{12} \frac{r_*^4}{r_{**}^4}}, \quad (4.72)$$

where it is taken in the chiral limit $m = 0$ and at the Fermi surface $k_F = q\mu$, and the dimensionless variables introduced before are used. We rewrite this expression in terms of Q and H , using eq.(2.8), as

$$\nu_{k_F} = \sqrt{\frac{k_F^2}{\sqrt{12}Q\sqrt{1+(H/Q)^2}} + \frac{\Delta^2}{6} - \frac{q^2 g_F^2}{12(1+(H/Q)^2)}}. \quad (4.73)$$

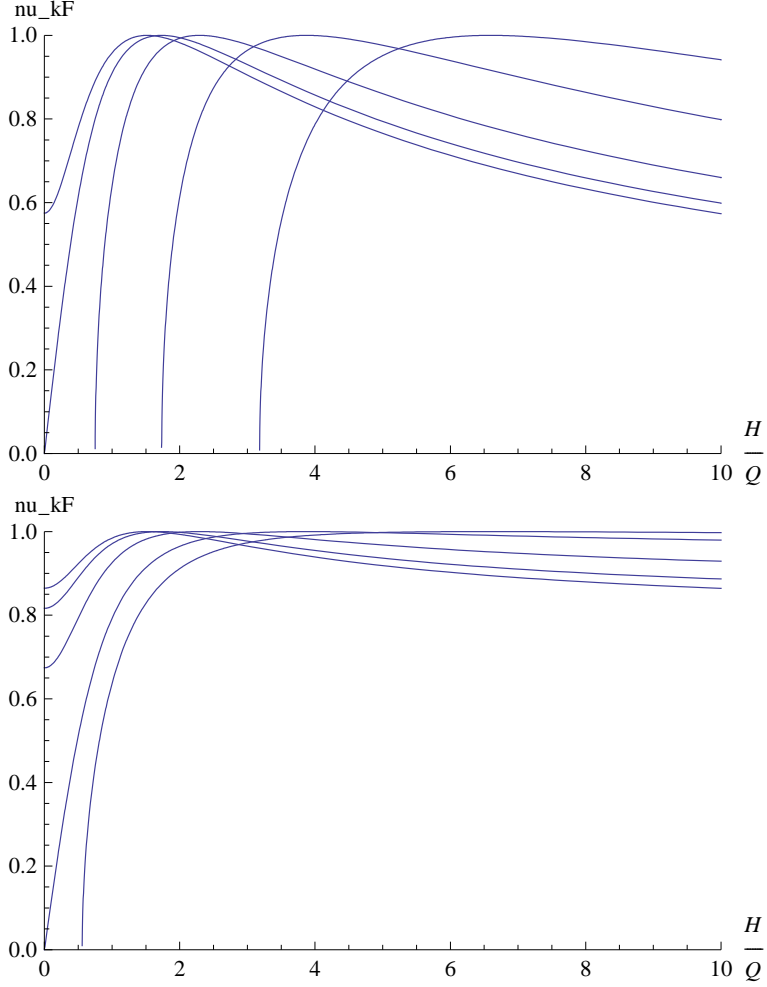


Figure 6: Conformal dimension of the fermion operator in the *IR CFT* ν_{k_F} as a function of the ratio $\frac{H}{Q}$ for different values for q' . We used parametrization $\nu \sim \sqrt{a/\sqrt{1+x^2} + b - c/(1+x^2)}$ with $x = \frac{H}{Q}$. The curves from right to left correspond to increasing charges q' , $a = \{0.3, 0.5, 0.8, 1, 1.1\}$, while b and $c = 1$ are kept fixed. Top plot is for $b = 0$, zero gap, and bottom plot is for $b = 0.5$, nonzero gap. At small and intermediate charges, the Fermi liquid regime and hence the particle-hole pairing are realized at a threshold value of the magnetic field, which is consistent with magnetic catalysis in graphene with impurities.

Writing ν_{k_F} as a function of $x = H/Q$, $\nu \sim \sqrt{\frac{a}{\sqrt{1+x^2}} + b - \frac{c}{1+x^2}}$, we plot ν_{k_F} vs. x for different parameters a, b, c , Fig.(6). Multiple curves correspond to increasing values for a starting from the right to left curves, while b and c are kept constant. This corresponds to increase of the fermion charge q . At small charges the Fermi momentum k_F is small (see Fig.(1)), that corresponds to small a (curves to the right). All curves show the rapid growth at the beginning, then saturation at some maximum, and fall off which happens at large enough x where we are not interested any more. For small charges, the rise to $\nu = \frac{1}{2}$ happens relatively quickly, and means there is a narrow window of magnetic field for non-

Fermi liquids. However, the region for $\frac{1}{2} < \nu < 1$, the case of Fermi liquids, corresponds to a much wider range of the magnetic field. For small and intermediate charges, regime of the Fermi liquid requires a threshold magnetic field, when $\nu = \frac{1}{2}$ is reached. This is consistent with the magnetic catalysis in a system with dissipations, e.g., graphene with impurities, where there is a nonzero width and the particle-hole gap is induced at a threshold value of the magnetic field [1]. For large charges, corresponding to curves to the left, there is only a regime of Fermi liquids (no non-Fermi liquids are possible) and pairing is supported for any magnetic field. Top and bottom pannels are plots for zero and nonzero gaps, respectively.

In this paper we have imagined the existance of an “experiemntal knob” which can be used to adjust the UV scaling dimension of fermionic operator. As noted in [22], the most useful knob will likely depend on the UV geometry into which this AdS_2 is embedded. In our case, an external magnetic field \mathcal{H} will allow one to tune the IR scaling dimension and to explore different sectors of the boundary field theory.

In analogy to the superconducting instability $\langle \psi\psi \rangle$ of the black hole, we find that the Breitenlohner-Freedman bound can also be broken in case of $\langle \bar{\psi}\psi \rangle$ condensate for large enough fermion charges q . Using the dimensionless variables, the conformal dimension of the bosonic operator in the IR CFT in the presence of a magnetic field is

$$\nu = \sqrt{\frac{1}{6} \left(\frac{2|q\mathcal{H}|l}{r_{**}^2} + m^2 \right) - \frac{q^2 g_F^2 r_*^4}{12 r_{**}^4} + \frac{1}{4}}, \quad (4.74)$$

which is obtained from eq.(A.45) by $k_F^2 \rightarrow 2|q\mathcal{H}|l$, the mass gap $\Delta \rightarrow m$ with m being the mass of the bosonic field living in the bulk. Here the last term $\frac{1}{4}$ distinguishes the bosonic case from the fermionic one. The conformal dimension of the bosonic operator in the UV CFT , Δ_ϕ , in the dimensionless variables is given by

$$\Delta_\phi = \frac{3}{2} + \sqrt{m^2 + \left(\frac{3}{2}\right)^2}. \quad (4.75)$$

Breitenlohner-Freedman (BF) bound is broken when conformal dimension becomes imaginary. As in the case with superconductor, there is a parameter range where the conformal dimension in the IR (coming from the near AdS_2 horizon) is imaginary and the conformal dimension in the UV (coming from the AdS_4 bulk) is real. Expressing the mass m through Δ_ϕ , the condition breaking the BF bound is

$$q^2 g_F^2 \frac{r_*^4}{r_{**}^4} \geq 2\Delta_\phi(\Delta_\phi - 3) + 3 + \frac{4R^4 |q\mathcal{H}|l}{r_{**}^2}. \quad (4.76)$$

Here we restored the dimension.

5. Equation of state and transport properties of the boundary field theory at zero magnetic field

In this section we consider thermodynamics of the boundary field theory, namely we obtain an equation of state and find the scaling behavior of the specific heat with temperature.

Then we consider transport properties of the system on the boundary, specifically we calculate the DC conductivity and analyze its scaling behavior. We do not specify the boundary theory. Instead we use the “dressed” by the gravity fermion propagators obtained from the AdS_{3+1}/CFT_{2+1} analyzes in [18]. As a result we obtain behavior of systems with properties ranging from Fermi and marginal liquids to non-Fermi liquids. In particular we reproduce correct temperature scaling for the DC conductivity and specific heat in case of the Fermi and marginal liquids. Since the two-point Green function of the boundary theory has been obtained using the AdS/CFT correspondence, it is “exact” in terms of gauge coupling corrections. Therefore the lowest order diagrams on the field theory side should suffice. Of course we lack the knowledge of the “dressed” by the gravity gauge-fermion vertex. For the quantities considered below, the scaling behavior does not change when vertex corrections are added.

5.1 Equation of state and specific heat

An effective potential in the CJT formalism is given by [25]

$$\Gamma_{eff} = \frac{1}{2}\text{Tr} \ln S^{-1} + \frac{1}{2}\text{Tr}(S_0^{-1}S - 1) + \Gamma_2[S], \quad (5.1)$$

where S is a dressed fermion propagator, Γ_2 is the sum of all two-particle irreducible (2PI) diagrams, and trace Tr involves integration $\int d^2x$. The last two terms can be simplified with the help of Dyson-Schwinger equation, to give

$$\Gamma_{eff} = \frac{1}{2}\text{Tr} \ln S^{-1} - \frac{1}{4}\text{Tr}(\Sigma S), \quad (5.2)$$

where the self-energy is $\Sigma = S^{-1} - S_0^{-1}$.

We use “dressed” by the gravity retarded and advanced fermion propagators [18]

$$\begin{aligned} G_R(\omega, \vec{k}) &= \frac{(-h_1 v_F)}{\omega - v_F k_\perp + \Sigma(\omega, k_F)}, \\ G_A(\omega, \vec{k}) &= -G_R(\omega, \vec{k})^* = -\frac{(-h_1 v_F)}{\omega - v_F k_\perp + \Sigma^*(\omega, k_F)}, \end{aligned} \quad (5.3)$$

where the momentum is counted from the Fermi surface $k_\perp = k - k_F$, h_1 and v_F are real constants (we keep the same notations for the constants as in [18]). The self energy $\Sigma = h v_F c(k_F) \omega^{2\nu_{k_F}}$ contains the real and imaginary parts, $\Sigma = \Sigma_1 + i\Sigma_2$, with imaginary part coming from scattering processes of a fermion in the bulk, e.g. via pair creation, and scattering into the black hole. The spectral function defined as $A(\omega, \vec{k}) = \frac{1}{\pi} \text{Im} G_R(\omega, \vec{k})$ is

$$A(\omega, \vec{k}) = \frac{1}{\pi} \frac{h_1 v_F \Sigma_2(\omega, k_F)}{(\omega - v_F k_\perp + \Sigma_1(\omega, k_F))^2 + \Sigma_2(\omega, k_F)^2}. \quad (5.4)$$

Exactly due to inelastic/dissipative processes we are able to calculate transport coefficients, which will be infinite otherwise. However, the imaginary self energy gives rise to a branch cut in the fermion propagator along $\text{Im}\omega = 0$ in a complex ω plane [16, 26, 27]. Therefore

in calculation of Matsubara sum we should take into account contributions from poles and discontinuities along branch cuts [26, 27]

$$T \sum_{\text{odd } m} F(i\omega_m) = \sum_{\text{poles}} n(z_i) \text{Res}(F, z = z_i) - \sum_{\text{cuts}} \int_{-\infty}^{\infty} \frac{d\zeta}{2\pi i} n(\zeta) \text{Disc } F, \quad (5.5)$$

with analytical continuation $i\omega_m \rightarrow z$, and $n(x)$ is the Fermi distribution function. One can use either $n(x) \equiv n(\frac{x}{T})$ or $\tanh(\frac{x}{2T})$ functions with prefactors $(-\frac{1}{2\pi i})$ and $(-\frac{1}{4\pi i})$ respectively in the contour integral which give the same result for the observables. Calculation of Matsubara sums using perturbative expansion in the imaginary part of the self-energy has been developed in [28].

For simplicity we take $(-h_1 v_F) \rightarrow 1$ which will not change our results qualitatively. Using the retarded fermion propagator eq.(5.3), an effective potential is

$$\Gamma_{eff} \rightarrow -\frac{1}{4\pi i} \frac{V_2}{T} \int \frac{d^2 k}{(2\pi)^2} \int_C dz \tanh \frac{z}{2T} \times T \left(\frac{1}{2} \ln \frac{z - v_F k_{\perp} + \Sigma(z, k_F)}{T} - \frac{1}{4} \frac{\Sigma(z, k_F)}{z - v_F k_{\perp} + \Sigma(z, k_F)} \right), \quad (5.6)$$

where we substituted Matsubara sum by the contour integral. The original contour C_0 going around the poles along imaginary z -axis was deformed in the contour C going along the real z axis and Γ being arcs at infinity with vanishing contribution [26]. In case of a real self-energy the result for the contour integration is (see Appendix C and [16])

$$\Gamma_{eff} \rightarrow \frac{V_2}{T} \int \frac{d^2 k}{(2\pi)^2} \sum_{z_*} \left(\frac{1}{2} T \ln \left(2 \cosh \frac{z_*}{2T} \right) + \frac{1}{4} \Sigma(z_*) \tanh \frac{z_*}{2T} \right), \quad (5.7)$$

where z_* are the poles of the retarded propagator, and the sum over all possible poles is taken. As was shown in [16], when a self-energy and hence poles include imaginary part, the following substitution of hyperbolic functions with Γ functions should be made [24]

$$\begin{aligned} |\Gamma(\frac{1}{2} + iz)|^2 &= \frac{\pi}{\cosh(\pi z)}, \\ |\Gamma(iz)|^2 &= \frac{\pi}{z \sinh(\pi z)}. \end{aligned} \quad (5.8)$$

Using the relation between the effective potential and the pressure, $p = \frac{T}{V_2} \Gamma_{eff}$, we get an equation of state

$$p = \int \frac{d^2 k}{(2\pi)^2} \sum_{z_*} \left(-\frac{1}{2} T \ln \left(\frac{1}{2\pi} \left| \Gamma\left(\frac{iz_*}{2\pi T} + \frac{1}{2}\right) \right|^2 \right) + \frac{1}{4} \frac{\Sigma(z_*) \left| \Gamma\left(\frac{iz_*}{2\pi T} + \frac{1}{2}\right) \right|^2}{\frac{|z_*|}{2\pi T} \left| \Gamma\left(\frac{iz_*}{2\pi T}\right) \right|^2} \right), \quad (5.9)$$

where summation over complex poles z_* is performed. As in our previous calculations we take only the contribution of the nearest to $\omega = 0$ pole eqs.(3.20),(3.21),(3.22), and the self-energy $\Sigma(z) \sim z^{2\nu}$. Near the Fermi surface, the one-loop contribution dominates over the self-energy term for the Fermi liquids $\nu > \frac{1}{2}$, while the self-energy becomes important for the non-Fermi liquids $\nu < \frac{1}{2}$.

Having calculated the pressure, we can obtain other thermodynamic quantities, e.g. the entropy, the specific heat, and the particle number density, respectively,

$$s = \frac{\partial p}{\partial T}, \quad c = T \frac{\partial s}{\partial T}, \quad n = \frac{\partial p}{\partial \mu} \quad (5.10)$$

with $\mu \equiv k_F$.

We find the temperature dependence for the specific heat. The first term in eq.(5.9) contributes to the specific heat

$$\begin{aligned} & \sim \frac{1}{T^2} \int \frac{d^2 k}{(2\pi)^2} \text{Re} \left(z_*^2 \Psi' \left(\frac{iz_*}{2\pi T} + \frac{1}{2} \right) + z_*^{*2} \Psi' \left(-\frac{iz_*^*}{2\pi T} + \frac{1}{2} \right) \right), \\ & \frac{1}{T^2} \int \frac{d^2 k}{(2\pi)^2} \text{Re} \left(\sim z_* T \Psi \left(\frac{iz_*}{2\pi T} + \frac{1}{2} \right); \sim z_*^* T \Psi \left(\frac{-iz_*^*}{2\pi T} + \frac{1}{2} \right) \right) \end{aligned} \quad (5.11)$$

where $\Psi'(x) = \frac{d\Psi}{dx} = \frac{d^2 \ln \Gamma}{dx^2}$. The second term in eq.(5.9) gives to the specific heat the following contributions

$$\frac{1}{T^2} \int \frac{d^2 k}{(2\pi)^2} \text{Re} \left(\sim T \Sigma(z_*) F[\Gamma]; \sim z_* \Sigma(z_*) F[\Gamma]; \sim \frac{z_*^2 \Sigma(z_*)}{T} F[\Gamma] \right), \quad (5.12)$$

where $F[\Gamma]$ denotes a combination of Γ functions and its first and second derivatives. Here momentum integration is performed around the Fermi surface, $d^2 k \rightarrow k_F dk_\perp$ with $k_\perp = k - k_F$, the poles $z_* = \omega_c - i\Gamma$ are given by eqs.(3.20),(3.21),(3.22) for the three cases of interest, and $\Sigma(z) \sim z^{2\nu}$.

For the Fermi liquid $\nu > \frac{1}{2}$, $z_\perp \sim k_\perp$ (the real part is dominant). The first term gives $\frac{1}{T^2} \int dk_\perp z_*^2 \rightarrow T$ and the same behavior from the other combination. In the second term we have $\Sigma \sim k_\perp^{2\nu}$. Therefore the second term gives $\frac{1}{T^2} \int dk_\perp \Sigma(z_*) z_* \rightarrow T^{2\nu}$ and the same behavior for the other two combinations. In eq.(5.9) for the pressure, the one-loop term dominates over the self-energy for $\nu > \frac{1}{2}$. Therefore for Fermi liquid at low temperatures we have

$$c \sim T. \quad (5.13)$$

This result reproduces correctly the linear temperature behavior of the heat capacity known for the Fermi liquids.

For the non-Fermi liquid $\nu < \frac{1}{2}$, $z_\perp \sim k_\perp^{\frac{1}{2\nu}}$ (for both real and imaginary parts). The first term gives $\frac{1}{T^2} \int dk_\perp k_\perp^{\frac{1}{2\nu}} \rightarrow T^{\frac{1}{2\nu}-1}$ and $\frac{1}{T^2} \int dk_\perp k_\perp^{\frac{1}{2\nu}} T \rightarrow T^{\frac{1}{2\nu}}$. The second term gives $\frac{1}{T^2} \int dk_\perp \Sigma(z_*) T \rightarrow T^{2\nu}$ and subleading behavior for the other two combinations. For $\nu < \frac{1}{2}$, the self-energy dominates over the one-loop in the pressure. Therefore for non-Fermi liquid at low temperatures we have

$$c \sim T^{2\nu}. \quad (5.14)$$

This result for the heat capacity reflects the scaling behavior of the self-energy.

For $\nu = \frac{1}{2}$ all obtained above terms are $\sim T$. Therefore for the marginal liquids we have $c \sim T$.

We repeat derivation of equation of state using the spectral function eq.(5.4). Density of states can be written through a spectral function as follows

$$n = T \sum_m \int \frac{d^2k}{(2\pi)^2} A(i\omega_m, \vec{k}) \rightarrow -\frac{1}{4\pi i} \int \frac{d^2k}{(2\pi)^2} \int_C dz A(z, \vec{k}) f(z), \quad (5.15)$$

where $f(z) = \tanh(\frac{z}{2T})$. One can use also the Fermi distribution function $f(z) = n(z)$ with a prefactor $(-\frac{1}{2\pi i})$, which gives the same result for observables. The pressure is given by

$$p = \int_{-\infty}^{\mu} d\mu' n, \quad (5.16)$$

where in our case $\mu \equiv k_F$. For simplicity we again take $h_1 v_F \rightarrow 1$. We expand the spectral function eq.(5.4) with respect to the imaginary part of the self-energy, which we consider to be small in this calculation [28]

$$\begin{aligned} A(z, \vec{k}) &\approx 2\pi\delta(z - z_*) - \Sigma_2(z, k_F) \mathcal{P}' \frac{1}{z - z_*}, \\ \mathcal{P}' \frac{1}{z - z_*} &\equiv \frac{\partial}{\partial z} \left(\mathcal{P} \frac{1}{z - z_*} \right), \end{aligned} \quad (5.17)$$

where the pole of the propagator z_* is a solution of the equation $z - v_F k_{\perp} - \Sigma_1(z, k_F) = 0$, which does not contain imaginary part of the self energy Σ_2 . Substituting this representation in the equation for the pressure, we have

$$p = -\frac{1}{4\pi i} \frac{d^2k}{(2\pi)^2} \int_{-\infty}^{k_F} dk'_F \int_{-\infty}^{\infty} dz \left(2\pi\delta(z - z_*) + \Sigma_2(z) \mathcal{P}' \frac{1}{z_* - z} \right) f(z). \quad (5.18)$$

The frequency integral in the first term gives familiar expression for the number density

$$n = \int \frac{d^2k}{(2\pi)^2} f(z_*), \quad (5.19)$$

where usually f is a Fermi distribution function, and the dispersion relation is given by z_* (in standard notations $z_* \rightarrow \varepsilon_k$). Here we have $f(x) = \tanh(\frac{x}{2})$. Therefore integrating over k_F gives $\int dk'_F \tanh \frac{z_*}{2} \rightarrow \ln(2 \cosh \frac{z_*}{2})$ where to the leading order $z_* \sim (k - k_F)$. In the second term we interchange the order of integration in z and k_F . Therefore, $\int_{-\infty}^{k_F} dk'_F \mathcal{P}' \frac{1}{z_*(k'_F) - z} \rightarrow -\frac{1}{z_*(k_F) - z}$, to the leading order there is no k_F dependence in $\Sigma_2(z) \sim z^{2\nu}$. The second integral is $\frac{1}{2\pi i} \int_{-\infty}^{\infty} dz \Sigma_2(z, k_F) f(z) \frac{1}{z_* - z} \rightarrow \Sigma_2(z_*) f(z_*)$. Combining all the terms together we have

$$p = \int \frac{d^2k}{(2\pi)^2} \sum_{z_*} \left(\frac{1}{2} T \ln \left(2 \cosh \frac{z_*}{2T} \right) + \frac{1}{4} \Sigma_2(z_*) \tanh \frac{z_*}{2T} \right), \quad (5.20)$$

where z_* is the pole of the fermion propagator without the imaginary part Σ_2 , and there is a summation over poles. If we take z_* to be the pole of the full propagator, z_* becomes imaginary and generalization of hyperbolic functions to the Γ functions is necessary eq.(5.8). We arrive then at eq.(5.9) for the pressure of the system.

5.2 DC conductivity

We calculate the DC conductivity in the boundary theory using the “dressed” by gravity retarded/advanced fermion propagators eq.(5.3). To make the calculations complete, we need the “dressed” vertex, to satisfy Ward identities. As was argued in [22], the boundary vertex which is obtained from the bulk one can be approximated by a constant in the low temperature limit. Also, according to [26], the vertex has only singularities of the product of the Green functions. Therefore, dressing the vertex will not change temperature dependence of the DC conductivity [26].

Using linear response theory, we have

$$\sigma = -\frac{\partial}{\partial\omega}\text{Im}\Pi_{AA}(\omega, \vec{k} = 0)|_{\omega=0}, \quad (5.21)$$

which is a Kubo formula for conductivity. Here the polarization operator is given by

$$\Pi_{AA}(i\nu_n, 0) = \int \frac{d^2k}{(2\pi)^2} T \sum_{\omega_m} G(i\omega_m + i\nu_n, \vec{k}) \Lambda_A(i\omega_m + i\nu_n, i\omega_m, \vec{k}) G(i\omega_m, \vec{k}) \Lambda_A^{(0)}(\vec{k}), \quad (5.22)$$

where the fermion frequency is $\omega_m = (2m + 1)\pi T$, and boson frequency is $\nu_n = 2n\pi T$, and in the low temperature limit $\Lambda_A(i\omega_m + i\nu_n, i\omega_m, \vec{k}) = \Lambda_A^{(0)}(\vec{k})$. Usually the most difficult step is to take the Matsubara sum. Here we do it in two ways. First, analytically continuing in the complex plane $i\omega_m \rightarrow z$ and replacing the Matsubara sum by the contour integral with the Fermi distribution function $n(x) = \frac{1}{e^x + 1}$ whose poles are at the Matsubara frequencies along the imaginary axis. Second, using the spectral representation. In both cases we follow [26], where transport coefficients are calculated with propagators including imaginary parts.

In the first way, we have for the fermion Matsubara sum

$$H(i\nu_n, \vec{k}) = T \sum_{\omega_m} G(i\omega_m + i\nu_n, \vec{k}) G(i\omega_m, \vec{k}) \rightarrow -\frac{1}{2\pi i} \int_C dz G(z + i\nu_n, \vec{k}) G(z, \vec{k}) n(z), \quad (5.23)$$

where the contour along the imaginary z-axis can be deformed to contour C which goes along the two brunch cuts, $\text{Im}Z = 0$ and $\text{Im}z = -\nu_n$, and the large arcs Γ with vanishing contribution [26]. The fermion propagator has a branch cut along $\text{Im}z = 0$ [27],[26]. Therefore we can rewrite

$$\begin{aligned} H(i\nu_n) &= -\frac{1}{2\pi i} \int_{-\infty}^{\infty} d\zeta n(\zeta) G(i\nu_n + \zeta) (G_R(\zeta) - G_A(\zeta)) \\ &\quad - \frac{1}{2\pi i} \int_{-\infty}^{\infty} d\zeta n(\zeta) G(-i\nu_n + \zeta) (G_R(\zeta) - G_A(\zeta)), \end{aligned} \quad (5.24)$$

where the difference of the retarded and advanced functions in the first bracket is due to the discontinuity along $\text{Im}z = 0$ and in the second bracket due to the discontinuity along $\text{Im}z = -\nu_n$. This contribution corresponds to the second term in eq.(5.23), and there are

no pole contributions [26]. We use the usual prescription for the retarded and advanced Green functions, $G_R = G(\omega + i0^+)$ and $G_A = G(\omega - i0^+)$. We suppress momentum indices. Taking $i\nu_n \rightarrow \omega + i0^+$, we have

$$H(\omega) = -\frac{1}{2\pi i} \int_{-\infty}^{\infty} d\zeta n(\zeta) G_R(\omega + \zeta) (G_R(\zeta) - G_A(\zeta)) - \frac{1}{2\pi i} \int_{-\infty}^{\infty} d\zeta n(\zeta + \omega) G_A(\omega + \zeta) (G_R(\zeta + \omega) - G_A(\zeta + \omega)), \quad (5.25)$$

where we changed the integration variable in the second integral $\zeta - \omega \rightarrow \zeta$. In the limit $\omega \rightarrow 0$, the dominant contribution comes from the pair $G_R G_A$, and it is inversely proportional to the distance between the poles given by the imaginary part Σ_2 . Combinations $G_R G_R$ and $G_A G_A$ with the poles on one side of real axis make a much smaller contribution due to cancellation between the residues at the poles. Therefore, as $\omega \sim 0$, we have

$$H(\omega, \vec{k}) \rightarrow -\frac{1}{2\pi i} \int_{-\infty}^{\infty} d\zeta (n(\zeta + \omega) - n(\zeta)) G_R(\zeta + \omega) G_A(\zeta), \quad (5.26)$$

and

$$\text{Im}\Pi_{AA}(\omega, 0) = \frac{1}{2\pi} \int \frac{d^2 k}{(2\pi)^2} \Lambda_A^{(0)}(\vec{k}) \int_{-\infty}^{\infty} \frac{d\zeta}{2\pi} (n(\zeta + \omega) - n(\zeta)) G_R(\zeta + \omega, \vec{k}) \times \Lambda_A(\zeta + \omega + i0^+, \zeta - i0^-, \vec{k}) G_A(\zeta, \vec{k}). \quad (5.27)$$

In small T limit the vertex is a constant. We integrate around the Fermi surface, therefore momentum integral is $\int \frac{d^2 k}{(2\pi)^2} \rightarrow \frac{k_F dk_{\perp}}{(2\pi)^2}$ with $k_{\perp} = k - k_F$. We exchange the order of integration and do first the momentum integral [14],[22]. For $\omega \sim 0$, we have

$$\int_{-\infty}^{\infty} \frac{dk_{\perp}}{2\pi} \frac{1}{(\frac{\zeta}{v_F} - k_{\perp} + \Sigma(\zeta, k_F) + i0^+)(\frac{\zeta}{v_F} - k_{\perp} + \Sigma^*(\zeta, k_F) - i0^+)} = \frac{i}{\Sigma(\zeta, k_F) - \Sigma^*(\zeta, k_F)} = \frac{1}{2\text{Im}\Sigma(\zeta, k_F)}. \quad (5.28)$$

Writing $n'(\zeta) = -\beta n(\zeta)(1 - n(\zeta))$, we have for $\omega \sim 0$

$$\sigma \rightarrow \Lambda^{(0)} 2k_F h_1^2 \int_{-\infty}^{\infty} \frac{\beta d\zeta n(\zeta)(1 - n(\zeta))}{2\pi \text{Im}\Sigma(\zeta, k_F)}, \quad (5.29)$$

where we did not include constants. Note that we get the same result for conductivity when we use $\tanh \frac{x}{2}$ in the contour integral eq.(5.23) since $n'(x) = -2 \tanh'(\frac{x}{2})$.

For the Landau Fermi liquid $\Sigma(\omega) \sim \omega^2$ at small T [29],[22]. We get

$$\sigma \sim T^{-2}, \quad (5.30)$$

that means we recover the standard result for the resistivity of the Fermi liquid, $\rho \sim T^2$.

In our case, $\Sigma(\omega) \sim \omega^{2\nu_{k_F}}$,

$$\sigma \sim T^{-2\nu_{k_F}}, \quad (5.31)$$

where ν_{k_F} is the IR conformal dimension. This result agrees with the DC conductivity obtained in [22]. For the marginal liquid, $\nu_{k_F} = \frac{1}{2}$, we recover the resistivity $\rho \sim T$, which is known for strange metals. It is interesting that the scaling behavior of the DC conductivity is the same as the single particle scattering rate. In the gravity calculations it is explained by the fact that the dissipative part of the current-current correlator is controlled by the rate of the bulk fermion falling in the horizon, given by the single particle scattering rate.

To check our calculation, we get the DC conductivity using the spectral representation

$$G(i\omega_m, \vec{k}) = \int \frac{dk_0}{2\pi} \frac{A(k_0, \vec{k})}{k_0 - i\omega_m}, \quad (5.32)$$

where the spectral function $A(k_0, \vec{k})$ is given in eq.(5.4). For the product of the Green functions we use the following formula

$$T \sum_m \frac{1}{i\omega_m - \omega_1} \frac{1}{i\omega_m + i\nu_n - \omega_2} = \frac{n(\omega_1) - n(\omega_2)}{i\nu_n + \omega_1 - \omega_2}. \quad (5.33)$$

Taking $i\nu_n \rightarrow \omega + i0^+$, the polarization operator is given by

$$\Pi_{AA}(\omega, 0) = \int \frac{d^2k}{(2\pi)^2} \frac{d\omega_1}{2\pi} \frac{d\omega_2}{2\pi} \frac{n(\omega_1) - n(\omega_2)}{\omega + \omega_1 - \omega_2} \Lambda_A^{(0)2} A(\omega_1, k_\perp) A(\omega_2, k_\perp). \quad (5.34)$$

Performing integration over ω_2 , we have

$$\text{Im}\Pi_{AA}(\omega, 0) = \int \frac{d^2k}{(2\pi)^2} \frac{d\omega_1}{2\pi} (n(\omega_1) - n(\omega_2)) \Lambda_A^{(0)2} A(\omega_1, k_\perp) A(\omega_1 + \omega, k_\perp). \quad (5.35)$$

In the limit $\omega \sim 0$, the momentum integration is

$$\int \frac{d^2k}{(2\pi)^2} A^2(\omega_1, k_\perp) \rightarrow k_F \int \frac{dk_\perp}{2\pi} A^2(\omega_1, k_\perp) \rightarrow \frac{k_F h_1^2}{\Sigma_2(\omega_1, k_F)}, \quad (5.36)$$

with $\Sigma_2 = \text{Im}\Sigma$. Therefore the DC conductivity given by eq.(5.21) is

$$\sigma \rightarrow \Lambda_A^{(0)2} k_F h_1^2 \int \frac{\beta d\omega_1}{2\pi} \frac{n(\omega_1)(1 - n(\omega_1))}{\text{Im}\Sigma(\omega_1, k_F)} \quad (5.37)$$

which is the same as eq.(5.29) obtained by the contour integration.

6. Discussion

In this article we studied the particle-hole pairing in the context of the magnetic catalysis. The Reissner-Nordstrom charged black hole can carry Fermi surfaces [14], in a sense that one has a Fermi liquid in the bulk: there are Fermi surfaces and free fermions fill all the levels up to the Fermi surface. It is natural to expect pairing between fermions (particle and hole in this case) when an attractive interaction is introduced. At the *CFT* boundary, we indeed get pairing instability for the Fermi liquids. However, quite surprisingly, there is no pairing realized for the non-Fermi liquids. We show that in variational calculations where

both terms in the r.h.s. of the gap equation vanish near the Fermi surface. In the bulk Ginsburg-Landau calculations, we obtain the critical temperature which vanish exactly at the *IR CFT* conformal dimension $\nu_{k_F} = \frac{1}{2}$, which is the border between Fermi and non-Fermi liquids. T_c stays zero for $\nu_{k_F} < \frac{1}{2}$. The same conclusion has been reached for the superconducting instability in [14]. Probably the reason is that there are no well defined quasiparticles in case of non-Fermi liquids, in particular the residue for the fermion pole vanishes around the Fermi surface [18]. Note, that we have well defined particle degrees of freedom in the bulk, while the situation is different when it is projected to the boundary. As suggested in [14], the momentum/frequency dependent four-Fermi interaction may help to realize pairing for the non-Fermi liquids.

Our calculations are different from the corresponding calculations in the field theory in several aspects. We have imagined the existence of an “experimental knob” which can be used to adjust the UV scaling dimension Δ of an operator, and therefore an ability to get different *CFT*’s, e.g., describing Fermi and non-Fermi liquids. As discussed in [18], the most useful knob will likely depend on the UV geometry into which this *AdS*₂ is embedded. For example, in our case an external magnetic field will allow one to tune the *IR* scaling dimension ν . We obtain a radial profile for the order parameter $\Delta(r) \sim \psi^0(r)^\dagger \sigma^1 \psi^0(r)$ where $\psi^0(r)$ are the zero modes with $\omega = 0$ and $k = k_F$. For the Fermi liquids, $\nu_{k_F} > \frac{1}{2}$, $\Delta(r)$ is supported near the *CFT* boundary, and for the non-Fermi liquids, $\nu_{k_F} < \frac{1}{2}$, $\Delta(r)$ is supported near the horizon where the Fermi velocity is considerably smaller than the speed of light $v_F \ll c$. The radial profile of $\Delta(r)$ with correct fall off is important to insure convergence of the radial integrals.

In the presence of the particle-hole condensate $\langle \bar{\psi} i \Gamma^{\hat{2}} \Gamma^{\hat{5}} \psi \rangle$, the Fermi momenta corresponding to the bulk fermions with spin up and down are shifted in the opposite directions. We did not introduce spins in the boundary theory. Therefore association with the bulk spins is understood as upper and lower components of the 4-component fermion field. For a fixed fermion charge we obtain multiple Fermi surfaces. This is the consequence of the *AdS* geometry effectively behaving as a box potential. It is interesting to understand the physical picture behind the multiple Fermi surfaces, and if pairing between different Fermi surfaces brings new physics.

In this paper the particle-hole pairing was considered on a very general ground. Therefore its evidence can be relevant for the chiral spirals [3] in the chiral magnetic effect [30] and the spin density waves, and can serve as a guide to construct an antiferromagnetic and Mott insulating states of the cuprate superconductors. In particular, it can be useful to describe the coexisting AFM and SC order parameters in the iron pnictides [31]. Recent work on non-abelian holographic superconductors [9] makes applications to color superconductivity possible.

It will be instructive to obtain, in analogy to the superconducting instability, to obtain the particle-hole condensation from the classical Einstein gravity calculations with the neutral scalar field.

We considered thermodynamic and transport properties of the boundary field theory. We did not specify the boundary theory. Using the “dressed” by the gravity fermion propagator G_R we obtained the equation of state, which includes a sum over all the poles

of G_R . We use prescription of [16],[17] to treat imaginary poles. Imaginary self-energy is a consequence of inelastic scattering by the black hole, and will be present in any gravity calculations. In particular the imaginary part provides finite transport coefficients. The scaling behavior for the heat capacity is $c \sim T$ for the Fermi liquid and $c \sim T^{2\nu}$, while it is the same in both cases for the DC conductivity $\sigma \sim T^{-2\nu}$. It reflects the fact that the specific heat depends on the dispersion relation, in particular on the real part of ω , while the DC conductivity is sensitive only to the scaling of the self-energy.

The presented approach has an advantage of unifying description of the Fermi and non-Fermi liquids within one framework. It uses the language of poles and branch cuts instead of quasiparticles, that may be more adequate description for some strongly correlated systems.

Acknowledgements

I am grateful to Dirk Rischke for giving me an opportunity to complete this work. The author thanks Tom Faulkner, Daniel Fernandez-Fraile, Tom Hartman, Nabil Iqbal, Tomoi Koide, Hong Liu, Mark Mezei, Volodya Miransky, Andreas Schmitt and Igor Shovkovy for helpful inputs and discussions, and Armen Sedrakian for useful suggestions and work on the manuscript. The work was supported in part by the Alliance program of the Helmholtz Association, contract HA216/EMMI “Extremes of Density and Temperature: Cosmic Matter in the Laboratory” and ITP of Goethe University, Frankfurt.

A. Dirac equation in the AdS_4

Here we discuss the Dirac equation in the presence of the magnetic field the AdS_4 , and show how Landau levels appear for the (x, y) part, dimensions of the boundary theory. The (x, y) part of the Dirac equation decouples from the radial part and can be solved exactly due to the translational invariance in perpendicular directions. Then we find the conformal dimension of the spinor operator in the $IR CFT$. Depending on the IR conformal dimension the boundary theory describes Fermi, marginal and non-Fermi liquids.

A.1 Dirac equation with magnetic field in a charged black hole geometry AdS_4

Here we solve analytically the part of the Dirac which depends on magnetic field and space-time coordinates of the boundary theory. The free spinor action in the geometry eq.(2.2) and in the presence of magnetic field eq.(2.3) is given by

$$S_0 = i \int d^4x \sqrt{-g} \bar{\psi} (\Gamma^M \mathcal{D}_M - m) \psi, \quad (A.1)$$

where $\bar{\psi} = \psi^\dagger \Gamma^{\hat{t}}$, and

$$\mathcal{D}_M = \partial_M + \frac{1}{4} \omega_{abM} \Gamma^{ab} - iq A_M, \quad (A.2)$$

with ω_{abM} the spin connection, and $\Gamma^{ab} = \frac{1}{2}[\Gamma^a, \Gamma^b]$; here M and a, b denote the bulk space-time and tangent space indices respectively, and μ, ν denote indices along the boundary directions, i.e. $M = (r, \mu)$; indices with hat refer to tangent space ones, i.e. converting

from bulk to tangent indices $\Gamma^M = e^M_{\hat{a}} \Gamma^{\hat{a}}$ with $e^{\hat{a}} = e^{\hat{a}}_M dx^M$ are the tetrads defined by the metric eq.(2.2), $ds^2 = g_{MN} dx^M dx^N = \eta_{\hat{a}\hat{b}} e^{\hat{a}} e^{\hat{b}}$ and $\eta_{\hat{a}\hat{b}} = \text{diag}(-1, 1, 1, 1)$ is the flat metric.

Using the translational invariance,

$$\psi(t, x, y, r) = \int d\omega dk e^{-i\omega t + ikx} \psi(\omega, k, y, r), \quad (\text{A.3})$$

with $k \equiv k_x$, the Dirac equation is given by

$$\left(\frac{1}{\sqrt{-g_{tt}}} \Gamma^{\hat{t}} (-i\omega + \frac{1}{2} \omega_{\hat{t}\hat{r}} \Gamma^{\hat{t}\hat{r}} - iqA_t(r)) + \frac{1}{\sqrt{g_{rr}}} \Gamma^{\hat{r}} \partial_r + \frac{1}{\sqrt{g_{ii}}} \Gamma^{\hat{x}} (ik + \frac{1}{2} \omega_{\hat{x}\hat{r}} \Gamma^{\hat{x}\hat{r}} - iqA_x(y)) \right. \\ \left. + \frac{1}{\sqrt{g_{ii}}} \Gamma^{\hat{y}} (\partial_y + \frac{1}{2} \omega_{\hat{y}\hat{r}} \Gamma^{\hat{y}\hat{r}}) - m \right) \psi(\omega, k, y, r) = 0, \quad (\text{A.4})$$

where $g_{ii} \equiv g_{xx} = g_{yy}$, and $A_t(r) = \mu(1 - r_0/r)$, $A_x(y) = -\mathcal{H}y$. From the torsion-free condition, $\omega_b^a \wedge e^b = -de^a$, we find the spin connection [32] for the metric 2.2,

$$\omega_{\hat{t}\hat{r}} = -\frac{\partial_r(\sqrt{-g_{tt}})}{\sqrt{g_{rr}}} dt, \quad \omega_{\hat{x}\hat{r}} = \frac{\partial_r(\sqrt{g_{ii}})}{\sqrt{g_{rr}}} dx^i, \quad (\text{A.5})$$

where $i = x, y$. Note that

$$-\Gamma^{\hat{t}} \Gamma^{\hat{t}\hat{r}} = \Gamma^{\hat{x}} \Gamma^{\hat{x}\hat{r}} = \Gamma^{\hat{y}} \Gamma^{\hat{y}\hat{r}} = \Gamma^{\hat{r}}, \quad (\text{A.6})$$

and

$$\frac{1}{4} e^M_{\hat{a}} \Gamma^{\hat{a}} \omega_{\hat{b}\hat{c}M} \Gamma^{\hat{b}\hat{c}} = \frac{1}{4} \frac{1}{\sqrt{-g_{tt}}} \frac{\partial_r(\sqrt{-g_{tt}})}{\sqrt{g_{rr}}} \Gamma^{\hat{r}} + \frac{2}{4} \frac{1}{\sqrt{g_{ii}}} \frac{\partial_r \sqrt{g_{ii}}}{\sqrt{g_{rr}}} \Gamma^{\hat{r}} \\ = \frac{1}{\sqrt{g_{rr}}} \Gamma^{\hat{r}} \partial_r \ln \left(-\frac{g}{g_{rr}} \right)^{1/4}, \quad (\text{A.7})$$

where g is the determinant of the metric. Therefore, we can rescale the spinor field

$$\psi = \left(-\frac{g}{g_{rr}} \right)^{-1/4} \Phi, \quad (\text{A.8})$$

and remove the spin connection completely. The new action is given by

$$S_0 = \int d^4x \sqrt{g_{rr}} i \bar{\Phi} (\Gamma^M \mathcal{D}'_M - m) \Phi, \quad (\text{A.9})$$

where the covariant derivative does not contain spin connection, $\mathcal{D}'_M = \partial_M - iqA_M$.

In new field variables, the Dirac equation is given by

$$\left(\frac{\sqrt{g_{ii}}}{\sqrt{g_{rr}}} \Gamma^{\hat{r}} \partial_r - \frac{\sqrt{g_{ii}}}{\sqrt{-g_{tt}}} \Gamma^{\hat{t}} i(\omega + q\mu(1 - \frac{r_0}{r})) - \sqrt{g_{ii}} m + \Gamma^{\hat{x}} i(k + q\mathcal{H}y) \right. \\ \left. + \Gamma^{\hat{y}} \partial_y \right) \Phi(\omega, k, y, r) = 0. \quad (\text{A.10})$$

We separate y and r dependences,

$$P(r) = \frac{\sqrt{g_{ii}}}{\sqrt{g_{rr}}} \Gamma^{\hat{r}} \partial_r - \frac{\sqrt{g_{ii}}}{\sqrt{-g_{tt}}} \Gamma^{\hat{t}} i(\omega + q\mu(1 - \frac{r_0}{r})) - \sqrt{g_{ii}} m, \\ Q(y) = \Gamma^{\hat{x}} i(k + q\mathcal{H}y) + \Gamma^{\hat{y}} \partial_y, \quad (\text{A.11})$$

and the Dirac equation is

$$(P(r) + Q(y))\Phi = 0. \quad (\text{A.12})$$

Though, $[P(r), Q(y)] \neq 0$, one can find a transformation matrix U such that $[UP(r), UQ(y)] = 0$, and then look for common eigenvectors of $UP(r)$ and $UQ(y)$ since they are commuting hermitian operators, i.e. the Dirac equation reads

$$UP(r)\Phi_n = -UQ(y)\Phi_n = \lambda_n\Phi_n, \quad (\text{A.13})$$

where n will label the Landau levels. In the main text we use l for the Landau index, in order not to confuse with the Matsubara frequency index n . Transformation matrix U should satisfy conditions

$$\{U, \Gamma^{\hat{r}}\} = 0, \quad \{U, \Gamma^{\hat{t}}\} = 0, \quad [U, \Gamma^{\hat{x}}] = 0, \quad [U, \Gamma^{\hat{y}}] = 0, \quad (\text{A.14})$$

which do not fix U completely. It is convenient to use the following basis [18],

$$\begin{aligned} \Gamma^{\hat{r}} &= \begin{pmatrix} -\sigma^3 & 0 \\ 0 & -\sigma^3 \end{pmatrix}, \quad \Gamma^{\hat{t}} = \begin{pmatrix} i\sigma^1 & 0 \\ 0 & i\sigma^1 \end{pmatrix}, \quad \Gamma^{\hat{x}} = \begin{pmatrix} -\sigma^2 & 0 \\ 0 & \sigma^2 \end{pmatrix}, \\ \Gamma^{\hat{y}} &= \begin{pmatrix} 0 & \sigma^2 \\ \sigma^2 & 0 \end{pmatrix}, \quad \Gamma^{\hat{z}} = \begin{pmatrix} 0 & i\sigma^2 \\ -i\sigma^2 & 0 \end{pmatrix}. \end{aligned} \quad (\text{A.15})$$

Note, that the usual relation holds

$$\Gamma^{\hat{z}} = \Gamma^{\hat{0}}\Gamma^{\hat{1}}\Gamma^{\hat{2}}\Gamma^{\hat{3}}, \quad (\text{A.16})$$

with $0 \rightarrow t, 1 \rightarrow x, 2 \rightarrow y, 3 \rightarrow r$. In the representation of eq.(A.15), we can choose

$$U = \begin{pmatrix} -i\sigma^2 & 0 \\ 0 & -i\sigma^2 \end{pmatrix}. \quad (\text{A.17})$$

Writing $\Phi = (F_1, F_2)^T$, and using eq.(A.31), we get the Dirac equation written in a compact form, eq.(A.13),

$$\left(-\frac{\sqrt{g_{ii}}}{\sqrt{g_{rr}}}\sigma^1\partial_r + \sqrt{g_{ii}}i\sigma^2m - \frac{\sqrt{g_{ii}}}{\sqrt{-g_{tt}}}\sigma^3(\omega + q\mu(1 - r_0/r)) - \lambda_n \right) \otimes 1 \begin{pmatrix} F_1 \\ F_2 \end{pmatrix} = 0 \quad (\text{A.18})$$

$$1 \otimes \begin{pmatrix} -(k + q\mathcal{H}y) + \lambda_n & -i\partial_y \\ -i\partial_y & (k + q\mathcal{H}y) + \lambda_n \end{pmatrix} \begin{pmatrix} F_1 \\ F_2 \end{pmatrix} = 0, \quad (\text{A.19})$$

where in $X \otimes Y$, X acts inside F_1 or F_2 and Y acts between F_1 and F_2 . In eq.(??), the 1 in the first equation shows that there is no mixing of F_1 and F_2 by the operator $UP(r)$ and the 1 in the second equation means that there is no mixing inside F_1 or F_2 by the operator $UQ(y)$. Therefore solution can be represented as

$$\begin{pmatrix} F_1 \\ F_2 \end{pmatrix} = \begin{pmatrix} f_n^{(1)}(r)g_n^{(1)}(y) \\ f_n^{(2)}(r)g_n^{(1)}(y) \\ f_n^{(1)}(r)g_n^{(2)}(y) \\ f_n^{(2)}(r)g_n^{(2)}(y) \end{pmatrix}, \quad (\text{A.20})$$

we do not write ω and k dependences. Dirac equations for each component are

$$\begin{aligned} \left(\frac{\sqrt{g_{ii}}}{\sqrt{g_{rr}}} \partial_r + \sqrt{g_{ii}} m \right) f_n^{(1)}(r) + \left(-\frac{\sqrt{g_{ii}}}{\sqrt{-g_{tt}}} (\omega + q\mu(1 - r_0/r)) + \lambda_n \right) f_n^{(2)}(r) &= 0, \\ \left(\frac{\sqrt{g_{ii}}}{\sqrt{g_{rr}}} \partial_r - \sqrt{g_{ii}} m \right) f_n^{(2)}(r) + \left(\frac{\sqrt{g_{ii}}}{\sqrt{-g_{tt}}} (\omega + q\mu(1 - r_0/r)) + \lambda_n \right) f_n^{(1)}(r) &= 0, \end{aligned} \quad (\text{A.21})$$

$$\begin{aligned} -i\partial_y g_n^{(1)}(y) + ((k + q\mathcal{H}y) + \lambda_n) g_n^{(2)} &= 0, \\ -i\partial_y g_n^{(2)} + (-(k + q\mathcal{H}y) + \lambda_n) g_n^{(1)} &= 0. \end{aligned} \quad (\text{A.22})$$

In equations A.22 for the y dependence, we rescale $\tilde{y} = \sqrt{|Q\mathcal{H}|} (y + k/q\mathcal{H})$ and $\lambda_n = \sqrt{|q\mathcal{H}|} \tilde{\lambda}_n$, and get

$$\begin{aligned} -i\partial_{\tilde{y}} g_n^{(1)} + (\tilde{y} + \tilde{\lambda}_n) g_n^{(2)} &= 0, \\ -i\partial_{\tilde{y}} g_n^{(2)} + (-\tilde{y} + \tilde{\lambda}_n) g_n^{(1)} &= 0. \end{aligned} \quad (\text{A.23})$$

The second order ODE

$$\begin{aligned} \partial_{\tilde{y}}^2 g^{(1)} - \frac{1}{\tilde{y} + \tilde{\lambda}} \partial_{\tilde{y}} g^{(1)} + (\tilde{\lambda}^2 - \tilde{y}^2) g^{(1)} &= 0, \\ \partial_{\tilde{y}}^2 g^{(2)} - \frac{1}{-\tilde{y} + \tilde{\lambda}} \partial_{\tilde{y}} g^{(2)} + (\tilde{\lambda}^2 - \tilde{y}^2) g^{(2)} &= 0, \end{aligned} \quad (\text{A.24})$$

are solved by substitution $g^{(1)} = e^{-\tilde{y}^2/2} \tilde{g}^{(1)}$ and $g^{(2)} = \pm i e^{-\tilde{y}^2/2} \tilde{g}^{(2)}$. The eigenfunctions are Hermite polynomials. We get the same eigenvalues, but slightly different eigenfunctions for different signs of $q\mathcal{H}$. Putting all together, for $q\mathcal{H} > 0$, we have

$$\begin{aligned} \tilde{\lambda}_{-1} &= 0 : \\ g_{-1}^{(1)}(\tilde{y}) &= e^{-\tilde{y}^2/2}, \quad g_{-1}^{(2)}(\tilde{y}) = -i e^{-\tilde{y}^2/2} \\ \tilde{\lambda}_n^\pm &= \pm \sqrt{2(n+1)} : \\ g_n^{(1)\pm}(\tilde{y}) &= e^{-\tilde{y}^2/2} \left(H_n(\tilde{y}) \pm \frac{1}{\sqrt{2(n+1)}} H_{n+1}(\tilde{y}) \right), \\ g_n^{(2)\pm}(\tilde{y}) &= i e^{-\tilde{y}^2/2} \left(H_n(\tilde{y}) \mp \frac{1}{\sqrt{2(n+1)}} H_{n+1}(\tilde{y}) \right), \end{aligned} \quad (\text{A.25})$$

and for $q\mathcal{H} < 0$, we have

$$\begin{aligned} \tilde{\lambda}_{-1} &= 0 : \\ g_{-1}^{(1)}(\tilde{y}) &= e^{-\tilde{y}^2/2}, \quad g_{-1}^{(2)}(\tilde{y}) = i e^{-\tilde{y}^2/2} \\ \tilde{\lambda}_n^\pm &= \pm \sqrt{2(n+1)} : \\ g_n^{(1)\pm}(\tilde{y}) &= e^{-\tilde{y}^2/2} \left(H_n(\tilde{y}) \mp \frac{1}{\sqrt{2(n+1)}} H_{n+1}(\tilde{y}) \right), \\ g_n^{(2)\pm}(\tilde{y}) &= -i e^{-\tilde{y}^2/2} \left(H_n(\tilde{y}) \pm \frac{1}{\sqrt{2(n+1)}} H_{n+1}(\tilde{y}) \right), \end{aligned} \quad (\text{A.26})$$

The case $q\mathcal{H} < 0$ can be obtained from the case $q\mathcal{H} > 0$ by replacing $g^{(1)}[q\mathcal{H} < 0] = -ig^{(2)}[q\mathcal{H} > 0]$ and $g^{(2)}[q\mathcal{H} < 0] = -ig^{(1)}[q\mathcal{H} > 0]$. Using the eigenvalues, eqs.(A.26,A.27), in the equation for the radial part, eq.(A.21), we get

$$\begin{aligned} & \left(\frac{\sqrt{g_{ii}}}{\sqrt{g_{rr}}} \partial_r + \sqrt{g_{ii}m} \right) f_n^{(1)\pm}(r) \\ & + \left(-\frac{\sqrt{g_{ii}}}{\sqrt{-g_{tt}}} (\omega + q\mu(1 - r_0/r)) \pm \sqrt{2|q\mathcal{H}|(n+1)} \right) f_n^{(2)\pm}(r) = 0, \\ & \left(\frac{\sqrt{g_{ii}}}{\sqrt{g_{rr}}} \partial_r - \sqrt{g_{ii}m} \right) f_n^{(2)\pm}(r) \\ & + \left(\frac{\sqrt{g_{ii}}}{\sqrt{-g_{tt}}} (\omega + q\mu(1 - r_0/r)) \pm \sqrt{2|q\mathcal{H}|(n+1)} \right) f_n^{(1)\pm}(r) = 0. \end{aligned} \quad (\text{A.27})$$

These equations can be obtained by replacing

$$k \rightarrow \pm \sqrt{2|q\mathcal{H}|(n+1)}, \quad (\text{A.28})$$

in the Dirac equation at zero magnetic field [16]. Equation (A.28) also gives a prescription how to treat the limit of zero magnetic field, i.e. the $\mathcal{H} \rightarrow 0$ limit is taken keeping $2|q\mathcal{H}|(n+1) \equiv k^2$ fixed as $\mathcal{H} \rightarrow 0$. In a compact form the Dirac equation, eq.(A.18), in a magnetic field reads

$$\begin{aligned} & \left(-\frac{1}{\sqrt{g_{rr}}} \sigma^3 \partial_r - m + \frac{1}{\sqrt{-g_{tt}}} \sigma^1 (\omega + q\mu(1 - r_0/r)) \right. \\ & \left. \mp \frac{1}{\sqrt{g_{ii}}} i\sigma^2 \sqrt{2|q\mathcal{H}|(n+1)} \right) \otimes 1 \begin{pmatrix} F_1 \\ F_2 \end{pmatrix} = 0, \end{aligned} \quad (\text{A.29})$$

which coincides with eq. (A14) in [18] with the replacement eq.(A.28). The starting Dirac equation in a magnetic field, eq.(A.10), is given by

$$\begin{aligned} & \left(\frac{1}{\sqrt{g_{rr}}} \Gamma^{\hat{r}} \partial_r - \frac{1}{\sqrt{-g_{tt}}} \Gamma^{\hat{t}} i(\omega + q\mu(1 - \frac{r_0}{r})) - m \right. \\ & \left. \mp \frac{1}{\sqrt{g_{ii}}} U^{-1} \sqrt{2|q\mathcal{H}|(n+1)} \right) \Phi(r) = 0, \end{aligned} \quad (\text{A.30})$$

we do not write ω dependence, $\Phi = (F_1, F_2)^T$, $n = -1, 0, 1, \dots$; and where U^{-1} is the inverse matrix to the transformation matrix eq.(A.31)

$$U^{-1} = \begin{pmatrix} i\sigma^2 & 0 \\ 0 & i\sigma^2 \end{pmatrix}. \quad (\text{A.31})$$

We use equation (A.30) in the main text.

A.2 Dirac equation. Conformal dimension in the low frequency limit

As outlined in [16, 17], the fermion determinant in the black hole background is given by a sum over the quasinormal frequencies $z_* = i\omega_n$, that are obtained as complex frequencies which give zero eigenvalues, $\lambda = 0$, of the Dirac equation. The eigenvalues are given by

$$\left(\Gamma^M \mathcal{D}_M - m - \Delta i \Gamma^{\hat{2}} \Gamma^{\hat{5}} \pm q\mathcal{H} \Gamma^{\hat{t}} \right) \psi = \lambda \psi. \quad (\text{A.32})$$

In Appendix A.1, we simplified the Dirac equation obtained from the free fermion action eq.(3.2). We rescaled the original fermion field, eq.(A.8), as was done in [18], and removed the spin connection, with the result eq.(A.9) and eq.(A.10). In new field variables, the Dirac equation is

$$\left(\Gamma^M \mathcal{D}'_M - m - \Delta i \Gamma^{\hat{2}} \Gamma^{\hat{5}} \pm q \mathcal{H} \Gamma^{\hat{t}}\right) \Phi = 0, \quad (\text{A.33})$$

where $\mathcal{D}_M = \partial_M - iqA_M$. It is written in the geometry eq.(2.2) and in the Landau gauge as

$$\left(\frac{1}{\sqrt{g_{rr}}} \Gamma^{\hat{r}} \partial_r - \frac{1}{\sqrt{-g_{tt}}} i \Gamma^{\hat{t}} (\omega + q\mu(1 - \frac{r_0}{r})) - m + \frac{1}{\sqrt{g_{ii}}} i \Gamma^{\hat{x}} (k + q\mathcal{H}y) + \frac{1}{\sqrt{g_{ii}}} \Gamma^{\hat{y}} \partial_y - i \Delta \Gamma^{\hat{2}} \Gamma^{\hat{5}} \pm q \mathcal{H} \Gamma^{\hat{t}}\right) \Phi = 0, \quad (\text{A.34})$$

with $k \equiv k_x$, $k_y = 0$. At the boundary, $r \rightarrow \infty$, the frequency ω is measured from the effective chemical potential $q\mu$. The dependence on charge q of ψ -field enters only through the combination $q\mu$. Also as given in Appendix A, in the Landau gauge eq.(2.9) the radial and y dependences decouple, eq.(A.18) and eq.(A.19), and y dependence reduces to the harmonic oscillator. We solve the y dependent part of the Dirac equation, eqs.(A.26) and (A.27), and use the result in the radial part of the Dirac equation. The procedure of obtaining the Dirac equation at nonzero magnetic field amounts to replacing

$$k \rightarrow \pm \sqrt{2|q\mathcal{H}l} \quad (\text{A.35})$$

in the Dirac equation at zero magnetic field. As compared to eq.(A.28), eq.(A.35) takes into account the Zeeman splitting term. The result for non-interacting fermions is given by eq.(A.30), which agrees with [16, 17]. The Dirac equation is written as

$$\left(\frac{1}{\sqrt{g_{rr}}} \Gamma^{\hat{r}} \partial_r - \frac{1}{\sqrt{-g_{tt}}} i \Gamma^{\hat{t}} (\omega + q\mu(1 - \frac{r_0}{r})) - m \mp \frac{1}{\sqrt{g_{ii}}} U^{-1} \sqrt{2|q\mathcal{H}l} - \Delta i \Gamma^{\hat{2}} \Gamma^{\hat{5}}\right) \Phi = 0, \quad (\text{A.36})$$

where $l = 0, 1, \dots$. The Γ matrices are defined in eq.(A.15) as in [18] and U^{-1} is given by eq.(A.31).

We split the 4-component spinors into two 2-component spinors (we do not write zero entries) $F = (F_1, F_2)^T$ where the index $\alpha = 1, 2$ is the Dirac index of the boundary theory, using projectors

$$\Pi_\alpha = \frac{1}{2}(1 - (-1)^\alpha \Gamma^{\hat{r}} \Gamma^{\hat{t}} \Gamma^{\hat{1}}), \quad \alpha = 1, 2, \quad \Pi_1 + \Pi_2 = 1, \quad (\text{A.37})$$

which commute with the Dirac operator of eq.(A.42), and $F_\alpha = \Pi_\alpha \Phi$, $\alpha = 1, 2$, decouple from each other. Gamma matrices were chosen in such a way that this decoupling is possible. The Dirac equation for two components is given by

$$\left(-\frac{1}{\sqrt{g_{rr}}} \sigma^3 \partial_r - m + \frac{1}{\sqrt{-g_{tt}}} \sigma^1 (\omega + q\mu(1 - r_0/r)) \mp \frac{1}{\sqrt{g_{ii}}} i \sigma^2 \sqrt{2|q\mathcal{H}l} + (-1)^\alpha s \Delta\right) F_\alpha = 0, \quad (\text{A.38})$$

where $s = \pm \text{sgn}(q\mathcal{H})$. To obtain the retarded Green function for fermionic operator O in the boundary theory, we need to find a solution Φ which satisfies the ingoing boundary conditions at the horizon, and to expand it near the boundary at $r \rightarrow \infty$ as

$$\begin{aligned} F_1 &\approx a_1 r^{m_1 R} \begin{pmatrix} 0 \\ 1 \end{pmatrix} + b_1 r^{-m_1 R} \begin{pmatrix} 1 \\ 0 \end{pmatrix}, \\ F_2 &\approx a_2 r^{m_2 R} \begin{pmatrix} 0 \\ 1 \end{pmatrix} + b_2 r^{-m_2 R} \begin{pmatrix} 1 \\ 0 \end{pmatrix}, \end{aligned} \quad (\text{A.39})$$

where a_α is the source and b_α is the v.e.v. in the Green function terminology, and the two masses are $m_1 \equiv m + \Delta$, $m_2 \equiv |m - \Delta|$. The conformal dimension Δ_ψ of \mathcal{O} is given in terms of the mass of ψ field by eq.(3.1), $\Delta_\psi = \frac{3}{2} + m_i R$. The two spinors $(1, 0)$ and $(0, 1)$ are eigenspinors of $\Gamma^{\hat{r}}$ with opposite eigenvalues, implying that a_α and b_α are canonically conjugate (in a radial Hamiltonian slicing) [23]. Depending on the value of the exponent, we impose different boundary condition for a_α and/or b_α . The retarded Green function is given by [33, 23, 34]

$$G_R(\omega, k) = \begin{pmatrix} G_1(\omega, k) & 0 \\ 0 & G_2(\omega, k) \end{pmatrix}, \quad \text{with } G_\alpha(\omega, k) = \frac{b_\alpha}{a_\alpha}, \quad \alpha = 1, 2, \quad (\text{A.40})$$

with $k \rightarrow \sqrt{2|q\mathcal{H}|\bar{l}}$.

For a general Reissner-Nordstrom black hole background there is no mixing between F_1 and F_2 (interaction term S_{int} is diagonal), and in the absence of Δ -term two fields F_1 and F_2 have coincident Fermi surfaces (at $\omega + q\mu = 0$ at the boundary $r \rightarrow \infty$). With the Δ term, there is a relative shift of the Fermi surface in the spectrum of F_1 and F_2 . In the following, we consider only one component, e.g., F_1 .

We could have solved eq.(A.38) with the ingoing boundary conditions at the horizon numerically. Instead, we use analytical results of [18], and for that we need to extract information from the low-energy limit of the theory. In section 4, we follow [14] and solve the Dirac equation at zero frequency, and then use the matching procedure to extract the retarded Green function of the boundary theory. For now we use results from [18, 20]. We will be interested in the poles of the retarded Green function. As was shown in [18], the nonanalytic part of the retarded Green function in the extremal Reissner-Nordstrom black hole background eq.(2.2) comes from the IR region, which has a simpler geometry than AdS_4 . At small frequencies, $\omega \rightarrow 0$, the metric reduces to $\text{AdS}_4 \rightarrow \text{AdS}_2 \times R_2$ at the horizon

$$ds^2 = \frac{R_2^2}{\zeta^2} (-d\tau^2 + d\zeta^2) + \frac{r_{**}^2}{R^2} d\bar{x}^2, \quad A_\tau = \frac{g_F}{\sqrt{12}} \frac{r_*^2}{r_{**}^2} \frac{1}{\zeta}, \quad A_x = -\mathcal{H}y, \quad (\text{A.41})$$

which is called the IR region [18]. In the IR region, the Dirac equation (A.38) becomes

$$\left(-\frac{1}{\sqrt{g_{\zeta\zeta}}} \sigma^3 \partial_\zeta - m + \frac{1}{\sqrt{-g_{\tau\tau}}} \sigma^1 \left(\omega + \frac{qg_F}{\sqrt{12}} \frac{r_*^2}{r_{**}^2} \frac{1}{\zeta} \right) - \frac{1}{\sqrt{g_{ii}}} i\sigma^2 \sqrt{2|q\mathcal{H}|\bar{l}} - s\Delta \right) F = 0, \quad (\text{A.42})$$

where we omit index by the spinor field. We can write explicitly

$$\begin{pmatrix} \frac{\zeta}{R_2} \partial_\zeta + m + s\Delta & -\frac{\zeta}{R_2} \left(\omega + \frac{qg_F}{\sqrt{12}} \frac{r_*^2}{r_{**}^2} \frac{1}{\zeta} \right) + \frac{R}{r_{**}} \sqrt{2|q\mathcal{H}|l} \\ \frac{\zeta}{R_2} \left(\omega + \frac{qg_F}{\sqrt{12}} \frac{r_*^2}{r_{**}^2} \frac{1}{\zeta} \right) + \frac{R}{r_{**}} \sqrt{2|q\mathcal{H}|l} & \frac{\zeta}{R_2} \partial_\zeta - m - s\Delta \end{pmatrix} \begin{pmatrix} y \\ z \end{pmatrix} = 0. \quad (\text{A.43})$$

At the AdS_2 boundary, $\zeta \rightarrow 0$, the Dirac equation to the leading order is

$$\zeta \partial_\zeta \Phi = -U \Phi, \quad U = \begin{pmatrix} R_2(m + s\Delta) & -\frac{qg_F}{\sqrt{12}} \frac{r_*^2}{r_{**}^2} + \frac{R_2 R}{r_{**}} \sqrt{2|q\mathcal{H}|l} \\ \frac{qg_F}{\sqrt{12}} \frac{r_*^2}{r_{**}^2} + \frac{R_2 R}{r_{**}} \sqrt{2|q\mathcal{H}|l} & -R_2(m + s\Delta) \end{pmatrix} \quad (\text{A.44})$$

Diagonalizing matrix U , we obtain the conformal dimension for the operator \mathcal{O} in the IR CFT dual to Φ ,

$$\begin{aligned} \delta_\psi &= \frac{1}{2} + \nu, \\ \nu &= \sqrt{\left((m + s\Delta)^2 + \frac{R^2}{r_{**}^2} 2|q\mathcal{H}|l \right) R_2^2 - \frac{q^2 g_F^2}{12} \frac{r_*^4}{r_{**}^4}}, \end{aligned} \quad (\text{A.45})$$

where the AdS_2 curvature radius is $R_2 = R/\sqrt{6}$, the Landau level index $l = 0, 1, \dots$ and $s = \pm \text{sign}(q\mathcal{H})$. The conformal dimension of the fermionic operator in the IR CFT in the chiral limit $m = 0$ and at the Fermi surface is given by

$$\nu_{k_F} = \sqrt{\left(\frac{k_F^2 R^2}{r_{**}^2} + \Delta^2 \right) R_2^2 - \frac{q^2 g_F^2}{12} \frac{r_*^4}{r_{**}^4}}, \quad (\text{A.46})$$

with $k_F = q\mu$, $\mu = \sqrt{3}g_F \frac{r_*^2}{R^2 r_0}$. We use the IR conformal dimension of the fermionic operator in the main text.

B. Dirac equation in the AdS_2

Here we discuss the Dirac equation in the AdS_2 . We obtain the conformal dimension of the spinor operator in the CFT_1 , which gives (with trivial modifications) the conformal dimension of the operator in the original CFT_{2+1} in the IR region. It controls the behavior of the theory, e.g., Fermi liquid or non-Fermi liquid regimes. Then, we derive analytically the two point Green function, which up to a nonimportant constant defines the self-energy in the fermion propagator of the CFT_{2+1} .

B.1 Dirac equation and conformal dimension

We consider the following action for a two-component spinor field ψ

$$S = i \int d^2x \sqrt{-g} \bar{\psi} \left(\Gamma^\alpha D_\alpha - m + i\Gamma\lambda - \tilde{\Gamma}\Delta \right) \psi, \quad (\text{B.1})$$

with $D_\alpha = \partial_\alpha - iqA_\alpha$ and the background metric and gauge field given by

$$ds^2 = \frac{R_2^2}{\zeta^2} (-d\tau^2 + d\zeta^2), \quad A_\tau = \frac{g_F r_*^2}{\sqrt{12} r_{**}^2} \frac{1}{\zeta}. \quad (\text{B.2})$$

In eq.(B.1), we included a time-reversal violating λ term which in our application will be related to k_x momentum in \mathbb{R}^2 , and hence the eigenvalue λ_n incorporating effect of the magnetic field; we also included Δ term to mimic the gap in \mathbb{R}^2 . We choose the following Gamma matrices

$$\Gamma^{\hat{\zeta}} = -\sigma^3, \quad \Gamma^{\hat{\tau}} = i\sigma^1, \quad \Gamma = -\sigma^2, \quad \tilde{\Gamma} = 1, \quad (\text{B.3})$$

where the hat indices denote those in tangent frame and σ^i are standard sigma matrices. Writing $\psi(\tau, \zeta) = (-g/g_{\zeta\zeta})^{-1/4} \int d\omega e^{-i\omega\tau} \Phi(\omega, \zeta)$ the equations of motion are

$$\left(-\frac{1}{\sqrt{g_{\zeta\zeta}}} \sigma^3 \partial_{\zeta} - m_{**} + \frac{1}{\sqrt{-g_{\tau\tau}}} \sigma^1 (\omega + qA_{\tau}) - i\sigma^2 \lambda \right) \Phi = 0, \quad (\text{B.4})$$

where we introduced $m_{**} = m + \Delta$. In a matrix form we have

$$\begin{pmatrix} \frac{\zeta}{R_2} \partial_{\zeta} + m_{**} & -\frac{\zeta}{R_2} \left(\omega + \frac{qg_F r_*^2}{\sqrt{12} r_{**}^2} \frac{1}{\zeta} \right) + \lambda \\ \frac{\zeta}{R_2} \left(\omega + \frac{qg_F r_*^2}{\sqrt{12} r_{**}^2} \frac{1}{\zeta} \right) + \lambda & \frac{\zeta}{R_2} \partial_{\zeta} - m_{**} \end{pmatrix} \begin{pmatrix} y \\ z \end{pmatrix} = 0. \quad (\text{B.5})$$

To find the conformal dimension of the operator \mathcal{O} dual to Φ , we solve the Dirac equation near the boundary. Near the AdS_2 boundary $\zeta \rightarrow 0$, equation (B.5) to the leading order is

$$\zeta \partial_{\zeta} \Phi = -U \Phi, \quad U = \begin{pmatrix} m_{**} R_2 & -\frac{qg_F r_*^2}{\sqrt{12} r_{**}^2} + \lambda R_2 \\ \frac{qg_F r_*^2}{\sqrt{12} r_{**}^2} + \lambda R_2 & -m_{**} R_2 \end{pmatrix}. \quad (\text{B.6})$$

As $\zeta \rightarrow 0$, Φ can be written to the leading order in the form

$$\Phi = A v_+ \zeta^{-\nu} + B v_- \zeta^{\nu}, \quad (\text{B.7})$$

where v_{\pm} are real eigenvectors of U with eigenvalues $\pm\nu$ respectively

$$\nu = \sqrt{((m + \Delta)^2 + \lambda^2) R_2^2 - \frac{q^2 g_F^2 r_*^4}{12 r_{**}^4}}, \quad (\text{B.8})$$

with $R_2 = R/\sqrt{6}$. Here ν determines the scaling dimension of the fermionic operator in the CFT_1 dual to the spinor field in the AdS_2 . With small modifications this gives the scaling dimension of the CFT_3 in the IR region, since as $\omega \rightarrow 0$ the metric reduces $AdS_4 \rightarrow AdS_2 \times R_2$ near the AdS_4 horizon. The eigenvectors of U can be chosen from eq.(B.6) as

$$v_{\pm} = \begin{pmatrix} (m + \Delta) R_2 \pm \nu_{\psi} \\ \lambda R_2 + \frac{qg_F r_*^2}{\sqrt{12} r_{**}^2} \end{pmatrix}. \quad (\text{B.9})$$

Imposing the ingoing boundary condition for Φ at the AdS_2 horizon, the retarded Green function for the boundary operator in the IR CFT_1 dual to Φ can be written as

$$G_R^{IR}(\omega) = \frac{B}{A} \omega^{2\nu}, \quad (\text{B.10})$$

meaning that the operator conformal dimension is given by

$$\delta_{\psi} = \frac{1}{2} + \nu, \quad (\text{B.11})$$

where ν is the scaling exponent with respect to ω , given by eq.(B.8). In eq.(B.10), we used the fact that in the solution Φ , ω and ζ scale with the same power [18].

B.2 Two-point functions for charged fermions in AdS₂

We calculate G^{IR} analytically. The equation of motion (B.4) can be written as

$$\partial_\zeta \Phi = i\sigma^2 \left(\omega + \frac{qg_F r_*^2}{\sqrt{12} r_*^2} \frac{1}{\zeta} \right) \Phi - \frac{R_2}{\zeta} (\sigma^3 m_{**} + \sigma^1 \lambda) \Phi, \quad (\text{B.12})$$

where $m_{**} = m + \Delta$. The equation of motion for two components $\Phi = (y, z)^T$ is given by

$$\begin{aligned} (\zeta \partial_\zeta + m_{**} R_2) y - (\omega \zeta + \frac{qg_F r_*^2}{\sqrt{12} r_*^2} - \lambda R_2) z &= 0, \\ (\zeta \partial_\zeta - m_{**} R_2) z + (\omega \zeta + \frac{qg_F r_*^2}{\sqrt{12} r_*^2} + \lambda R_2) y &= 0, \end{aligned} \quad (\text{B.13})$$

which contain ζ dependence in the mixing term proportional to $i\sigma^2$, that makes it difficult to solve for one component. We therefore transform to another basis to make all ζ dependent terms diagonal [?]. We make the following basis rotation

$$\begin{pmatrix} \tilde{y} \\ \tilde{z} \end{pmatrix} = M \begin{pmatrix} y \\ z \end{pmatrix}, \quad \text{with } M = \begin{pmatrix} 1 & -i \\ -i & 1 \end{pmatrix}, \quad M^{-1} = \frac{1}{2} \begin{pmatrix} 1 & i \\ i & 1 \end{pmatrix}. \quad (\text{B.14})$$

Transforming the sigma matrices, $M\sigma^i M^{-1}$, we have $i\sigma^2 \rightarrow i\sigma^3$, $\sigma^3 \rightarrow -\sigma^2$, $\sigma^1 \rightarrow \sigma^1$. The equation of motion becomes

$$\partial_\zeta \tilde{\Phi} = i\sigma^3 \left(\omega + \frac{qg_F r_*^2}{\sqrt{12} r_*^2} \frac{1}{\zeta} \right) \tilde{\Phi} + \frac{R_2}{\zeta} (\sigma^2 m_{**} - \sigma^1 \lambda) \tilde{\Phi}, \quad (\text{B.15})$$

and for two components $\tilde{\Phi} = (\tilde{y}, \tilde{z})^T$,

$$\begin{aligned} (\zeta \partial_\zeta - i(\omega \zeta + \frac{qg_F r_*^2}{\sqrt{12} r_*^2})) \tilde{y} + (im_{**} + \lambda) R_2 \tilde{z} &= 0, \\ (\zeta \partial_\zeta + i(\omega \zeta + \frac{qg_F r_*^2}{\sqrt{12} r_*^2})) \tilde{z} - (im_{**} - \lambda) R_2 \tilde{y} &= 0. \end{aligned} \quad (\text{B.16})$$

Expressing \tilde{y} from the second equation

$$\tilde{y} = \frac{\zeta \partial_\zeta + i(\omega \zeta + \frac{qg_F r_*^2}{\sqrt{12} r_*^2})}{(im_{**} - \lambda) R_2} \tilde{z}, \quad (\text{B.17})$$

we get the equation for \tilde{z} . The equations for both components are given by

$$\begin{aligned} \left(\zeta \partial_\zeta + i(\omega \zeta + \frac{qg_F r_*^2}{\sqrt{12} r_*^2}) \right) \left(\zeta \partial_\zeta - i(\omega \zeta + \frac{qg_F r_*^2}{\sqrt{12} r_*^2}) \right) \tilde{y} &= (m_{**}^2 + \lambda^2) R_2^2 \tilde{y}, \\ \left(\zeta \partial_\zeta - i(\omega \zeta + \frac{qg_F r_*^2}{\sqrt{12} r_*^2}) \right) \left(\zeta \partial_\zeta + i(\omega \zeta + \frac{qg_F r_*^2}{\sqrt{12} r_*^2}) \right) \tilde{z} &= (m_{**}^2 + \lambda^2) R_2^2 \tilde{z}. \end{aligned} \quad (\text{B.18})$$

Rewriting these equations, we get

$$\begin{aligned} \zeta^2 \partial_\zeta^2 \tilde{y} + \zeta \partial_\zeta \tilde{y} + \left(-i\zeta \omega + (\omega \zeta + \frac{qg_F r_*^2}{\sqrt{12} r_*^2})^2 - (m_{**}^2 + \lambda^2) R_2^2 \right) \tilde{y} &= 0, \\ \zeta^2 \partial_\zeta^2 \tilde{z} + \zeta \partial_\zeta \tilde{z} + \left(i\zeta \omega + (\omega \zeta + \frac{qg_F r_*^2}{\sqrt{12} r_*^2})^2 - (m_{**}^2 + \lambda^2) R_2^2 \right) \tilde{z} &= 0. \end{aligned} \quad (\text{B.19})$$

MATHEMATICA gives the following solutions for equations (B.19)

$$\begin{aligned}\tilde{y}(\zeta) &= e^{-i\omega\zeta}\zeta^\nu \left(c_1 U\left(1 + \nu + i\frac{qgFr_*^2}{\sqrt{12}r_{**}^2}, 1 + 2\nu, 2i\omega\zeta\right) + c_2 L\left(-1 - \nu - i\frac{qgFr_*^2}{\sqrt{12}r_{**}^2}, 2\nu, 2i\omega\zeta\right) \right), \\ \tilde{z}(\zeta) &= e^{-i\omega\zeta}\zeta^\nu \left(c_3 U\left(\nu + i\frac{qgFr_*^2}{\sqrt{12}r_{**}^2}, 1 + 2\nu, 2i\omega\zeta\right) + c_4 L\left(-\nu - i\frac{qgFr_*^2}{\sqrt{12}r_{**}^2}, 2\nu, 2i\omega\zeta\right) \right),\end{aligned}\quad (\text{B.20})$$

where $\nu = \sqrt{(m_{**}^2 + \lambda^2)R_2^2 - \frac{q^2 g_F^2 r_*^4}{12r_{**}^4}}$, $U(a, b, z)$ is the tricomi confluent hypergeometric function (of the second kind) and $L(\nu, \lambda, z) \equiv L_\nu^\lambda(z)$ is the generalized Laguerre function (for $\nu = n$ the associated Laguerre polynomial). We substitute solutions (B.20) into the system of first order ODE, eq.(B.16), and consider this system at the AdS₂ boundary, $\zeta \rightarrow 0$, where it is considerably simplified. As a result we get the relations between the constants

$$\begin{aligned}\frac{c_1}{c_3} &= (im_{**} + \lambda)R_2 \\ \frac{c_2}{c_4} &= \frac{(im_{**} + \lambda)R_2}{\nu + i\frac{qgFr_*^2}{\sqrt{12}r_{**}^2}} = \frac{\nu - i\frac{qgFr_*^2}{\sqrt{12}r_{**}^2}}{(-im_{**} + \lambda)R_2},\end{aligned}\quad (\text{B.21})$$

to simplify we use $\Gamma(z)\Gamma(1-z) = \pi/\sin(\pi z)$. Both equations in the system give the same relations eq.(B.21). As a consistency check, we found the same relations considering the system at the AdS₂ horizon, $\zeta \rightarrow \infty$. In order to insure the ingoing wave $\sim e^{i\omega\zeta}$ at the horizon $\zeta \rightarrow \infty$ for each of the solutions, we have one more relation between the constants

$$\frac{c_1}{c_2} = -\frac{\Gamma(1 + \nu + i\frac{qgFr_*^2}{\sqrt{12}r_{**}^2})}{\pi}.\quad (\text{B.22})$$

Relations (B.21,B.22) fix all the constants up to overall normalization constant. Using the relations (B.21,B.22), the solution of the system (B.16) at $\zeta = 0$ becomes

$$\tilde{y} \rightarrow (2i\omega)^{-2\nu} \frac{\Gamma(2\nu)\Gamma(1 - \nu - i\frac{qgFr_*^2}{\sqrt{12}r_{**}^2})}{\nu + i\frac{qgFr_*^2}{\sqrt{12}r_{**}^2}} \zeta^{-\nu} + \frac{\Gamma(-2\nu)\Gamma(1 + \nu - i\frac{qgFr_*^2}{\sqrt{12}r_{**}^2})}{-\nu + i\frac{qgFr_*^2}{\sqrt{12}r_{**}^2}} \zeta^\nu, \quad (\text{B.23})$$

$$\tilde{z} \rightarrow (2i\omega)^{-2\nu} \frac{\Gamma(2\nu)\Gamma(1 - \nu - i\frac{qgFr_*^2}{\sqrt{12}r_{**}^2})}{(im_{**} + \lambda)R_2} \zeta^{-\nu} + \frac{\Gamma(-2\nu)\Gamma(1 + \nu - i\frac{qgFr_*^2}{\sqrt{12}r_{**}^2})}{(im_{**} + \lambda)R_2} \zeta^\nu. \quad (\text{B.24})$$

At $\zeta \rightarrow 0$, solution to the original system of equations (B.13) is given by

$$\begin{aligned}\begin{pmatrix} y \\ z \end{pmatrix} &= \frac{1}{2} \begin{pmatrix} \tilde{y} + i\tilde{z} \\ \tilde{z} + i\tilde{y} \end{pmatrix} = (2i\omega)^{-2\nu} \frac{\Gamma(2\nu)\Gamma(1 - \nu - i\frac{qgFr_*^2}{\sqrt{12}r_{**}^2})}{2(\nu + i\frac{qgFr_*^2}{\sqrt{12}r_{**}^2})} \begin{pmatrix} 1 + i\frac{\nu + i\frac{qgFr_*^2}{\sqrt{12}r_{**}^2}}{(im_{**} + \lambda)R_2} \\ \frac{\nu + i\frac{qgFr_*^2}{\sqrt{12}r_{**}^2}}{(im_{**} + \lambda)R_2} + i \end{pmatrix} \zeta^{-\nu} \\ &+ \frac{\Gamma(-2\nu)\Gamma(1 + \nu - i\frac{qgFr_*^2}{\sqrt{12}r_{**}^2})}{2(-\nu + i\frac{qgFr_*^2}{\sqrt{12}r_{**}^2})} \begin{pmatrix} 1 + i\frac{-\nu + i\frac{qgFr_*^2}{\sqrt{12}r_{**}^2}}{(im_{**} + \lambda)R_2} \\ \frac{-\nu + i\frac{qgFr_*^2}{\sqrt{12}r_{**}^2}}{(im_{**} + \lambda)R_2} + i \end{pmatrix} \zeta^\nu.\end{aligned}\quad (\text{B.25})$$

The system of equations (B.13) near the AdS₂ boundary has a solution which can be written in a general form as, eq.(B.7),

$$\begin{pmatrix} y \\ z \end{pmatrix} = Av_+\zeta^{-\nu} + Bv_-\zeta^\nu = A \begin{pmatrix} m_{**}R_2 + \nu \\ \lambda R_2 + \frac{qgFr_*^2}{\sqrt{12r_*^2}} \end{pmatrix} \zeta^{-\nu} + B \begin{pmatrix} m_{**}R_2 - \nu \\ \lambda R_2 + \frac{qgFr_*^2}{\sqrt{12r_*^2}} \end{pmatrix} \zeta^\nu. \quad (\text{B.26})$$

then the Green function is $G_R^{IR}(\omega) = B/A$. We put solution eq.(B.25) into this form,

$$\begin{aligned} \begin{pmatrix} y \\ z \end{pmatrix} &= (2i\omega)^{-2\nu} \Gamma(2\nu) \Gamma(1 - \nu - i \frac{qgFr_*^2}{\sqrt{12r_*^2}}) \frac{1 + \frac{\nu + i \frac{qgFr_*^2}{\sqrt{12r_*^2}}}{(m_{**} - i\lambda)R_2}}{2(\nu + i \frac{qgFr_*^2}{\sqrt{12r_*^2}})(m_{**}R_2 + \nu)} \begin{pmatrix} m_{**}R_2 + \nu \\ \lambda R_2 + \frac{qgFr_*^2}{\sqrt{12r_*^2}} \end{pmatrix} \zeta^{-\nu} \\ &+ \Gamma(-2\nu) \Gamma(1 + \nu - i \frac{qgFr_*^2}{\sqrt{12r_*^2}}) \frac{1 + \frac{-\nu + i \frac{qgFr_*^2}{\sqrt{12r_*^2}}}{(m_{**} - i\lambda)R_2}}{2(-\nu + i \frac{qgFr_*^2}{\sqrt{12r_*^2}})(m_{**}R_2 - \nu)} \begin{pmatrix} m_{**}R_2 - \nu \\ \lambda R_2 + \frac{qgFr_*^2}{\sqrt{12r_*^2}} \end{pmatrix} \zeta^{-\nu}, \end{aligned} \quad (\text{B.27})$$

and extract the IR Green function to be

$$\begin{aligned} G_R^{IR}(\omega) &= e^{-i\pi\nu} \frac{\Gamma(-2\nu) \Gamma(1 + \nu - i \frac{qgFr_*^2}{\sqrt{12r_*^2}})}{\Gamma(2\nu) \Gamma(1 - \nu - i \frac{qgFr_*^2}{\sqrt{12r_*^2}})} \times \\ &\frac{((m_{**} - i\lambda)R_2 + i \frac{qgFr_*^2}{\sqrt{12r_*^2}} - \nu)(i \frac{qgFr_*^2}{\sqrt{12r_*^2}} + \nu)(m_{**}R_2 + \nu)}{((m_{**} - i\lambda)R_2 + i \frac{qgFr_*^2}{\sqrt{12r_*^2}} + \nu)(i \frac{qgFr_*^2}{\sqrt{12r_*^2}} - \nu)(m_{**}R_2 - \nu)} (2\omega)^{2\nu}. \end{aligned} \quad (\text{B.28})$$

Simplifying the following ratio

$$\frac{((m_{**} - i\lambda)R_2 + i \frac{qgFr_*^2}{\sqrt{12r_*^2}} - \nu)(i \frac{qgFr_*^2}{\sqrt{12r_*^2}} + \nu)}{((m_{**} - i\lambda)R_2 + i \frac{qgFr_*^2}{\sqrt{12r_*^2}} + \nu)(i \frac{qgFr_*^2}{\sqrt{12r_*^2}} - \nu)} = \frac{((m_{**} + i\lambda)R_2 - i \frac{qgFr_*^2}{\sqrt{12r_*^2}} - \nu)}{((m_{**} + i\lambda)R_2 - i \frac{qgFr_*^2}{\sqrt{12r_*^2}} + \nu)}, \quad (\text{B.29})$$

we get the retarded IR Green function given by

$$G_R^{IR}(\omega) = e^{-i\pi\nu} \frac{\Gamma(-2\nu) \Gamma(1 + \nu - i \frac{qgFr_*^2}{\sqrt{12r_*^2}})}{\Gamma(2\nu) \Gamma(1 - \nu - i \frac{qgFr_*^2}{\sqrt{12r_*^2}})} \frac{((m_{**} + i\lambda)R_2 - i \frac{qgFr_*^2}{\sqrt{12r_*^2}} - \nu)}{((m_{**} + i\lambda)R_2 - i \frac{qgFr_*^2}{\sqrt{12r_*^2}} + \nu)} (2\omega)^{2\nu}, \quad (\text{B.30})$$

with $m_{**} = m + \Delta$. In eq.(B.30), we did not include a ratio $\frac{m_{**}R_2 + \nu}{m_{**}R_2 - \nu}$, since there is an ambiguity in definition of the Green function up to a real function of λ (or k with no magnetic field) and q, m . If the matching is done using our basis then this difference should not matter. This expression for the IR Green function agrees with the one obtained in [18].

C. One-loop calculations in a (2 + 1) dimensional field theory

We calculate here the free fermion energy and the gap equation. One-loop fermion effective action in the chiral limit, $m = 0$, is given by

$$S_{eff}^{1loop} = -i \ln \det(i\mathcal{D} - \Delta) = -\frac{i}{2} \ln \det(\mathcal{D}^2 + \Delta^2), \quad (\text{C.1})$$

where $i\mathcal{D} = (i\partial_t + \mu)\gamma^0 - v_F\vec{K}\vec{\gamma}$, and $\vec{K} = i\vec{\nabla} + q\vec{A}$. For simplicity, we added to the free part the interaction $G_{int}(\bar{\psi}\psi)(\bar{\psi}\psi) \rightarrow (\Delta(\bar{\psi}\psi) + h.c.) - \Delta^2/4G_{int}$, where the strength of interaction in $(2+1)$ -d is $G_{int} \sim \frac{1}{M_F}$. Here, the order parameter is $\Delta = 2G_{int} \langle \bar{\psi}\psi \rangle$. In the Landau gauge $\vec{A} = (-\mathcal{H}y, 0)$, and after the Fourier transform, we have

$$-\mathcal{D}^2 = (\omega + \mu)^2 - v_F^2\vec{K}^2 - iq\mathcal{H}v_F^2\gamma^1\gamma^2. \quad (\text{C.2})$$

To calculate the fermion determinant, eq.(C.1), we use $\ln \det G^{-1} = \text{Tr} \ln G^{-1}$. The eigenvalues of operator \vec{K}^2 are known $(2l+1)|q\mathcal{H}|$ (we also calculated them in Appendix A.1); the eigenvalues of operator $iv_F^2q\mathcal{H}\gamma^1\gamma^2$ are $\pm v_F^2|q\mathcal{H}|$ (in standard representation for γ matrices); i.e., the \mathcal{H} dependent part is $(2l+1)v_F^2|q\mathcal{H}| \pm v_F^2|q\mathcal{H}|$. One can rescale $l \rightarrow l-1$ for one of the signs and combine two terms with both signs together with the result $v_F^2 2|q\mathcal{H}|l$. After rescaling there will be however different prefactors for two signs from taking matrix elements under the trace, Tr (see [1] for details). Since we will consider only the lowest Landau level, we can ignore the difference in prefactors, and moreover

$$\int \frac{d^2k}{(2\pi)^2} \rightarrow \frac{V_2|q\mathcal{H}|}{(2\pi)}, \quad (\text{C.3})$$

that takes into account the degeneracy of Landau levels, since the Dirac equation eigenvalue λ and hence the quasiparticle spectrum do not depend on momentum k . Here $V_2 = L_x \times L_y$ is the size of the sample. We therefore have

$$S_{eff}^{1loop} = -\frac{V_2|q\mathcal{H}|}{2\pi} \sum_n \ln \frac{(\omega_n + i\mu)^2 + E_l^2}{T^2}, \quad (\text{C.4})$$

where the fermionic Matsubara frequencies at temperature T are $\omega_n = \frac{(2n+1)\pi T}{2}$ (we changed to Matsubara frequency by Wick rotation $\omega_n = i\omega$), and $E_l = \sqrt{2v_F^2|q\mathcal{H}|l + \Delta^2}$. Sum over the Landau levels l is implied. The Dirac equation eigenvalue is $\lambda = (\omega_n + i\mu)^2 + E_l^2$, which gives quasiparticle poles $z_*(l) = i\omega_n$ at $\lambda = 0$ equal to $z_*(l) = \mu \pm E_l$. We rewrite the Matsubara sum as a contour integral

$$\sum_n \ln \frac{(\omega_n + i\mu)^2 + E_l^2}{T^2} = \frac{i}{2} \int_C \frac{dz}{2\pi} \ln \frac{-(z - \mu)^2 + E_l^2}{T^2} \tanh \frac{z}{2T}, \quad (\text{C.5})$$

due to the fact that the poles of \tanh are situated along the imaginary axis at $z = i(2n+1)\pi T$. Differentiating both sides with respect to E_l , we take the r.h.s. integral

$$\sum_n \frac{2E_l}{(\omega_n + i\mu)^2 + E_l^2} = \frac{1}{2} \sum_{z_*} \tanh \frac{|z_*(l)|}{2T} = \frac{1}{2} \left(\tanh \frac{E_l - \mu}{2T} + \tanh \frac{E_l + \mu}{2T} \right). \quad (\text{C.6})$$

Integrating back over E_l , we have

$$\begin{aligned} T \sum_n \ln \frac{(\omega_n + i\mu)^2 + E_l^2}{T^2} &= T \sum_{z_*(l)} \ln \left(2 \cosh \frac{|z_*(l)|}{2T} \right) = T \sum_{z_*(l)} \left(\frac{|z_*(l)|}{2T} + \ln(1 + e^{-|z_*(l)|/T}) \right) \\ &= \frac{E_l - \mu}{2} + T \ln(1 + e^{-(E_l - \mu)/T}) + \frac{E_l + \mu}{2} + T \ln(1 + e^{-(E_l + \mu)/T}). \end{aligned} \quad (\text{C.7})$$

A useful formula following from eq.(C.6),

$$T \sum_n \frac{1}{(\omega_n + i\mu)^2 + E_l^2} = \frac{1}{2E_l} \sum_{z_*(l)} \frac{1}{2} \tanh \frac{|z_*(l)|}{2T} = \frac{1}{2E_l} \frac{\sinh \frac{E_l}{T}}{\cosh \frac{E_l}{T} + \cosh \frac{\mu}{T}}. \quad (\text{C.8})$$

Putting all together, an effective action for Δ is given by

$$S_{eff} = \frac{V_2}{T} \left(\frac{|\Delta|^2}{4G_{int}} - \frac{T|q\mathcal{H}|}{2\pi} \sum_{z_*(l)} \ln \left(2 \cosh \frac{z_*(l)}{2T} \right) \right), \quad (\text{C.9})$$

with $z_*(l) = \mu \pm E_l$, $E_l = \sqrt{2|q\mathcal{H}|l + \Delta^2}$, sum over the Landau levels l is implied. The free fermion energy can be obtained by dividing S_{eff} by the space-time volume, i.e., $\Omega_F = -S_{eff}/(TV_2)$. Minimizing effective action, $\delta S_{eff}/\delta \Delta = 0$, we get the gap equation

$$\Delta = \frac{G_{int}|q\mathcal{H}|}{\pi} \frac{\Delta}{E_l} \frac{\sinh \frac{E_l}{T}}{\cosh \frac{E_l}{T} + \cosh \frac{\mu}{T}}, \quad (\text{C.10})$$

with $E_l = \sqrt{2|q\mathcal{H}|l + \Delta^2}$, sum over l is implied. For the lowest Landau level, $l = 0$, the gap equation reads

$$\Delta = \frac{G_{int}|q\mathcal{H}|}{\pi} \frac{\sinh \frac{\Delta}{T}}{\cosh \frac{\Delta}{T} + \cosh \frac{\mu}{T}}. \quad (\text{C.11})$$

At $T = 0$, the solution is given by

$$\Delta = \frac{1}{\pi} G_{int}|q\mathcal{H}|, \quad (\text{C.12})$$

provided $\Delta > \mu$, and where $G_{int} = \frac{1}{M_F}$. At $T \neq 0$, from eq.(D.2), there is the second solution $\Delta = 0$, and the phase transition between $\Delta \neq 0$ and $\Delta = 0$. The character of the phase transition, first or second order depends on the values of parameters [1].

We calculate the critical temperature of the phase transition. We fix the charge density, n , and express the chemical potential through n . From the effective action eq.(C.9), the charge density and the gap equation for the lowest Landau level are given by

$$\begin{aligned} n &= \frac{|q\mathcal{H}|}{2\pi} \frac{\sinh(\frac{\mu}{T})}{\cosh(\frac{\Delta}{T}) + \cosh(\frac{\mu}{T})}, \\ \Delta &= \frac{G_{int}|q\mathcal{H}|}{\pi} \frac{\sinh(\frac{\Delta}{T})}{\cosh(\frac{\Delta}{T}) + \cosh(\frac{\mu}{T})}. \end{aligned} \quad (\text{C.13})$$

We introduce the filling factor

$$\eta_{\mathcal{H}} = \frac{2\pi n}{|q\mathcal{H}|} \equiv \frac{\mathcal{H}_c}{\mathcal{H}}, \quad (\text{C.14})$$

then from the expression for the charge density, we have

$$\cosh\left(\frac{\mu}{T}\right) = \frac{\eta_{\mathcal{H}}^2 \cosh\left(\frac{\Delta}{T}\right) + \sqrt{1 + \eta_{\mathcal{H}}^2 \sinh^2\left(\frac{\Delta}{T}\right)}}{1 - \eta_{\mathcal{H}}^2}. \quad (\text{C.15})$$

Therefore the gap equation becomes

$$\Delta = \frac{G_{int}|q\mathcal{H}|}{\pi} \frac{(1 - \eta_{\mathcal{H}}^2) \sinh(\frac{\Delta}{T})}{\cosh(\frac{\Delta}{T}) + \sqrt{1 + \eta_{\mathcal{H}}^2 \sinh^2(\frac{\Delta}{T})}}. \quad (\text{C.16})$$

At $T=0$, the solution is given by

$$\Delta = \frac{G_{int}|q\mathcal{H}|}{\pi} (1 - \eta_{\mathcal{H}}). \quad (\text{C.17})$$

There is no nonzero gap for the filling factor $\eta_{\mathcal{H}} > 1$. The condition $\eta_{\mathcal{H}} < 1$ to have a nonzero gap translates for the charge density to be smaller than critical one, $n < n_c$, with $n_c = n(\eta_{\mathcal{H}} = 1)$, or for the magnetic field to be larger than the critical one, $\mathcal{H} > \mathcal{H}_c$. For $\eta_{\mathcal{H}} > 1$, i.e. $n > n_c$ or $\mathcal{H} < \mathcal{H}_c$ the symmetry is restored, $\Delta = 0$. Around the critical temperature, when the gap is vanishing, the gap equation gives the following critical temperature

$$T_c = \frac{G_{int}|q\mathcal{H}|}{2\pi} (1 - \eta_{\mathcal{H}}^2), \quad (\text{C.18})$$

where $T_c = 0$ for $\eta_{\mathcal{H}} > 1$, i.e. for $\mathcal{H} < \mathcal{H}_c$. For $\mathcal{H} > \mathcal{H}_c$, T_c grows linearly with magnetic field, $T_c \sim |q\mathcal{H}|$, in the vicinity of the phase transition. Away from the phase transition one should solve the following gap equation for the lowest Landau level numerically

$$\Delta = \frac{2T_c \sinh(\frac{\Delta}{T})}{\cosh(\frac{\Delta}{T}) + \sqrt{1 + \eta_{\mathcal{H}}^2 \sinh^2(\frac{\Delta}{T})}}. \quad (\text{C.19})$$

We use this procedure to derive the gap equation and to calculate T_c in the AdS_4 .

D. Critical temperature from the AdS_4 variational calculations

We calculate the critical temperature T_c for the case of Landau Fermi liquid, $\nu_{k_F} > \frac{1}{2}$. Let us introduce an analog of the charge density in the AdS_4 by differentiating an effective action eq.(3.23) with respect to the Fermi momentum k_F , $n(r) = \frac{\delta S_{eff}}{\delta(v_F k_F)}$. Together with the gap equation, $\frac{\delta S_{eff}}{\delta \Delta(r)} = 0$, we have

$$n = \frac{|q\mathcal{H}|}{2\pi R} \frac{1}{\pi} \sum_{z_*[\Delta(r)]} \left(\frac{\delta \omega_*[\Delta(r)]}{\delta(v_F k_F)} \text{Im} \Psi \left(\frac{iz_*[\Delta(r)]}{2\pi T} + \frac{1}{2} \right) - \frac{\delta \Gamma[\Delta(r)]}{\delta(v_F k_F)} \text{Re} \Psi \left(\frac{iz_*[\Delta(r)]}{2\pi T} + \frac{1}{2} \right) \right), \quad (\text{D.1})$$

$$\Delta(r) = \frac{G_{int}|q\mathcal{H}|}{\pi} \frac{1}{\pi} \sum_{z_*[\Delta(r)]} \left(\frac{\delta \omega_*[\Delta(r)]}{\delta \Delta(r)} \text{Im} \Psi \left(\frac{iz_*[\Delta(r)]}{2\pi T} + \frac{1}{2} \right) - \frac{\delta \Gamma[\Delta(r)]}{\delta \Delta(r)} \text{Re} \Psi \left(\frac{iz_*[\Delta(r)]}{2\pi T} + \frac{1}{2} \right) \right). \quad (\text{D.2})$$

Here sum goes over the two poles. For the lowest Landau level, $l = 0$,

$$n = \frac{|q\mathcal{H}|}{2\pi R} \frac{1}{\pi} \text{Im} \left(-\Psi \left(\frac{iv_F(\delta k_F[\Delta(r)] - k_F)}{2\pi T} + \frac{1}{2} \right) + \Psi \left(\frac{iv_F(\delta k_F[\Delta(r)] + k_F)}{2\pi T} + \frac{1}{2} \right) \right), \quad (\text{D.3})$$

$$\Delta(r) = \frac{G_{int}|q\mathcal{H}|}{\pi} \frac{1}{\pi} \text{Im} \left(\Psi \left(\frac{iv_F(\delta k_F[\Delta(r)] - k_F)}{2\pi T} + \frac{1}{2} \right) + \Psi \left(\frac{iv_F(\delta k_F[\Delta(r)] + k_F)}{2\pi T} + \frac{1}{2} \right) \right) \frac{\psi^0(r)^\dagger \sigma^1 \psi^0(r)}{R^4}, \quad (\text{D.4})$$

where the shift of the Fermi momentum is given by

$$\delta k_F[\Delta(r)] = \frac{1}{v_F R^4} \int dr \sqrt{-g} \psi^0(r)^\dagger \sigma^1 \psi^0(r) \Delta(r). \quad (\text{D.5})$$

For $T \sim T_c$, we expand in $\Delta \ll T$,

$$n = \frac{|q\mathcal{H}|}{2\pi R} \frac{1}{\pi} \text{Im} \left(-\Psi \left(\frac{-iv_F k_F}{2\pi T} + \frac{1}{2} \right) + \Psi \left(\frac{iv_F k_F}{2\pi T} + \frac{1}{2} \right) \right), \quad (\text{D.6})$$

$$\Delta(r) = \frac{G_{int}|q\mathcal{H}|}{\pi} \frac{1}{\pi} \text{Im} \frac{i \int dr \sqrt{-g} \psi^0(r)^\dagger \sigma^1 \psi^0(r) \Delta(r)}{2\pi T R^4} \times \left(\Psi' \left(\frac{-iv_F k_F}{2\pi T} + \frac{1}{2} \right) + \Psi' \left(\frac{iv_F k_F}{2\pi T} + \frac{1}{2} \right) \right) \frac{\psi^0(r)^\dagger \sigma^1 \psi^0(r)}{R^4}, \quad (\text{D.7})$$

where $\Psi'(x)$ is the derivative of the digamma function $\Psi'(x) = \frac{d^2 \ln \Gamma(x)}{dx^2}$; the subleading term $\sim \Delta$ in n and the leading term ~ 1 in Δ vanish due to the imaginary part. We use that the solution of the gap equations at zero temperature is given by eq.(3.32). Therefore the radial profile is given by

$$\Delta(r) \sim \psi^0(r)^\dagger \sigma^1 \psi^0(r). \quad (\text{D.8})$$

Substituting it into eq.(D.7), we have

$$1 = \frac{G_{int}|q\mathcal{H}|}{\pi} \frac{1}{\pi} \text{Im} \frac{i}{2\pi T} \left(\Psi' \left(\frac{-iv_F k_F}{2\pi T} + \frac{1}{2} \right) + \Psi' \left(\frac{iv_F k_F}{2\pi T} + \frac{1}{2} \right) \right) \frac{\int dr \sqrt{-g} (\psi^0(r)^\dagger \sigma^1 \psi^0(r))^2}{R^8}. \quad (\text{D.9})$$

Simplifying the digamma functions and their derivatives, we obtain

$$n = \frac{|q\mathcal{H}|}{2\pi R} \tanh \frac{v_F k_F}{2T}, \quad (\text{D.10})$$

$$1 = \frac{G_{int}|q\mathcal{H}|}{\pi} \frac{1}{2T} \frac{1}{\cosh^2 \frac{v_F k_F}{2T}} \frac{\int dr \sqrt{-g} (\psi^0(r)^\dagger \sigma^1 \psi^0(r))^2}{R^8}. \quad (\text{D.11})$$

We introduce the filling factor

$$\eta_{\mathcal{H}}(r) = \frac{2\pi R n}{|q\mathcal{H}|} \equiv \frac{\mathcal{H}_c}{\mathcal{H}}. \quad (\text{D.12})$$

From the equation (D.10) for the charge density, we have

$$\cosh^2\left(\frac{v_F k_F}{2T}\right) = \frac{1}{1 - \eta_{\mathcal{H}}^2}. \quad (\text{D.13})$$

Using it in the gap equation (D.11), we get the critical temperature for the lowest Landau level

$$T_c = \frac{G_{int}|q\mathcal{H}|}{2\pi R^8} (1 - \eta_{\mathcal{H}}^2) \int dr \sqrt{-g} (\psi^0(r)^\dagger \sigma^1 \psi^0(r))^2. \quad (\text{D.14})$$

For the filling factor $\eta_{\mathcal{H}} > 1$, the critical temperature vanishes, $T_c = 0$, and for $\eta_{\mathcal{H}} < 1$, which means either $\mathcal{H} > \mathcal{H}_c$ or $n < n_c$, the critical temperature grows with the magnetic field in the vicinity of the phase transition. The integral over the profile agrees with the critical temperature given in eq.(4.24). In eq.(4.24), $v_F h_1$ introduces the dependence $v_F h_1 \sim 1/\int dr \sqrt{g/g_{tt}} \psi^0(r)^\dagger \psi^0$, which probably follows from a more careful definition for the density n in the above calculations.

References

- [1] E. V. Gorbar, V. P. Gusynin, V. A. Miransky, I. A. Shovkovy, “Dynamics in the quantum Hall effect and the phase diagram of graphene,” *Phys. Rev. B* **78**, 085437 (2008) [arXiv:0806.0846[hep-ph]], E. V. Gorbar, V. P. Gusynin, V. A. Miransky, “Toward theory of quantum Hall effect in graphene,” *LowTemp. Phys.* **34**, 790 (2008) [arXiv:0710.3527[hep-ph]].
- [2] E. V. Gorbar, V. A. Miransky, I. A. Shovkovy, “Chiral asymmetry of the Fermi surface in dense relativistic matter in a magnetic field,” *Phys. Rev. C* **80**, 032801 (2009) [arXiv:0904.2164 [hep-ph]].
- [3] G. Basar, G. V. Dunne, D. E. Kharzeev, “Chiral Magnetic Spiral,” [arXiv:1003.3464[hep-ph]], T. Kojo, Y. Hidaka, L. McLerran, R. D. Pisarski, “Quarkyonic Chiral Spirals,” [arXiv:0912.3800[hep-ph]].
- [4] S. A. Hartnoll, J. Polchinski, E. Silverstein, D. Tong, “Towards strange metallic holography,” *JHEP* **1004**, 120 (2010) [arXiv:0912.1061[hep-th]].
- [5] N. Iqbal, H. Liu, M. Mezei, Q. Si “Quantum phase transitions in holographic models of magnetism and superconductors,” [arXiv:1003.0010[hep-th]].
- [6] T. Faulkner, J. Polchinski, “Semi-Holographic Fermi Liquids,” [arXiv:1001.5049[hep-th]].
- [7] C. P. Herzog, P. K. Kovtun, D. T. Son, “Holographic model of superfluidity,” [arXiv:0809.4870[hep-th]].
- [8] C. P. Herzog, “An Analytic Holographic Superconductor,” [arXiv:1003.3278[hep-th]].
- [9] S. S. Gubser, F. D. Rocha, A. Yarom, “Fermion correlators in non-abelian holographic superconductors,” [arXiv:1002.4416[hep-th]].
- [10] S. S. Gubser, “Breaking an Abelian gauge symmetry near a black hole horizon,” *Phys. Rev. D* **78**, 065034 (2008) [arXiv:0801.2977 [hep-th]].
- [11] S. A. Hartnoll, C. P. Herzog and G. T. Horowitz, “Building a Holographic Superconductor,” *Phys. Rev. Lett.* **101**, 031601 (2008) [arXiv:0803.3295 [hep-th]].
- [12] S. S. Lee, “A Non-Fermi Liquid from a Charged Black Hole: A Critical Fermi Ball,” *Phys. Rev. D* **79**, 086006 (2009) [arXiv:0809.3402 [hep-th]].

- [13] M. Cubrovic, J. Zaanen and K. Schalm, “String Theory, Quantum Phase Transitions and the Emergent Fermi-Liquid,” *Science* **325**, 439 (2009) [arXiv:0904.1993 [hep-th]].
- [14] T. Hartman, S. A. Hartnoll, “Cooper pairing near charged black holes,” [arXiv:1003.1918[hep-th]]
- [15] S. A. Hartnoll, “Lectures on holographic methods for condensed matter physics,” arXiv:0903.3246 [hep-th].
- [16] F. Denef, S. A. Hartnoll and S. Sachdev, “Quantum oscillations and black hole ringing,” arXiv:0908.1788 [hep-th].
- [17] F. Denef, S. A. Hartnoll and S. Sachdev, “Black hole determinants and quasinormal modes,” arXiv:0908.2657 [hep-th].
- [18] T. Faulkner, H. Liu, J. McGreevy and D. Vegh, “Emergent quantum criticality, Fermi surfaces, and AdS2,” [arXiv:0907.2694 [hep-th]].
- [19] M. Alford, G. Cowan, “Single-flavour and two-flavour pairing in three-flavour quark matter,” *J. Phys. G* **32**, 511 (2006) [arXiv:hep-ph/0512104].
- [20] H. Liu, J. McGreevy and D. Vegh, “Non-Fermi liquids from holography,” arXiv:0903.2477 [hep-th].
- [21] T. Faulkner, G. T. Horowitz, J. McGreevy, M. M. Roberts and D. Vegh, “Photoemission ‘experiments’ on holographic superconductors,” [arXiv:0911.3402 [hep-th]].
- [22] T. Faulkner, N. Iqbal, H. Liu, J. McGreevy and D. Vegh “From black holes to strange metals,” [arXiv:1003.1728[hep-th]].
- [23] N. Iqbal and H. Liu, “Real-time response in AdS/CFT with application to spinors,” *Fortsch. Phys.* **57**, 367 (2009) [arXiv:0903.2596 [hep-th]].
- [24] I. S. Gradshteyn, I. W. Ryzhik, “Tables of integrals, series, and products,” Academic press, 1965.
- [25] S. B. Ruster, I. A. Shovkovy, D. H. Rischke, “Phase diagram of dense neutral three-flavor quark matter,” *Nucl. Phys. A* **743**, 127-146 (2004) [arXiv:hep-ph/0405170]; S. B. Ruster, D. H. Rischke, “Effect of color superconductivity on the mass and radius of a quark star,” *Phys. Rev. D* **69**, 045011 (2004) [arXiv:nucl-th/0309022]
- [26] M. A. V. Basagoiti, “Transport coefficients and ladder summation in hot gauge theories,” *Phys. Rev. D* **66**, 045005 (2002) [arXiv:hep-ph/0204334]; J. M. M. Resco, M. A. V. Basagoiti, “Color conductivity and ladder summation in hot QCD,” *Phys. Rev. D* **63**, 056008 (2001), [arXiv:hep-ph/0009331].
- [27] Unpublished notes on branch cut in the integrals $\ln z = \int_1^z \frac{d\xi'}{\xi'}$ where z is imaginary.
- [28] A. Sedrakian, G. Röpke, “A quantum kinetic equation for Fermi-systems including three-body correlations,” *Annals Phys.* **266**, 524 (1998). [arXiv:nucl-th/9712074].
- [29] Landau, Lifshitz., Vol. 10. “Physical Kinetics”, chapter 76.
- [30] K. Fukushima, D. E. Kharzeev, H. J. Warringa, “ The Chiral Magnetic Effect,” [arXiv:0808.3382[hep-ph]]
- [31] R. M. Fernandes, J. Schmalian, “Competing order and nature of the pairing state in the iron pnictides,” [arXiv:1005.2437[hep-th]]

- [32] S. M. Carroll, “Spacetime and Geometry: An Introduction to General Relativity,” Publisher: Benjamin Cummings (2003).
- [33] D. T. Son and A. O. Starinets, “Minkowski-space correlators in AdS/CFT correspondence: Recipe and applications,” *JHEP* **0209**, 042 (2002) [arXiv:hep-th/0205051].
- [34] E. S. C. Ching, P. T. Leung, W. M. Suen and K. Young, “Wave propagation in gravitational systems: Late time behavior,” *Phys. Rev. D* **52**, 2118 (1995) [arXiv:gr-qc/9507035].